Design of a Heat Exchanger with Thermal Storage using PCM

M.T. van Heyningen



TUDelft

Quooker

Design of a Heat Exchanger with Thermal Storage using PCM

by

M.T. van Heyningen

Student number: 4363132

Project duration: February 1, 2022 – February 20, 2023 Supervisors: Dr. R. Delfos, TU Delft

Ir. M. Disselkoen, Quooker
Prof. dr. ir. K. Hooman, TU Delft

Thesis committee: Prof. dr. ir. K. Hooman, TU Delft

Dr. ir. M. J. Tummers, TU Delft





Preface

This report signifies the end of another chapter in my educational journey. Working on this multifaceted project has enriched me in many ways that I had not expected at the outset. I want to thank Micha Disselkoen and René Delfos for their supervision and guidance during my master's thesis graduation project. Their input, feedback and expertise were invaluable for the successful completion of my thesis. I want to thank Anthony Kok for inspiring me to think outside the box and come up with creative solutions, and I would like to thank Lucas van Ballegoijen de Jong for his help throughout the project. Furthermore, I also want to thank all the other colleagues at Quooker who were always open to help in any way, shape or form at a moment's notice. I want to thank my parents for always putting education as the highest priority on the agenda and thus giving me all the opportunities to achieve my goals. Finally, I would like to thank all my family and friends who gave me inspiration, insights and support during this project and throughout my studies.

M.T. van Heyningen Delft, February 2023

Abstract

Energy efficiency is a key goal for the Quooker system. To further increase the energy efficiency of the Quooker system, this study investigates a possible heat integration system where the waste heat from the refrigeration cycle for chilled drinking water is implemented to preheat water before entering the boiling water reservoir.

Due to the intermittent nature of both the supply of heat, which is coupled to the control scheme of the chilled water reservoir and the demand for heat, which is determined by the user, a thermal storage system is required. Literature showed that the best refrigeration system for this application was a vapour compression system using a natural refrigerant such as isobutane. The most efficient heat storage could be done using organic phase change materials (PCM). Using a PCM allows the system to retain more energy in the same volume due to the latent heat in the system. To enhance the heat transfer between the fluid streams and the PCM, a fin-and-tube heat exchanger concept was designed. This concept, coupled with existing Quooker system demands, leads to a preliminary set of design requirements as well as a set of variables left to be optimised by modelling. The heat transfer from the refrigerant to the tubes was modelled using known correlations for condensation in tubes. The heat transfer between tubes and fins was modelled using a two-dimensional finite difference scheme. The heat transfer between the tubes and the water was modelled using forced convection models. The models gave dimensions for the size of the PCM container, the number of passes for each fluid stream and the thickness and spacing of the heat transfer fins.

An experimental setup based on the optimal design was created to validate the models. The results showed that PCM storage is an effective manner to store thermal energy. Heat transfer was significant in the regions surrounding the tubes. Further away from the tubes, the fins did not provide enough heat transfer to utilise the whole storage capacity effectively. In its current design state, the system would have an economic payback time of around 20 years. With small design improvements, such as increasing the fin thickness and decreasing the fin distance, the payback period can be brought down significantly. The added product value from being a more efficient product makes the concept promising for future implementation.

Contents

1	Intro	duction
	1.1	Current Product
	1.2	Problem Description
	1.3	Product Requirements
		1.3.1 Reservoir Temperatures
		1.3.2 External Requirements
	1.4	Problem Definition
	1.5	Motivation
	1.6	Structure
	1.0	Structure
2	Вас	ground Information 5
	2.1	Refrigeration Technologies
		2.1.1 Vapour Compression
		2.1.2 Thermoelectric
		2.1.3 Alternative Cooling Methods
	22	Energy Storage Methods
	2.2	2.2.1 Sensible Heat Storage
		-
	2.2	2.2.2 Latent Heat Storage
	2.3	Customer Demand
3	Sys	em Design 19
	3.1	Refrigeration System Selection
		3.1.1 Refrigeration Technology Weighting
		3.1.2 Refrigeration Technology Selection
	3.2	Storage Method Selection
	0.2	3.2.1 Sensible Heat Storage
		3.2.2 Latent Heat Storage
		3.2.3 Selection of Storage Technique
		3.2.4 Storage Medium Selection
		3.2.5 Heat Transfer Enhancement Selection
	3.3	Product Configuration
		3.3.1 Prototype Requirements
		3.3.2 Variables to be Determined Through Calculation and Modelling
4	Mod	elling 25
•	4.1	Finite Difference Model
	7.1	4.1.1 Bulk
		4.1.2 Boundary Conditions
		4.1.2 Boundary Conditions
		4.1.4 Fin Thickness
		4.1.5 Fin Distance
	4.2	Condenser side
	4.3	Preheating side
5	Prof	otype design 33
-		Design Considerations
	٠. ١	5.1.1 Heat Conduction from Tube to Fin
		5.1.2 Materials
		5.1.3 PCM Expansion
		5.1.3 POW Expansion
		J + + + + + + + + + + + + + + + + + + +

viii Contents

	5.2	Heat Storage Capacity	35
	5.3	Differences Between Prototype and End Product	
	5.4	Experimental Setup	
		5.4.1 Thermocouple Placement	
	5.5	Experimentation Method	
		5.5.1 Heat Storage	
		5.5.2 Heat Withdrawal	10
6	Res	ults	41
	6.1	Heat Delivery	11
	6.2	Heat Extraction	
	6.3	Key Points of Interest	15
7	Fco	nomic case	17
•		Costs	
		Monetary Gains.	
		7.2.1 Best-Case Scenario	
		7.2.2 Worst-Case Scenario	
		7.2.3 Average User Scenario	
	7.3	Economic Discussion	
8	Con	clusions and Recommendations	51
0	_	Conclusions	
		Recommendations	
Α	Sup	plementary Data	53
В	Man	ufacturing process	55
		Tubes	55
	B.2	Fins	55
	B.3	Pressing	57
	B.4	Container	31
	B.5	Thermocouple T-junctions	31
С	Mea	surements	35

List of Figures

1.1	Schematic dedication of the Quooker system	2
2.1	Vapor Compression Cycle. A shows the 4 stages of the cycle. B shows a Temperature entropy diagram of a typical vapour compression cycle [19]	6
2.3	Conventional vapour compression cycle (a) and a transcritical vapour compression cycle (b) [29]	10
2.4	Simplified diagram of the Peltier effect. Current flows through an N-type semiconductor pulling heat from the cooling side to the sink. The current flows through the cooling side into the P-type, where heat is again pulled from the cooling side to the sink [26]	11
2.5	Basic Absorption cycle [9]	12
2.6	Basic Ejector cycle [43]	13
2.7	Stirling refrigeration cycle [36]	13
2.8	Specific heat capacity and Thermal conductivity as a function of density for sensible heat materials. [17]	14
2.9	Cross sections of possible PCM configurations. The left image shows a compact tube in a tube. The Center image shows a packed bed of encapsulated PCM. The right image shows encapsulated cylinders.	16
3.1	Depiction of the vapour compression system. A backup condenser is implemented to make sure cooling capacity is always ensured. Work is applied in the compressor. In the evaporator, heat is absorbed. Heat is rejected into the primary condenser until it is full and will overflow into condenser	23 24
4.1	Schematic depiction of the modelled area	26
4.2	Partial enthalpy distribution of the PCM. Supplier data has been fitted with equation 4.4.	27
4.3 4.4	Diagram of Heat transfer through an interface node	28
	followed by PCM nodes. On the right-hand side, the furthest is the tube followed by an interface node.	28
4.5	Energy extraction per unit area as a function of fin thickness.	29
4.6	Energy extraction per unit area as a function of fin distance	30
4.7	Height of the system given as a function of the achievable ΔT for different tube diameters.	31
4.8	Pressure drop in the condenser for different tube lengths	32
5.1	Test strips used to dimension the collars. The thicker fins were capable of producing higher collars before tearing. The thicker fins are less flexible	33
5.2	Single cooling fin	34
5.3	Tube arrangement on the heat transfer fin. Dimensions are in mm. The heat withdrawal stream is made up of the five tubes at the bottom, all separated by 25 mm. The 18 tubes at the top are for heat delivery. They are arranged in two sections with a triangular pitch	
	with a 25 mm separation. The three layers are separated by 15 mm from each other.	35
5.4	Schematic depiction of the experimental setup	37
5.7		38

x List of Figures

5.5	have the same length and are thus placed at varying heights within the system. The tap on the left is purely used as a safety release valve for the boiling water reservoirs 39
5.6	Image of the experimental setup where the heat exchanger is visible due to most of the PCM being molten
6.1 6.2 6.3	First test where hot water was sent through the storage system. 42 Energy flow into the system during the three heating tests. 42 Logarithmic plot showing the forward difference of the temperature at each point in time for the first heating test. A low-pass filter has been applied to the temperature change data to remove random noise. 43
6.4 6.5 6.6	Example of a test where cold water was sent through the storage system
7.1	Graph showing the payback period of the system with an average user scenario 49
B.1	Tube bending process where the tube has been heated with a heat gun and subsequently bent into shape and placed in the mould to cool. The silicon tube with attached wire can be seen still present within the tubing
B.2	Left: The first iteration bending tube with a shorter handle and larger tube diameter. Right: The second iteration bending tube with a larger handle, increased chamfer, and a smaller diameter
B.3	Drawing of the first tube bending solution
B.4	Drawing of the mould for tube bending
B.5	Image of fins with pressed collars form optimal thermal contact
B.6	Image of the tool that was attached to the hydraulic press to press the fins over the tubes. 59
B.7	Drawing of the press-plate of the pressing tool
B.8	Drawing of the top plate of the pressing tool
	Drawing of the rods used in the pressing tool
	Drawing of the rack in which the tubes stand while pressing
	Drawing of the PCM container lid
	Image of a welded thermocouple t-junction
	Drawing of the short sides of the PCM container
B.13	Drawing of the long sides of the PCM container
B.14	Image of the glueing process of the PCM container
	Image of the PCM container leak test
	First heating measurement
	Second Heating measurement
	Third heating measurement
	First cooling measurement
	Second cooling measurement
	Third cooling measurement
	Heat transfer coefficients of the first heating measurement
	Heat transfer coefficients of the second heating measurement
	Heat transfer coefficients of the third heating measurement
	Heat transfer coefficients of the first cooling measurement
	Heat transfer coefficients of the second cooling measurement
	Heat transfer coefficients of the third cooling measurement
0.13	surement
C.14	Change in temperature per second at each thermocouple during the second heating measurement

List of Figures xi

C.15 Change in temperature per second at each thermocouple during the third heating mea-	
surement	73
C.16 Change in temperature per second at each thermocouple during the first cooling mea-	
surement	73
C.17 Change in temperature per second at each thermocouple during the second cooling	
measurement	74
C.18 Change in temperature per second at each thermocouple during the third cooling mea-	
surement	74

List of Tables

1.1	Design requirements of the product
2.1	Refrigerant properties of R600a [22]
2.2	Refrigerant properties of ammonia [23]
2.3	Refrigerant properties of CO ₂
2.4	Emerging refrigeration technologies [36]
3.1	Refrigeration method grading
3.2	PCM supplier data [30]
5.1	Diameters and centre distances of commercially available u-bends
7.1	System costs
_	
A.1	Thermocouple offsets

1

Introduction

Since the conception of the Quooker system in 1970, innovation and development have been central to the company. The product represents a radical change in consumer boiling water delivery from a time-consuming process to instant gratification. Further innovation has led to the addition of cooled drinking water as an extra option, and later the system added carbonated water to its capabilities. The product Quooker B.V. develops and sells is a household faucet capable of instant dispensing of chilled, carbonated, warm and boiling water.

Quooker was the first company to bring this product to market and has always strived to be a market leader. Innovation is critical to maintaining this competitive advantage. A key factor that has always been central to the product has been energy usage. While early models still had high energy demand, today's energy losses have been minimised to a standby loss of 10 W [25]. The continued lowering of the energy demand of the product is a crucial goal.

With the introduction of the refrigerated water dispenser to the product range, an opportunity arises to save more energy. One piece of equipment cools water with the removed heat thrown out. In the next piece of equipment, water is heated. Smartly integrating these systems can lead to a further decrease in energy demand. Lowering the energy demand of the product is multifaceted. It appeals to the consumer financially, and it also benefits the environment. Besides ensuring an innovative and competitive image, an integrated, more energy-efficient product will benefit all its users. A successful design will serve as the basis for future Quooker products.

1.1. Current Product

The Quooker system is built up of multiple elements. Figure 1.1 shows a schematic depiction of the system. The Quooker system has elements above the counter and below the sink. Above the counter, one or two faucets are present, depending on customer preference. The faucets, controlled by the user, dispense the water at different temperatures. These are boiling water, regular tap water ranging from hot to cold and further cooled water. The cooled water can also be dispensed with carbonation. Under the kitchen counter, one or two reservoirs are present. The primary reservoir is responsible for heating and storing water. From this point on, the primary reservoir will be called the Quooker. Water from the primary domestic water source flows into the Quooker, where a heating element at the bottom of the tank heats the water to 110 °C. This heating element has a capacity of 1600 W. The water is kept at a pressure of at least 1.2 bar to ensure it does not boil. A valve opens when a signal is sent from the faucet to the Quooker. The pressure causes the boiling water to be dispensed instantly. A specialised dispenser releases the pressure at the tap causing the water to boil on exit. A second reservoir can be purchased in addition to the first. This unit is called the Cube. The Cube cools the water using a vapour compression refrigeration cycle which can be seen in figure ??. This cycle operates at an evaporation temperature of 3 °C and a condensation temperature of 35 °C in normal operation. The cooling capacity is 140 W. In continuous operation, the coefficient of performance (COP) of the system is 3.6. The complete cycle can be seen in Appendix A. The Cube also possesses a carbon dioxide cylinder and a water filter. This reservoir can also be connected to the same faucet allowing the user to dispense cold and carbonated water.

2 1. Introduction



Figure 1.1: Schematic dedication of the Quooker system

1.2. Problem Description

Two areas can be looked at to improve the system's efficiency: the standby losses of the hot water reservoir and the heating and cooling efficiencies of the two systems. The standby losses in the current system have been minimised to 10 W. This has been achieved by the meticulous design of an insulated vacuum layer around the reservoir and by minimising contact surfaces. Therefore, minimising the standby losses is not an area where significant gains can still be made. The Quooker system warms its water using an electric heating element. This element is surrounded by water and thus nearly has 100% electrical efficiency. Improving this efficiency is also not reasonable. This thesis will look into the possibilities of reducing the total energy demand of the system. The current system involves two subsystems requiring energy as input, and both release heat to the surroundings. Due to the addition of the cooling system, more opportunities arise to save energy. Equations 1.1 and 1.2 show an energy balance of the current system:

$$W_{in,Q} = Q_{out,Q} \tag{1.1}$$

$$W_{in,C}(COP + 1) = Q_{out,C}$$
(1.2)

with $W_{in,Q}$ as the electrical power input to the Quooker and $W_{in,C}$ as the mechanical work by the compressor in the cooling cycle. $Q_{out,Q}$ is the heat loss to the surroundings from the Quooker, and $Q_{out,C}$ is the heat lost to the surroundings by the cooling cycle primarily from the condenser. The COP of the cooling cycle is given by:

$$COP = \frac{Q_{cool}}{W_{comp}} \tag{1.3}$$

where Q_{cool} is the cooling capacity and W_{comp} is the compressor work.

Examining these equations makes it clear that there is potential for energy saving as both $Q_{out,Q}$ and $Q_{out,C}$ are unwanted byproducts with potential uses. A fully integrated system could lead to new areas of energy reduction. Reusing waste heat from the refrigeration cycle will require less input work in the boiler. Heat transfer solutions will need to be tailor-made to fit the system. It is not plausible or even possible for a user to simultaneously demand boiling and cold water. Combined solutions will, for that reason, require buffering or energy storage components. Usage profiles will need to be applied to the design choices to decide the optimal design.

1.3. Product Requirements

The design aims to be an improvement on the current design. For this reason, the final design will need to have the same capabilities as the current system with lower energy demand.

Requirement	Value
Boiling Water storage	3 L
Chilled water storage	2. 5L
Boiling water flow rate	3 L/min
Chilled water flow rate	2.4 L/min
Carbonated water flow rate	2 L/min
Heating capacity	1600 W
Cooling capacity	140 W
Cooling COP	3.6
Boiling water dispensing Temperature	100 °C
Chilled water dispensing Temperature	4-6 °C

Table 1.1: Design requirements of the product

1.3.1. Reservoir Temperatures

The temperatures in the reservoirs themselves are not necessarily fixed. The current system keeps the temperature of the boiling water reservoir between 108 °C and 110 °C. The temperature in the cold water reservoir is held between 4 °C and 7 °C. These storage temperatures are practical as no further heat transfer is required to make the water reach the desired dispensing temperatures.

1.3.2. External Requirements

Besides the primary requirements mentioned above, the product also has some external requirements. Firstly it needs to comply with all environmental regulations. Besides these regulations, Quooker tries to design its products to be future-proof. This means that borderline cases and any ethical dilemmas are avoided. A long lifespan is desirable. Current aims are at least ten years, with many products lasting 20 or more. Health and safety considerations also apply. Dangerous substances should be avoided or adequately dealt with to ensure safe product delivery. When dealing with water at warm temperatures, legionella needs to be considered.

1.4. Problem Definition

This thesis aims to design a system with a lower energy demand than the current system while retaining all the current system's capabilities. To achieve this goal, a few questions will need to be answered.

- What is the best refrigeration technique for this application?
- Which energy storage method should be utilised to bridge the gap between energy production and need?
- How should these technologies be implemented in an integrated design?

1.5. Motivation

The motivation for this project is threefold. First, the use of energy from fossil fuels has caused a significant increase in greenhouse gas emissions. Global warming and climate change caused by these emissions are some of society's biggest challenges. Global energy demand is rising, and the energy transition is not happening fast enough. Reducing energy demand is thus as critical as ever. Reducing the energy demand of the Quooker system decreases the total energy requirement for society's hot water needs. Not only does this thesis aim to benefit society on an energetic level, but it also aims to innovate and advance the state of understanding. The successful design of this product could inspire other products to implement similar systems to save more energy in similar manners. Finally, there is a

4 1. Introduction

commercial aspect as well. A product with lower energy demand is a better product and hence, more marketable. This can be profitable for Quooker and the customer who spends less on energy.

1.6. Structure

This study begins with a review of the current literature and available technologies. Selection criteria are set up based on the accrued information, at which point a selection is made on heat transfer method, energy storage method and general process design. The design requirements will be set based on the chosen technologies. Modelling will then determine variables from the design. This will lead to a prototype design which is manufactured and tested. These results will be analysed and will be used to set up an economic case for the product. Conclusions and recommendations will be drawn based on the model, the prototype and the economic case.

Background Information

This chapter will discuss the literature and available information relevant to the research. Due to the nature of the assignment, the scope of literature retrieval is broad. More in-depth information may be needed when further design choices are made. The chapter is split into four sections. The first section discusses different refrigeration techniques. Energy storage possibilities are examined in the second section. The third section looks into the usage of the product.

2.1. Refrigeration Technologies

Refrigeration is the thermodynamic process of removing energy from a lower-temperature source and delivering it to a higher-temperature sink. Often this involves removing heat from a body or fluid to keep it at a temperature lower than its surroundings. Net positive work is applied to the system to achieve this goal. The ratio of the heat removed from the source to work applied to the system is the COP. The ideal refrigeration cycle is the Carnot cycle. The Carnot cycle reversibly transfers energy and entropy from the source to the sink. In other words, the Carnot cycle is the refrigeration cycle with the maximum COP. Actual refrigeration cycles will not achieve this efficiency level as the heat transfer between the refrigerant and the source and sink will not be reversible. A significant temperature delta is required to achieve significant heat transfer. This irreversible process causes reduced COP. There are multiple techniques to achieve this effect. The technique with the best COPs among existing refrigeration technologies is vapour compression [21].

2.1.1. Vapour Compression

Vapour Compression is the most mature refrigeration technology [8]. Ever since chlorofluorocarbons (CFC) and hydrochlorofluorocarbons (HCFC) were discovered to have efficient refrigerant properties, vapour compression has been the dominant source of cooling technology. A vapour compression refrigeration cycle consists of 4 steps:

- The refrigerant passes through the evaporator. The heat from the volume to be cooled causes the refrigerant to evaporate. The energy that passes through the heat exchanger here is the refrigeration capacity \dot{Q}_{in} .
- The refrigerant leaves the evaporator as a gas and enters the compressor, where it is compressed to higher pressures and temperatures. The compressor work is *W*.
- The refrigerant then passes through the condenser, where the gas condenses and releases its heat to the surroundings. \dot{Q}_{out} denotes the energy released.
- The refrigerant enters the expansion valve releasing the pressure to meet the evaporator pressure.

Figure 2.1 shows a schematic diagram of the steps and a temperature-entropy diagram of a typical cycle. The only power input to the system is the compressor. Thus the COP of the system is $\frac{\dot{Q}_{in}}{W}$. Vapour compressors fall into three different categories:

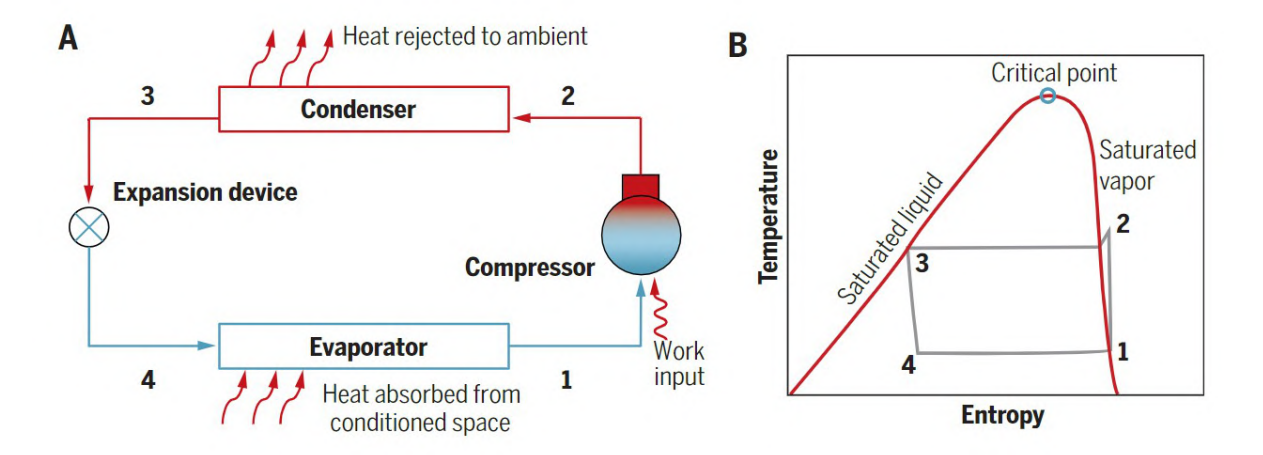


Figure 2.1: Vapor Compression Cycle. A shows the 4 stages of the cycle. B shows a Temperature entropy diagram of a typical vapour compression cycle [19].

- Reciprocating compressors
- · Rotary compressors
- · Kinematic compressors

An example of a reciprocating compressor is a bike pump. Rotary compressors increase the pressure by continuously decreasing the volume of cavities. Kinematic compressors apply kinetic energy to the gas. The kinetic energy is then converted to pressure.

Condenser selection

The condenser plays a vital role in transferring waste heat to the storage medium or the drinking water itself. The method of Sinnott and Towler details the condenser design method [38]. There are four categories of Shell and tube condensers:

- · Horizontal, with condensation in the shell and the cooling medium in the tubes
- Horizontal, with condensation in the tubes
- · Vertical, with condensation in the shell
- · Vertical, with condensation in the tubes

The most commonly used types are vertical tube-side condensation and horizontal shell-side condensation. A horizontal system with condensation in the tubes is not commonly utilised. This arrangement is used for heaters and vaporisers using condensing steam as the heating method. Sinnot and Towler give equations describing the heat transfer coefficients of each arrangement. The heat transfer coefficient of condensation outside horizontal tubes is given by:

$$(h_c)_1 = 0.95k_L \left[\frac{\rho_L (\rho_L - \rho_v) g}{\mu_L \Gamma} \right]^{1/3}$$
 (2.1)

Where $(h_c)_1$ is the mean condensation film coefficient for a single tube, k_L is the thermal conductivity of the condensate, ρ_L is the density of the condensate, ρ_v is the vapour density, μ_L is the viscosity of

the condensate, g is the gravitational acceleration, and Γ is the condensate flow per unit length of tube [38]. For condensation inside and outside vertical tubes, the condensation coefficient is given by:

$$(h_c)_v = 0.926k_L \left[\frac{\rho_L (\rho_L - \rho_v) g}{\mu_L \Gamma_v} \right]^{1/3}$$
 (2.2)

where $\Gamma_{\!\scriptscriptstyle \mathcal{V}}$ is the vertical tube loading [38]. This vertical tube loading is given by :

$$\Gamma_v = \frac{W_c}{N_r \pi d_o}$$
 or $\frac{W_c}{N_t \pi d_i}$ (2.3)

where W_c is the total condensate flow, N_t is the number of tubes and d_o and d_i are the outer and inner diameter respectively [38]. Equation 2.2 only applies when the Reynolds number is 30 or below. The Reynolds number in the condensate film is given by:

$$Re_{c} = \frac{4\Gamma_{v}}{\mu_{L}} \tag{2.4}$$

When Reynolds numbers exceed 30, waves form in the condensate, causing the heat transfer coefficient to increase. Equation 2.2 is thus still valid as a conservative, safe estimate. Condensation inside a horizontal tube depends heavily on the flow that is present. During condensation, the flow will vary from a single-phase vapour flow at the inlet to a single-phase liquid flow at the outlet. The coefficient for a condensing flow in a horizontal tube can be estimated using two equations. Equation 2.5 is for a stratified flow. Equation 2.6 is for annular flow. The higher of the two values should be used for the condensing flow coefficient.

$$(h_c)_s = 0.76k_L \left[\frac{\rho_L (\rho_L - \rho_v) g}{\mu_L \Gamma_k} \right]^{1/3}$$
 (2.5)

$$(h_c)_{RK} = h_t' \left[\frac{J_1^{L/2} + J_2^{1/2}}{2} \right]$$
 (2.6)

where

$$J = 1 + \left[\frac{\rho_L - \rho_V}{\rho_V} \right] x \tag{2.7}$$

for the inlet and outlet conditions. X is the vapour quality [38].

Superheating and subcooling

When the vapour enters the condenser above the condensation temperature, it is considered superheated, and when it is below the condensing temperature after leaving the condenser, it is considered subcooled. Figure 2.2 shows subcooling and superheating on an enthalpy-pressure chart for a typical refrigerant. The temperature profile may need to be split into two sections when dealing with superheating. The superheated vapour will condense onto the tubes if the tube wall temperature is below the dew point. If the superheat is less than 25% of the latent heat and the outlet coolant temperature is well below the vapour dew point, the desuperheating can be lumped with the latent heat. This condition allows the total heat transfer area to be calculated using the mean temperature difference based on saturation temperature and the film condensate heat transfer coefficient [38].

Refrigerant selection

An essential part of creating a vapour compression cycle is refrigeration selection. Multiple criteria must be considered when selecting a refrigerant, but they can all be placed in three categories: performance, safety and environmental impact [21]. Performance criteria include the required cooling or heating capacity, reliability and costs. Safety criteria usually involve decisions against toxic or flammable substances. Finally, environmental impact can be placed in two categories: global warming and ozone depletion.

First, the performance criteria are examined. The refrigerant choice depends on the temperatures of the cold and hot regions surrounding the evaporator and condenser. These temperatures determine the operating pressures in the evaporator and condenser. Large pressure differences are often

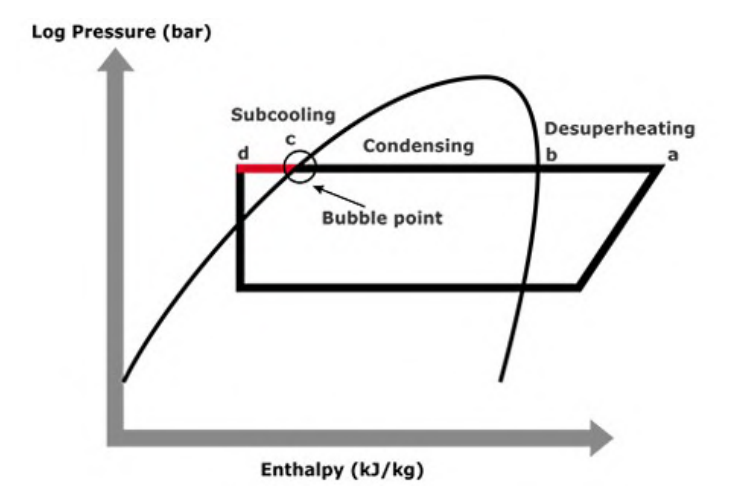


Figure 2.2: Superheating and subcooling on a pressure enthalpy diagram of a typical refrigerant [27].

undesirable, meaning the pressure-temperature relation of the medium in the desired range is of vital importance [21]. Another performance criterion is the chemical stability of the refrigerant. Higher chemical stability avoids depletion of the refrigerant and increases system lifetime. Practical performance criteria also apply, such as price and compatibility with materials [19].

The history of refrigerants is also very entangled with environmental effects. Before the 1930s, accidents associated with refrigerants were common due to the prevalent use of toxic and flammable refrigerants [12]. This led to the development of less hazardous synthetic refrigerants, namely CFCs and HCFCs. The refrigerants became widely used due to their highly stable structures. Towards the 1980s, it was discovered that refrigerants containing chlorines were harmful to the environment. The discovery of the damaging effects of CFCs on the ozone layer caused international bans on the use of these refrigerants. Refrigeration also accounts for 7.8% of the total greenhouse gas emissions. While a large part of this stems from the indirect emissions related to energy generation using fossil fuels, a significant portion also stems from the refrigerant itself [19]. All refrigerants are given a rating on these two environmental factors. The ozone depletion potential (ODP) and global warming potential (GWP). With all refrigerants with any ODP being banned, GWP became the leading metric. The GWP measures the climate impact of the refrigerant relative to carbon dioxide (CO₂). GWP values of refrigerants can range from 0 to above 20,000. Due to the high GWP of HCFCs, these are now being phased out worldwide [19]. These refrigerants are often replaced by natural refrigerants such as ammonia, CO₂ and hydrocarbons. These all have no ODP and low or no GWP. Only natural refrigerants will thus be considered here.

R600a

The current system implemented by Quooker to cool water uses R600a. R600a is the natural refrigerant, iso-butane. It has no ozone depletion and a low GWP of 3.3. It does come with the disadvantage of being flammable. This means that certain safety measures need to be taken. R600a is one of the most commonly used refrigerants in household refrigeration despite its flammability [10]. Table 2.1 shows the thermal properties of R600a. Next to the good thermal and environmental properties, iso-butane also has a low cost when implemented on a small scale. In large-scale implementations, flammability concerns raise the price, but the safety measures are still relatively cheap on a domestic scale [19]. Other hydrocarbons can also be used as refrigerants, and they will behave similarly to iso-butane with slightly different properties.

Ammonia

Ammonia is a refrigerant with very favourable thermodynamic properties. These can be seen in table 2.2. The cycle operates the same way as the isobutane cycle, meaning the heat rejection happens under the critical point using condensation. Due to the high enthalpy of vaporisation, ammonia has one of the highest refrigeration capacities per unit of mass. This makes ammonia an attractive choice. Other advantages are the environmental effects. Ammonia has no ODP or GWP. Ammonia is also

Table 2.1: Refrigerant properties of R600a [22]

Property	R600a
Formula	$C_4 H_{10}$
Molecular mass	58 g/mol
Ozone depletion potential	0
Global warming potential	3.3
Critical temperature	407.81 K
Critical pressure	3.63 MPa
Boiling point at 1 bar	261.4 K
Freezing point at 1 bar	113.73 K
Enthalpy of vaporisation at 273 K	355 kJ/kg

Table 2.2: Refrigerant properties of ammonia [23]

Property	Ammonia
Formula	NH ₃
Molecular mass	17 g/mol
Ozone depletion potential	0
Global warming potential	0
Critical temperature	405.5 K
Critical pressure	11.28 MPa
Boiling point at 1 bar	229.81 K
Freezing point at 1 bar	195.42 K
Enthalpy of vaporisation at 273 K	1263.2 kJ/kg

abundantly available, making the fluid cheap. There are three disadvantages to using ammonia as a refrigerant. Firstly, it is not compatible with copper, so copper pipes can not be used. Switching to steel installations causes higher prices. Secondly, ammonia is poisonous in high concentrations. Two factors lower this risk. Ammonia has a distinctive smell that is detectable at very low concentrations before these concentrations reach dangerous levels. Ammonia is also lighter than air. In the case of a leak, the ammonia will rise and disperse into the atmosphere. Thirdly, pure ammonia gas is highly toxic. This is the reason why domestic refrigerators do not use ammonia [24].

Trans-critical CO₂

 CO_2 is also a refrigerant returning to prevalence after CFCs were banned and HCFCs started getting limited. It is a natural refrigerant, and it has a comparatively low impact on the environment. It has no ozone depletion potential, and its global warming potential is one. It is also appealing when safety is considered as CO_2 is non-toxic and non-flammable, and non-corrosive. Economically it is also readily available and cheap, as it is a waste product in many industries. CO_2 is unique compared to other refrigerants as it has a low critical temperature. At 73.7 bar, CO_2 becomes supercritical at 31.1 °C [3]. A transcritical CO_2 cycle works slightly differently from a conventional vapour compression cycle. The difference is that the heat rejection occurs above the critical point of the CO_2 . There is no saturation condition at these conditions, and the pressure is independent of the temperature. In the transcritical cycle, a gas cooler replaces the role of the condenser in the conventional refrigeration cycle. The heat absorption still occurs similarly to a normal vapour compression cycle using an evaporator at low pressure [40]. Figure 2.3 shows the difference.

Table 2.3 shows the properties of CO_2 . One advantage of a CO_2 cycle is the use of sensible heat rejection by the gas cooler compared to the latent heat rejection in a condenser. This means that a large temperature difference can be addressed [3]. The major disadvantage of the transcritical system is the immense pressure difference that needs to be overcome to bring the CO_2 to the transcritical region. This requires an expensive compressor, and all surrounding parts need to be resistant to high pressures. Furthermore, increased regulations further raise the costs of CO_2 as a refrigerant.

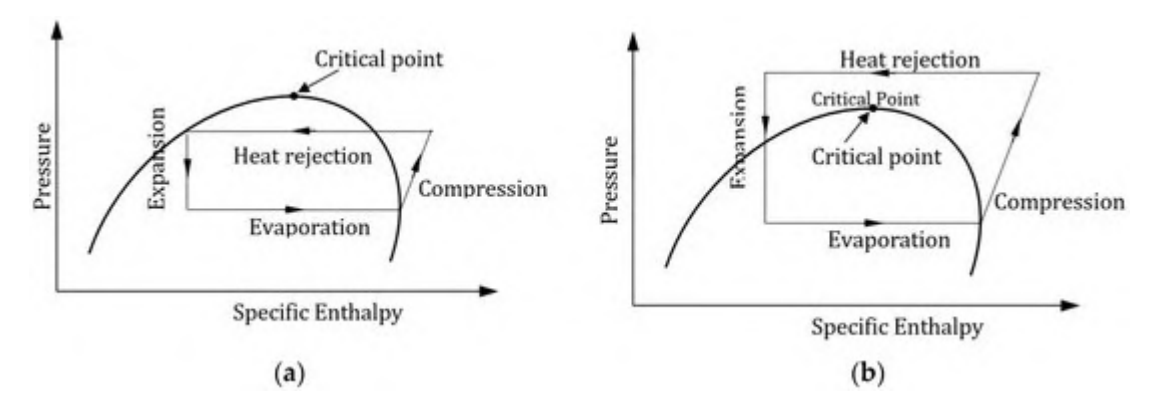


Figure 2.3: Conventional vapour compression cycle (a) and a transcritical vapour compression cycle (b) [29].

Table 2.3: Refrigerant properties of CO₂.

Property	Carbon Dioxide
Formula	CO ₂
Molecular mass (g/mol)	44
Ozone depletion potential	0
Global warming potential	1
Critical temperature (K)	304.1
Critical pressure (MPa)	7.37
Boiling point at 1 bar (K)	194,67

2.1.2. Thermoelectric

A thermoelectric cooler is based on the effect discovered by Peltier in 1834. Gurevich [13] defines the effect as "the absorption or evolution of heat (in addition to the Joule heat) at the junction between two conductors through which a dc electric current passes." This means that multiple thermocouples are connected electrically in series and thermally in parallel. The thermocouple, shown in figure 2.4, is made up of an n-type and p-type semiconductor. On one side, they are joined by a conductor. When the current flows, the electrons in the n-type semiconductor flow from the junction toward the bottom. Simultaneously, the positively charged holes in the p-type also flow towards the bottom. The energy to form these holes and electrons comes from the junction causing the junction to cool. On the other side, holes and electrons are recombined, releasing energy as heat.

This means that excellent conductors connect p and n-type doped semiconductors. A potential across the system drives current through the semiconductors and connectors. Conventional thermoelectric cooling devices consist of hundreds of pairs of semiconductors organised into grids, causing one side to be cooled and the other to be heated. Peltier elements can have certain advantages. They are highly reliable. They have no moving mechanical parts. They are small and lightweight. They also do not require any fluids. As a result, they benefit DC sources such as photovoltaics and fuel cells or dc sources in cars. The applications of Peltier cooling have been reviewed. When regarding high-performance electronic cooling applications, Peltier coolers are not appropriate. This is because thermoelectric materials do not have good enough COPs [34]. Thermoelectric coolers are essential for niche applications with limited cooling requirements, specifically under 25W, such as small coolers. They are also crucial for applications where the energy demand is not a critical issue(e.g., military applications) [28]. The performance of a thermoelectric household refrigerator is much lower than a conventional vapour compression refrigerator [4]. Disadvantages associated with thermoelectric cooling are often the cost and the low efficiency [42].

2.1.3. Alternative Cooling Methods

Many emerging cooling techniques are currently less commonly used. Tassou et al. [36] have reviewed the state of these technologies and their relevance to food refrigeration applications. Table 2.4 shows these technologies.

One of these techniques is absorption. The critical uniqueness of absorption is that it is heat-driven

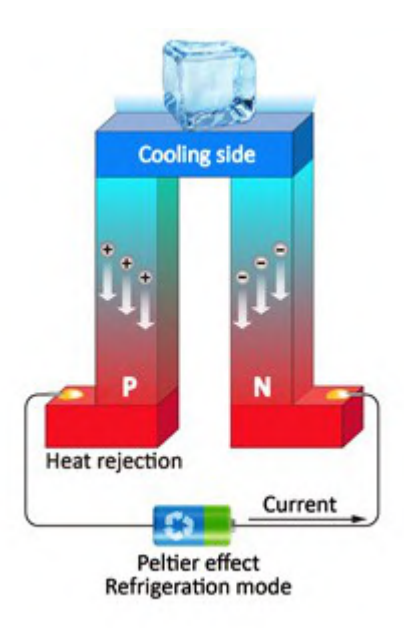


Figure 2.4: Simplified diagram of the Peltier effect. Current flows through an N-type semiconductor pulling heat from the cooling side to the sink. The current flows through the cooling side into the P-type, where heat is again pulled from the cooling side to the sink [26].

Table 2.4: Emerging refrigeration technologies [36].

Technology	State of Development	Cooling capacity of presently available or R&D systems	COP of presently available or R&D systems
Air cycle	Bespoke systems available	11 kW–700 kW	0.4–0.7
Sorption- Adsorption	Systems for refrigeration applications at R&D stage	35kW-MW	0.4-0.7
Ejector	Bespoke steam ejector systems available	kW to 50 MW	<0.3
Stirling	Small capacity 'Free' piston systems available. Larger systems at R&D stage	15-300 W	1-3
Thermoacoustic	R&D stage. Predicted commercialisation: 5–10 years.	<1 W	<1
Magnetic	R&D stage. Predicted commercialisation 10 plus years from now	<540 W	1.8

rather than work-driven, like vapour compression cycles. Figure 2.5 shows the absorption refrigeration cycle. Instead of the compressor, an absorber is used with a solution pump, a solution heat exchanger and a generator. The generator adds heat to the high-pressure solution made up of absorbent and refrigerant. This releases the refrigerant vapour that can be condensed and flashed to a lower pressure. The solution without refrigerant is sent back to the absorber through a heat exchange followed by a pressure release valve. The refrigerant at low pressure takes in heat which provides the refrigeration effect. The low-pressure refrigerant vapour then gets absorbed in the absorber, and the liquid is pumped to a higher pressure, where it enters the generator at a higher pressure. Heat is added here to repeat the cycle. Absorption cooling is generally preferential when a significant waste source of heat is available to be used in the generator. The economical range where absorption refrigerators are economical starts at a cooling capacity of 100 kW. Small absorption refrigerators are used in hotels or offices where compressor noise is highly undesirable. In these systems, the required heat is supplied by an electrical heater [7].

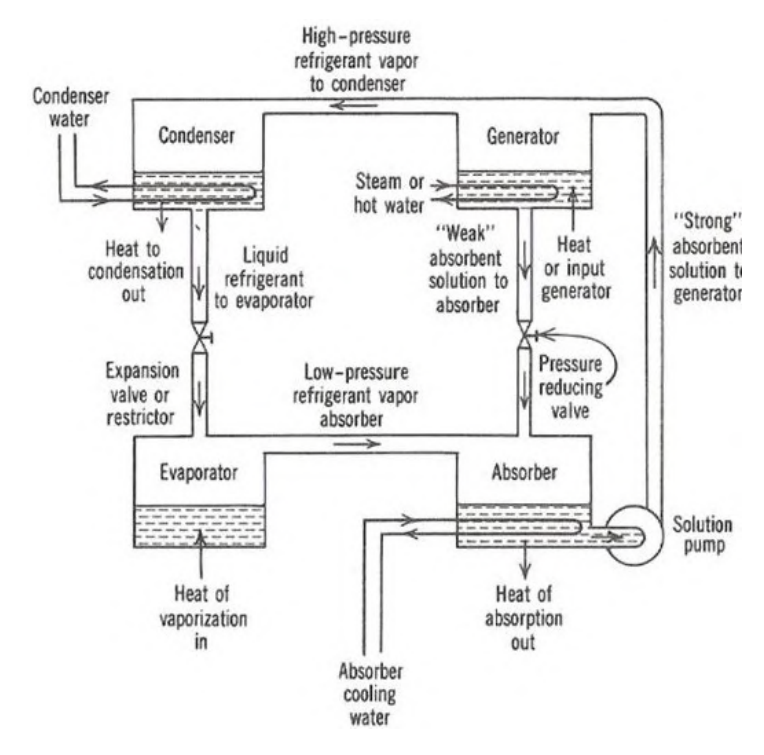


Figure 2.5: Basic Absorption cycle [9]

Air cycle systems are similar to vapour compression in that they involve compression and expansion. Refrigeration occurs by subjecting air to compression, cooling at constant pressure, and expansion to a lower temperature, which can be used to cool a medium. The difference to conventional vapour compression is the lack of phase change; thus, only sensible heat is used. Multi-stage compression with intercooling can be used to improve performance. Air cycles can achieve temperatures down to -100 °C but suffer from low COPs.

Ejector systems are thermally driven systems. Figure 2.6 shows the ejector cycle. The ejector system contains two loops. These are the refrigeration loop and the power loop. In the power loop, low-grade heat evaporates a high-pressure refrigerant. It then flows through the ejector nozzle, where it accelerates, reducing the pressure. This lower pressure pulls in vapour from the evaporator, which mixes, after which the pressure is recovered. The mixed fluid enters the condenser, where heat is rejected. Some of the fluid exiting the condenser is pumped to the boiler to completer the power cycle. The rest expands through an expansion valve to reach the evaporator, where the refrigeration occurs. This flows back into the ejector. The significant advantage of these systems is that they do not need moving parts. This makes them especially useful for waste heat sources or solar heat sources. The COPs of these systems are also relatively low.

Stirling engines use a free piston with a hot end space and a cold end space on either side of a displacer. The cycle begins with the piston moving in to compress the gas at the hot end, which causes heat rejection on the hot end. The displacer then moves the gas to the cold end. The piston then moves out, expanding the gas at the cold end and causing refrigeration. The displacer then moves the gas back to the warm end. While the COPs of Stirling engines are relatively high, they still can not compete with vapour compression cycles. As a result, the costs of Stirling engines are also higher.

Other systems exist that are in the early research & development stage. These systems operate on similar principles. A substance is heated using a unique property of this material, after which it rejects heat to the surroundings. The external effect is then removed. This further lowers the temperature to a point where it can cool another medium. Thermoacoustic cooling uses a working gas that heats up when it resonates with the sound waves. Magnetic cooling uses magnetocaloric fluids, which gain heat when a magnetic field is applied. Electrocaloric fluids work in the same way but then with an electric field. These systems still require development to improve efficiency or capacity.

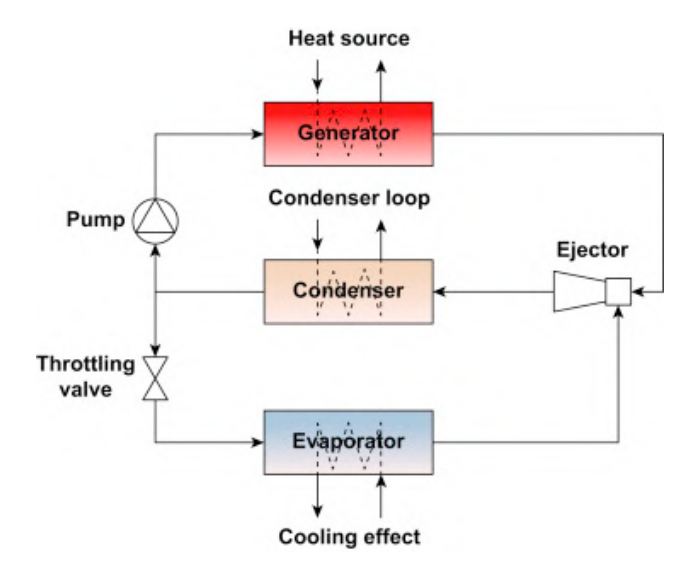


Figure 2.6: Basic Ejector cycle [43]

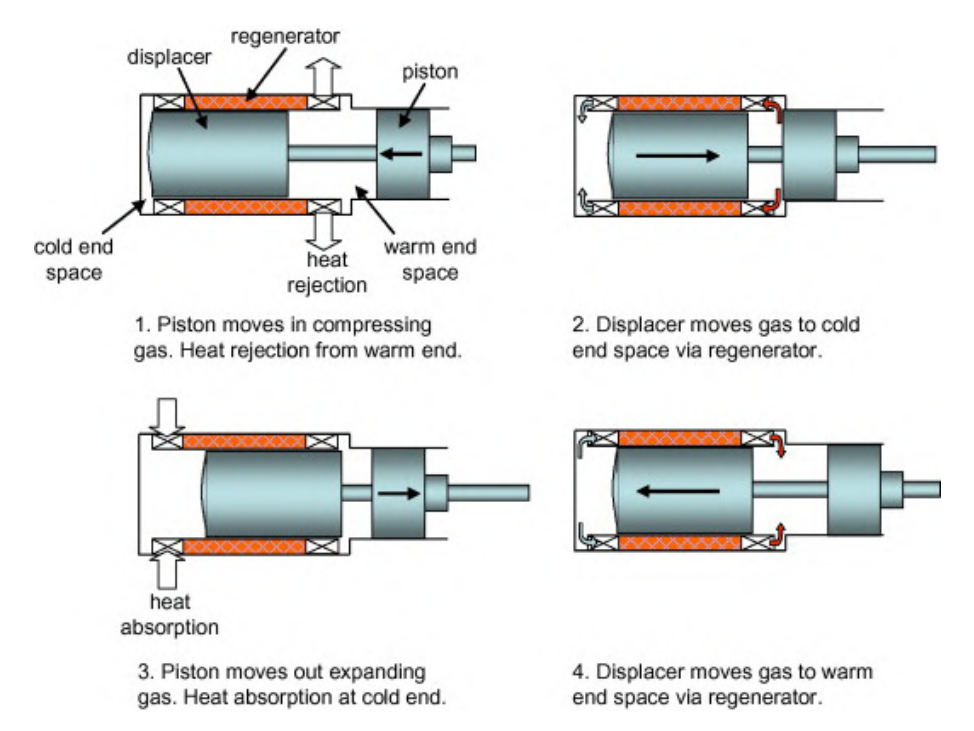


Figure 2.7: Stirling refrigeration cycle [36]

2.2. Energy Storage Methods

Because warm and cold water are not dispensed simultaneously in the Quooker system, energy will need to be stored somewhere in some shape or form. The usage scenarios will change the required energy storage. This section will look into different types of energy storage applicable to other systems. There are a multitude of energy storage techniques outside of thermal energy storage. These techniques can be placed in different categories. Mechanical storage techniques involve potential or kinetic energy storage, such as pumped hydro storage or flywheels. Electrical storage can be done using supercapacitors. Chemical storage is also possible using batteries or fuel cells [11]. The problem with all these techniques is that they involve conversion to other energy forms. The energy that is being dealt with in this project is all thermal. Losses always accompany conversion processes. For this reason, only thermal energy storage will be examined, which can be done in two methods: sensible heat and latent heat.

2.2.1. Sensible Heat Storage

Sensible heat storage stores energy in the temperature change of material. This material can be of any phase: solid, liquid or gas. The amount of energy that can be stored (Q) depends on the amount of material present, denoted by its mass (m), the specific heat capacity of the material (c_p) and the temperature change applied to the material (ΔT) .

$$Q = m \cdot c_p \cdot \Delta T \tag{2.8}$$

Water is a common sensible heat storage medium. Other materials, such as oils, molten salts, or liquid metals, can be used at higher temperatures. Sensible heating systems are very stable. Sensible heating materials are often low in cost. The main disadvantage of sensible heat storage, which is inherent to the storage mechanism, is the stability of the temperature during discharge. As the discharge process continues, the temperature difference between the storage medium and working fluid decreases gradually [16]. Another disadvantage is that compared to the latent heat capacity of materials, the specific heat capacity is up to 2 orders of magnitude smaller. This results in a lower energy density for sensible heat storage when the temperature differences are minor. Large temperature ranges can be implemented to counter this lower energy density [2].

Sensible Heat Storage Materials

The material choice is critical for a sensible heat storage system. Figure 2.8 shows the essential properties of sensible heat storage materials. A high energy density is crucial as less material is required to store the same amount of energy. High thermal conductivity is also preferential as heat can be stored in the medium more efficiently.

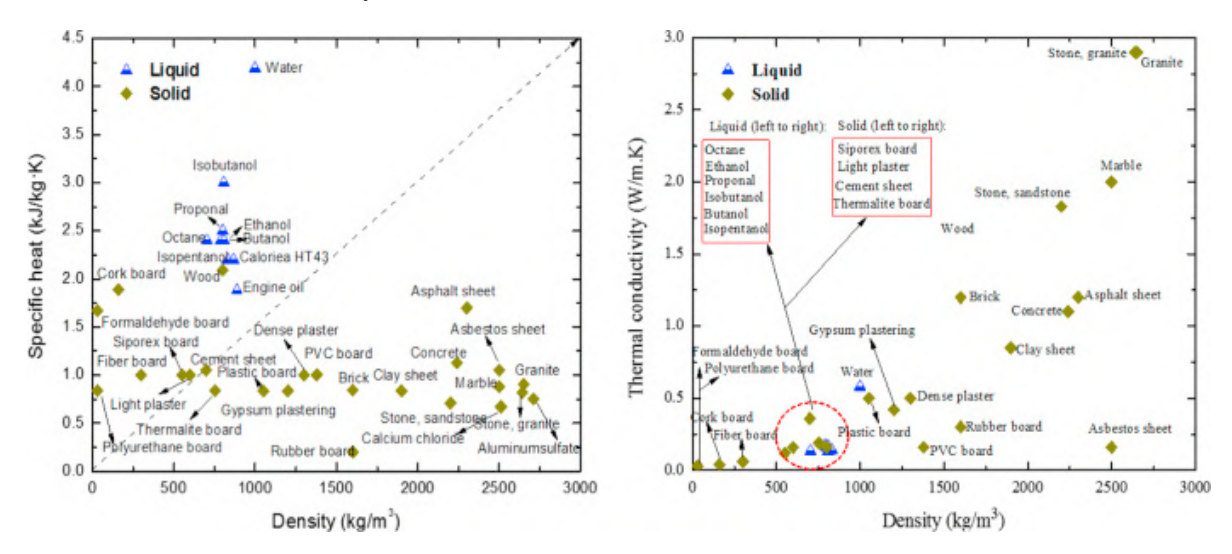


Figure 2.8: Specific heat capacity and Thermal conductivity as a function of density for sensible heat materials. [17].

Water is a common choice as it has a high specific heat capacity. Water can be used between 0 and 100 °C. It has a high specific heat capacity which makes it an attractive choice. Furthermore, water is abundant, relatively cheap and not dangerous or harmful [32]. It is also easily circulated. Depending on the situation, it can double as a heat transfer fluid and thermal energy storage medium. It is well suited for all domestic and food applications due to safety considerations. However, water does have some drawbacks. It is corrosive, which makes it unsuitable for some applications, and it can form a thermocline when liquid.

Thermal oils are another interesting material for sensible heat storage. These oils are organic fluids with good heat transfer properties. They are usually colourless liquids with higher boiling points than water. An example of an available temperature range of thermal oil is 12 °C to 400 °C. They also have low vapour pressures. Furthermore, they have low viscosity and good flow properties. However, they do suffer from poor thermal conductivity. Thermal oils, like water, can form a thermocline in a liquid state. Thermocline thermal energy storage systems typically have a packed bed of rocks or sand with the thermal oil acting as the heat transfer fluid. Due to the wide temperature range, thermal oils are not prone to freezing. Compared to water, they do have a lower specific heat capacity. They also have the

potential to degrade over time, especially when the temperature loading is severe. Finally, thermal oils can also be a fire risk as the vapours are flammable [2].

When the temperature range of thermal oils has been exceeded, molten salts become an interesting material. The preferred range for molten salts as heat transfer fluids or thermal energy storage is above 400 °C. The high temperature range is the main advantage of molten salts. They are also highly thermally stable. They are readily available and cheap. Safety-wise they are non-toxic and non-flammable. The temperature range starts above 200 °C, which can be a problem for many applications. Eutectics can be used to bring the melting point down. The heat transfer characteristics of molten salts are inferior but can be improved with certain additives.

Liquid metals can also be used to store energy. Some metals and alloys have low enough melting points close to ambient temperatures. Liquid metals are outstanding heat transfer fluids and thermal energy storage materials due to their low vapour pressure and low risk of freezing. They also have very high heat transfer. The problem is that they are costly. They are also prone to corrosion. The various metals that are used also have their issues. For example, sodium is a fire hazard, and lead-bismuth eutectic is toxic.

The earth materials are on the other side of the cost spectrum. Rocks, gravel and sand are cheap and readily available. There are also no health or safety issues associated with these materials. What sets these materials apart is that they can act as the heat transfer surface and the medium in one. This causes more efficient heat transfer and fewer costs associated with expensive heat exchangers. The thermal properties are dependent on the type of mineral. Some minerals, such as quartzite, have high thermal conductivity and heat capacity.

2.2.2. Latent Heat Storage

Latent energy storage uses the energy associated with changing the phase of a material. Commonly this is done between the solid and liquid phases, as these phases often have similar volumes. These materials are called phase change materials (PCM). Solid-solid phase changes are also possible, but these phase changes usually have low latent heat. Liquid-gas phase changes have the highest latent heats, but the associated change in volume brings too many problems [33]. The energy stored in latent heat is expressed with the following equation:

$$O = m \cdot L \tag{2.9}$$

where Q is the amount of energy stored, m is the mass, and L is the specific latent heat. PCM's are often split into two categories; Organics and Non-organics. Many organics are interesting phase change materials as they have their melting points at temperatures near ambient temperatures. They are also very chemically stable and easily found in nature. The disadvantages associated with organic phase change materials are low thermal conductivity and that they can decompose at high temperatures. Subcategories of these organic phase change materials include different kinds of paraffin, fatty acids and esters.

Inorganic phase change materials are other materials selected based on their phase transition temperature. Inorganics are often used in situations where organics are unavailable. An example of such a situation is high-temperature applications where organics would decompose. Typical materials include salts, salt eutectics, salt hydrates and metal alloys. Latent heat is 50-100 times denser than sensible heat. Therefore, using phase change materials is advantageous when making compact thermal energy storage systems. The output temperature of a PCM is constant, which is also a significant advantage. The main disadvantages of PCMs are their low thermal conductivities. Normal PCMS are all non-toxic, but organic PCMs are flammable.

PCM Systems

A latent heat system is built up of 3 main components:

- The PCM
- · The container of the PCM
- · Heat exchanger surface

The PCM should be selected based on the required temperature. The container is equally important as it needs to have the right characteristics. Depending on the requirements, a compact design can be chosen or an encapsulated design [31]. Figure 2.9 shows a few possible configurations involving these designs. The heat exchanger surface is important to consider as a limiting factor of latent heat storage systems is the thermal conductivity.

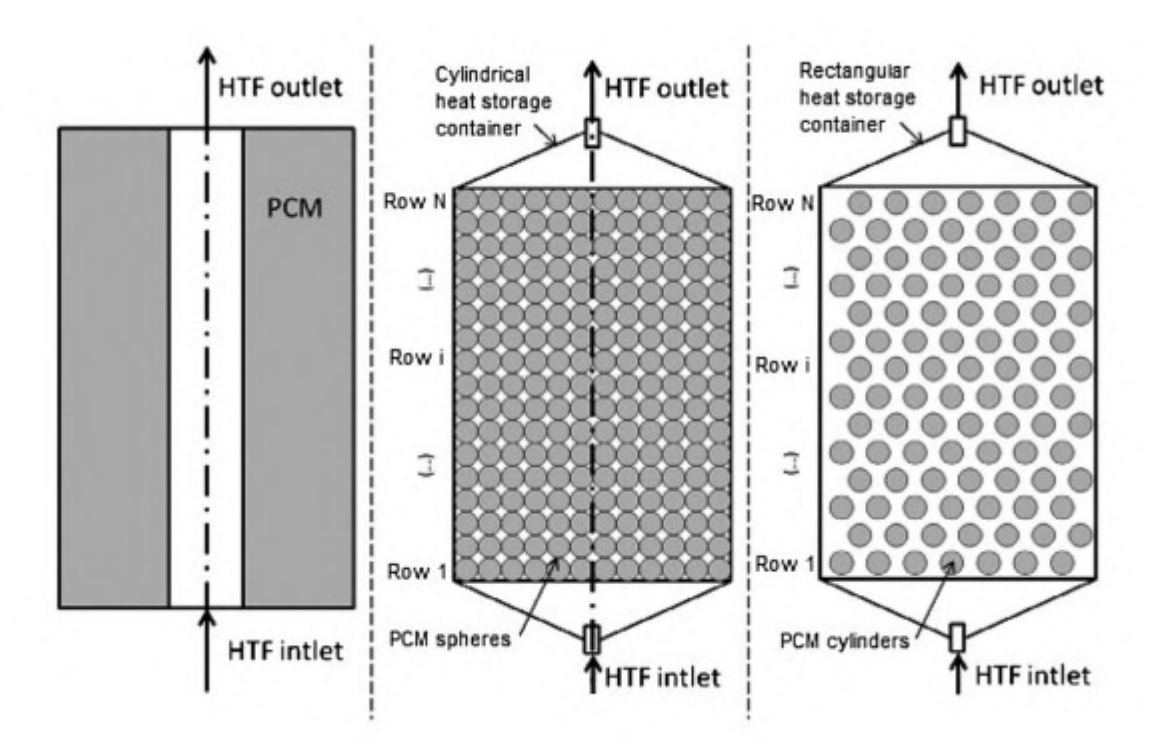


Figure 2.9: Cross sections of possible PCM configurations. The left image shows a compact tube in a tube. The Center image shows a packed bed of encapsulated PCM. The right image shows encapsulated cylinders.

Choosing a suitable PCM is critical for a successful latent heat storage system. The selection criteria can be put into three categories.

- · Thermo-physical properties
- · Chemical properties
- · Economic criteria

First of all, for a material to be a suitable PCM, it needs to have a high latent heat of fusion as this forms the basis for how much energy can be stored. Secondarily, thermal conductivity should be as high as possible to reduce reaction time. Chemically the materials should have limited super-cooling and long-term stability. Furthermore, all safety considerations should apply. Economic criteria should also be considered, such as cost and availability.

PCM Heat Transfer Enhancers

PCMs often struggle with low thermal conductivity. For this reason, latent storage systems often use different methods to enhance the thermal conductivity in the system:

- · Low-density materials
- Porous materials
- · Metal matrices
- · Encapsulation

2.3. Customer Demand 17

- · Extended surfaces and fins
- · Heat pipes
- · Cascaded storage
- · Direct heat transfer
- Scraping

One option for increasing conductivity is the addition of low-density materials. Conventional high thermal conducting materials such as metals often have a high density and thus do not mix well with many PCMs. An example would be using carbon fibres with high thermal conductivity. Porous materials with high thermal conductivity are also interesting as an additive. An example of this is a composite of paraffin and expanded graphite [15]. Adding metal matrices increases thermal conductivity. A matrix structure stops the metal from sinking to the bottom while conducting heat across the PCM. Metals with high thermal conductivity are the best options. Copper and aluminium are usually chosen as they are relatively cheap compared to other metals with high conductivity, such as gold or silver. Encapsulation can also be used to increase heat transfer into the PCM. The PCM is then placed in small capsules surrounded by the heat transfer fluid. Depending on the size of the capsules, the technique is called macro- (1-10 mm), micro- (1-1000 μm), or nano-encapsulation ($< 1 \mu m$). Fins or extended surfaces are among the most common systems to increase heat transfer. Heat pipes can also be implemented to increase thermal conductivity. Cascaded storage works by implementing multiple PCMs with different melting temperatures. By lowering the temperature differences within the PCM, the PCM will maintain a more constant temperature during solidification and melting, thus improving effectivity. Finally, in some situations, direct contact between the heat transfer fluid and the PCM can be used to increase the heat transfer. Direct contact does come with other issues, such as mixing of the PCM and the heat transfer fluid, and that energy may be required to keep part of the PCM liquefied to allow flow. Another option to increase thermal conductivity is scraping. The solidification process relies purely on heat conduction through the material to the heat sink. By scraping away the layer that has already solidified, new material is directly exposed to the heat sink. A downside of this system is that it is only applicable during solidification. A scraper would not be able to move through solid material during melting. Secondly, scraping may cause damage to the heat transfer surface. Expensive coatings may be required to protect this surface. Costs are also associated with adding an additional scraping system [14]. All PCM enhancement techniques are a trade-off between the speed at which the heat is delivered and the decrease in storage capacity coming from the reduction in PCM mass [18].

The advantages of PCMs are twofold. First, the latent heat capacity is often significantly higher than sensible heat capacities in operable temperature ranges. This makes the energy density high. Secondly, the lack of temperature change is also a significant advantage associated with PCMs. Small volume changes are also important when it comes to implementing PCMs. This allows them to be utilised in confined spaces [1].

PCMs still struggle with a few disadvantages, such as incongruent melting, supercooling, low thermal conductivity and poor long-term stability. Many hydrated salts melt with decomposition, forming another salt and water. The salt has a lower density and will sink to the bottom. This means that on refreezing, only a tiny layer will recrystallise. This phase separation is irreversible and will thus continuously decrease the storage capacity. Subcooling is an issue in some systems that have problems crystallising. Nucleation only occurs at lower temperatures causing the initial heat discharge to be sensible rather than latent heat. Long-term stability of the PCMs and their containers have been a limiting factor in their development. The PCMs have poor stability, and corrosion often occurs between containers and PCM [41]. The major disadvantage surrounding PCMs is their thermal conductivity. In the solid PCM, the heat transfer is purely conductive. Due to the PCM's low thermal conductivity, the heat transfer rate is low [37]. Due to these issues, the industry still struggles with the development of a reliable and practical system [5].

2.3. Customer Demand

The customers demand profile is highly relevant to the design of the system. In a situation where the demand for boiling water is high and chilled water is low, refrigeration efficiency is less critical as the

waste heat has the potential to be reused. In a situation where this is reversed, a very efficient cooling system is required. Time is also essential. When chilled water and boiling water are used quickly after one another, the reaction time of the heat transfer medium needs to be fast, but a small buffer may be enough. If the demands are at wildly different times, the buffer may need to be larger. With this in mind, the demand can be split into a few categories:

- · Average yearly demand of the different streams
- · Modal yearly demand of the different streams
- · Quantity demanded per batch
- · Average time between batches
- · Seasonal variation

The total amount of boiling water demanded by the client is known for all products returned to Quooker. A distribution of the average daily consumption of boiling water can be made using the data. The average usage of boiling water from these returned products is 6.3 litres per day. The modal usage is between 1 and 2.5 litres per day. The modal and mean usage differ significantly. While many users, such as families at home, use a few litres a day, the average skews heavily upwards due to high usage situations in offices or other communal spaces. The amount of warm water used can also be derived from the returned products. The average usage of warm water is 7.5 litres per day. The modal usage is significantly lower at 2.5 litres per day. The same factors as with the boiling water lead to a large discrepancy in the mean and modal usage.

Cold Water usage is currently unknown from returned products and will need to be estimated. To make this estimation, it is assumed that chilled water is only used for drinking. Any other domestic water usage for cooking or otherwise would not need to be cooled. An average person needs 2 L of water per day [20]. According to the ATUS, before the pandemic, an average non-institutionalised person spent 50% of waking hours at home [39]. Following this assumption, it is assumed that the average person drinks 1 litre of cold water per day at home. The average household size in the Netherlands is 2.14 [6]. This leads to a cold-water usage of 2.14 L per day.

The usage of cold and boiling water is a batch process. The quantity demanded per batch is important when considering the energy storage capacity. This type of data is not available. Different scenarios can be examined, ranging from emptying the whole reservoir in one go to pouring out many small quantities at fixed time intervals. The frequency will differ for the type of user, the situation, and the season. Most domestic users with a work schedule will see more intensive use in the evenings with longer breaks during the day and night. Systems, where people are present throughout the day, will see usage spread out more. Different frequencies will also need to be examined as this data is unavailable.

This knowledge of the demanded water can be used to size the equipment further in the design process. The amount of demanded boiling water gives a clear limit to the savings potential in the system. The total yearly energy demand of the system, ignoring standby losses, is around 70 kWh. Without additional cooling requirements due to cold water demand, the Cube produces 14 kJ every 20 minutes. This is a yearly loss of 105 kWh. This excludes extra heat generated from additional cooling due to cold water usage.

System Design

This chapter will discuss the steps that were taken to apply the background information to decide on crucial design choices. Furthermore, the required modelling and calculations will be laid out to make further detailed design decisions.

3.1. Refrigeration System Selection

The first system that needs to be defined is the refrigeration system, which forms the backbone of the product. It determines the rates at which heat is transferred, the temperatures at which the systems need to operate, and how heat transfer can occur. The selection of the refrigeration system will be made according to three criteria.

- · Efficiency
- Technology Readiness
- Cost

Efficiency of refrigeration systems is measured by the COP. It compares useful refrigeration heat to the input work. No heat recovery system is 100% efficient. By maximising the refrigeration system's efficiency, less heat is available to be recovered, but the total energy usage is even lower. Heat recovery is of more considerable importance when a low COP system is required, but as total efficiency is essential here, the higher COP systems are favourable. Technology readiness is also essential. The facilities and capabilities for implementing this system need to be available so the analysis can be carried out. Furthermore, the goal is to create a better product and sell it to clients. Time to market is thus also a factor of importance. If technological development is still lacking, many unforeseen issues can arise in developing the product. Cost is an important criterion. A simple calculation using the modal usage of 2 litres per day and a kWh price of €0.50 results in a yearly cost of €38, ignoring standby heating. Heavy users would also profit from a more expensive solution, but this solution will target the modal user. This price is very susceptible to shifts in energy prices. At the time of writing, the global energy supply is quite uncertain, so the available price range shifts significantly. Nevertheless, the order of magnitude of the calculation is still significant and does not leave much room for expensive solutions.

3.1.1. Refrigeration Technology Weighting

A weighting factor gives the relative importance of each criterion. Technology readiness is the most critical criterion as it determines the feasibility of the project and the time to market. Implementing a more established cooling technique will allow the focus of the research to be placed on the storage mechanism. Efficiency is the following most crucial criterion. As the design aims to create a system that is as efficient as possible, the cooling technique at the core of it should also be very efficient. Cost is the last criterion. While still significant, it is not as crucial as the other two in this process stage. This led to technology readiness receiving a weight of 3, COP a weight of 2 and cost a weight of 1.

20 3. System Design

3.1.2. Refrigeration Technology Selection

As mentioned in the previous section, there are multiple technologies available for cooling processes. Many of these methods are still in early research or development phases and thus will be omitted from this analysis. Instead, this analysis will examine vapour compression with a conventional refrigerant such as R600a, vapour compression with a new natural refrigerant, CO₂, and thermoelectric cooling. While Ammonia is also interesting as a refrigerant, the application of small-scale household refrigeration is not suitable for this refrigerant. These three technologies are ranked in the metrics named above, with the best technology receiving a 3 and the worst receiving a 1.

Ranking the technologies on efficiency, cost, and technology readiness, yields the results in table 3.1. The vapour compression system with CO_2 is listed as the most efficient. A cooling system with CO_2 as refrigerant can be designed where the heat rejection happens at a significantly higher temperature. This would allow much more efficient storage or preheating possibilities. Thermoelectric coolers have a very low COP compared to vapour compression with a conventional refrigerant. Vapour compression using R600a is also the most readily available. Thermoelectric coolers are also readily available, but the applications are different. Vapour compression systems using CO_2 are only available at very large scales and thus are not readily available for this application. Currently, the costs associated with CO_2 systems at small scales are very high. The high pressure requirements of the system will bring high costs for all surrounding equipment. The most conventional technology is also the cheapest, as economies of scale have driven the prices down for the components.

Technology	Efficiency	Technology Readiness	Cost	Score
Vapor compression using R600a	2	3	3	16
Vapor compression using CO ₂	3	1	1	10
Thermoelectric	1	3	2	10

Table 3.1: Refrigeration method grading

Table 3.1 shows that vapour compression with R600a is currently the best option. Further technological development in the field of CO₂ vapour compression could bring the price down along with the applicability to small-scale applications. Still, in its current state, it is not yet suitable.

3.2. Storage Method Selection

The choice between energy storage methods is made between two techniques: sensible heat storage and latent heat storage. All other types of energy storage would require energy transfer from one mode to another, bringing intrinsic inefficiencies. Sensible and latent heat storage both come in many forms.

3.2.1. Sensible Heat Storage

The most practical application of sensible heat storage in the required application would be using water as a storage medium. This would be the same water that would eventually flow into the boiling water reservoir and thus ultimately be consumed by the user. The advantage of this method is that there is no intermediate storage medium. This increases the systems' responsiveness as there is one less step in the heat transfer. Sensible heat storage is also more prevalent and widely used. Heat storage in water is widespread as it has a high specific heat capacity and good heat transfer. Disadvantages of this system include the fact that all surfaces must be approved for food and drink usage. Without an intermediate medium, the water directly comes into contact with all the systems parts. Another disadvantage is the capacity. By using the medium that requires heating as the storage medium, the volume of medium that can be preheated is limited by the volume that is available for the storage medium as its the same medium. The storage volume is limited by the energy density of the medium.

3.2.2. Latent Heat Storage

Latent heat storage is an attractive solution as it has a significant advantage compared to sensible heat storage. The energy density is much higher. This means a larger volume of water can be heated with a smaller storage volume. However, a latent heat system does bring additional complexity. First of all, the introduction of an intermediate adds a layer of complexity. Heat transfer must occur from the source to the storage medium and then to the water rather than travelling directly. This could mean additional components or design restrictions. Another layer of complexity associated with latent heat systems is

the heat transfer rate. Most latent heat mediums have low heat conductivity, causing these systems' responsiveness to be very low. Typical applications for latent heat systems use hours and days as an order of magnitude (for example, storage for solar energy) rather than seconds or minutes [41].

3.2.3. Selection of Storage Technique

The choice of storage method in the current application is dictated by a single factor, namely capacity. Sensible heat storage systems cannot store enough energy at low temperature differences. Even with a high specific heat capacity medium such as water, the energy density is too low at minor temperature differences. This application requires energy storage at a scale where the product still fits within the size requirements. This application requires higher energy densities than what sensible heat storage can deliver. The product requirements limit the space. This makes latent heat storage the best option.

3.2.4. Storage Medium Selection

Choosing the suitable latent heat storage medium or PCM is vital as it dictates many design parameters. The temperature at which the heat is recovered is critical in deciding the material's phase change temperature. The heat rejection temperature of the current Quooker system is heavily dependent on the conditions the system finds itself in as well as the usage of the system. To simplify the analysis, this temperature will be taken to be a constant 40 °C. Materials which have a phase change in this temperature range are different kinds of paraffin, salt hydrates and eutectic salts. Different kinds of organic PCM, such as paraffin, are cost-effective and have a high heat capacity at the required temperature ranges. The inorganic PCMs can have a higher heat capacity but suffer from poor thermal stability, corrosion and decomposition, which makes them complex to work with [1]. For these reasons, paraffin is the best option. The phase change temperature should be slightly lower than the heat rejection temperature of the cooling cycle. This maximises the potential gain from the storage. The total phase change range should be available for storage. If the PCM temperature is too close to the heat delivery temperature, the heat transfer rate will be too low, and the complete phase change will not be utilised during water withdrawal. On the other hand, if the phase change temperature is too low, a large portion of the heat will be delivered at a lower temperature to the water. This decreases the efficiency of the total system. Commercially available materials were compared, and a PCM was chosen based on the heat capacity and temperature. The chosen PCM is the RT35HC by Rubitherm. Its properties are shown in table 3.2. The heat storage capacity from the supplier is given as a combination of latent

Property	Value
Melting area	34-36°C
Congealing area	36-34°C
Heat storage capacity ±7.5%	230 kJ/kg
Specific heat capacity	$2 \text{ kJ kg}^{-1} \text{ K}^{-1}$
Density at 25°C	880 kg m^{-3}
Density at 40°C	770 kg m^{-3}
Thermal conductivity	$0.2~{\rm W}~{\rm m}^{-1}~{\rm K}^{-1}$
Volumetric expansion	12%
Flash Point	177°C
Maximum operating temperature	70°C
Price	7 €/kg

Table 3.2: PCM supplier data [30]

and sensible heat in the temperature range between 27 °C and 42 °C. Using the given specific heat capacity; the latent heat capacity can be calculated. This becomes 210 kJ/kg. Critical information from the supplier data is that phase change also brings a volumetric expansion, and the heat conductivity is extremely low. The volumetric expansion will require additional design requirements. The low heat conductivity can be amended using additives.

3.2.5. Heat Transfer Enhancement Selection

As the conductivity of the PCM is low, heat transfer enhancers are necessary. Many solutions exist that can solve this problem. First of all, there are different types of inserts that can be added to or placed

22 3. System Design

in the PCM. One example is adding expanded graphite in suspension to the PCM. This increases the heat conductivity throughout the material [15]. The problem with this solution is the workability and manufacturability. It is challenging to achieve effective suspension of the carbon throughout the PCM. The increased heat transfer would likely not be sufficient enough to disperse the heat throughout the PCM quickly.

Another heat transfer enhancer that was considered was the use of a porous or low-density material through which the PCM could be poured. This option is attractive as it can significantly increase heat transfer through systems depending on the materials used. The problem with this solution is that manufacturing these heat transfer enhancers to specification is complex and expensive. From a cost perspective, these solutions were ruled out. Direct contact between the heat transfer medium and PCM is not an option in the system being designed. Drinking water requirements would not allow the mixing of fluids due to health and safety considerations.

Encapsulation is often used in these situations to retain the advantages of direct contact but separate the materials. Unfortunately, encapsulation would not function optimally in this application as it would require heat delivery and heat extraction streams to run through the same volumes. This is not optimal for the vapour compression cycle as the fluids could mix. Health and safety regulations would also apply on the drinking water side. Additionally, this would require additional levels of control for the refrigeration cycle, where it would need to shut off as soon as the user starts withdrawing boiling water from the system. For these reasons, encapsulation is not suitable either. This leaves one of the more conventional options, namely heating fins. Fins can be used to transport heat from the tubes carrying the heat transfer fluid to the PCM and back from the PCM to the drinking water. A material with a high heat conductivity will need to be selected, and the dimensions will need to be optimised. Their thickness and spacing will determine the effectivity of the fins.

3.3. Product Configuration

A schematic depiction of the product is shown in figure 3.1. The system design will consist of a vapour compression cycle that cools the cold water reservoir. The heat recovered from this system when the compressor runs will be sent through a finned heat exchanger, transporting the heat to the PCM. When the user demands boiling water, water from the mains line will run through a different channel in the finned heat exchanger and pull heat from the PCM causing the water to be preheated before arriving in the boiling water reservoir. The cycle will contain a second ordinary condenser to ensure cooling capacity when the buffer is full.

3.3.1. Prototype Requirements

This design configuration has requirements and demands that must be met further in the design process. In short, they are detailed below:

- 120 mm width
- 300 mm depth
- · Minimal height
- · Maximum heat transfer to a 3L/min flow
- Leak tight
- Sanitary conditions, i.e. separation between drinking water and possible contaminants
- Ability to allow volumetric expansion of the PCM
- High thermal storage capacity
- Ability to fully condense the refrigerant at low temperature differences
- · Good thermal contact between tubes and fins

The configuration of the product is based on manufacturing, safety, and product-related decisions. Specific design parameters are fixed due to the application. The system's width should be at most 120

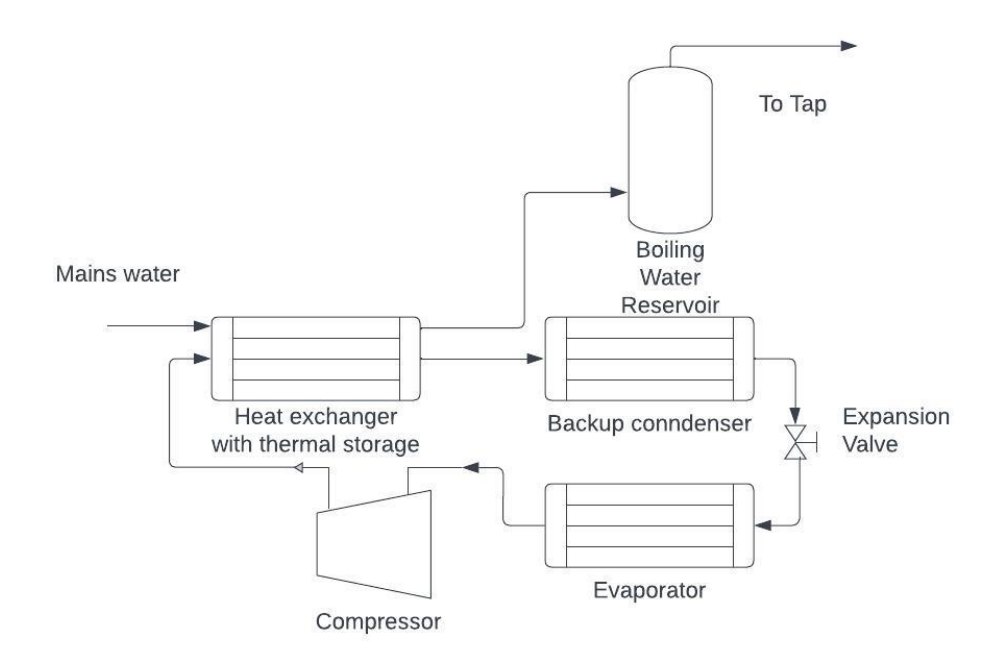


Figure 3.1: Depiction of the vapour compression system. A backup condenser is implemented to make sure cooling capacity is always ensured. Work is applied in the compressor. In the evaporator, heat is absorbed. Heat is rejected into the primary condenser until it is full and will overflow into condenser.

mm to fit inside the current product line. The depth of the product is also limited to 300 mm. The free dimension is the height. This will be optimised towards the minimum. The tubes should be designed so that optimum heat transfer occurs when a flow of 3L per minute of water is run through the system. Safety considerations regarding leak-tightness and separation of water and potential contaminants are essential and will be handled by the design phase. The expansion of the PCM during phase change needs to be considered. The volumetric expansion of the PCM amounts to 12% during melting. The reservoir should thus contain enough space for the PCM in the molten state. This means that once the PCM settles in a solidified state, it will have room for expansion above it due to gravity. A high capacity is desirable as it increases the number of demand profiles that can be encompassed by the design. The higher the capacity, the longer a user can add heat to the system before making use of the heat. A user with very intermittent demands would thus prefer a system with a larger capacity. Due to almost all the system's energy being stored in latent heat at the PCM temperature, a user with regular use should not notice the slight decrease in responsiveness due to the increased capacity. The design should also be made so that full condensation takes place at a low as possible temperature difference. This ensures that the most significant amount of heat is sent into the system and is not wasted. It is thus desirable to have a large condensation surface. The last requirement in the list is a sub-requirement to both heat transfer requirements, but it is nonetheless vital to focus on as it has a significant effect. Due to the fact that the design uses two separate parts for the fins and the tubes, the thermal contact between the two is of utmost importance. A poor connection between these two parts would cause a significantly increased thermal resistance rendering the fins almost useless. The fins will be identical and perpendicular to the tubes for manufacturability reasons. The most common solution for heat exchangers with fins is to have tubes running in a longitudinal direction with U-bends at both ends to increase the distance travelled by the fluid. The fins are made up of plates with holes through which the tubes run. The PCM will then surround the tubes and fins.

3.3.2. Variables to be Determined Through Calculation and Modelling

This leads to the following requirements to be determined through calculation and modelling:

- · Drinking water tube length
- · Drinking water tube diameter

24 3. System Design

- · Condenser tube length
- · Condenser tube diameter
- · Fin thickness
- · Fin distance
- · Reservoir dimensions

Figure 3.2 shows a schematic depiction of some of the relevant parameters of the design concept. The length of the drinking-water tube needs to be of such a length and diameter that it attracts enough heat while the hot water reservoir is being filled. The flow rate is fixed by the complete product design and is thus non-negotiable. The condenser tube length and diameter must be designed so the compressor can give off its heat at an as small as possible temperature difference and pressure drop. The achievable temperature difference will be a trade-off against the PCM storage reservoir size, as longer tubes will be required to achieve smaller temperature differences. The fin thickness and fin spacing are critical as high thickness and low spacing will lead to increased heat transfer but decrease the volume of PCM available. A trade-off will need to be made between storage capacity and heat transfer rate. The reservoir dimensions are limited in depth and width, so the PCM volume and the available tube space will vary using height, determining the PCM volume and space for tubes.

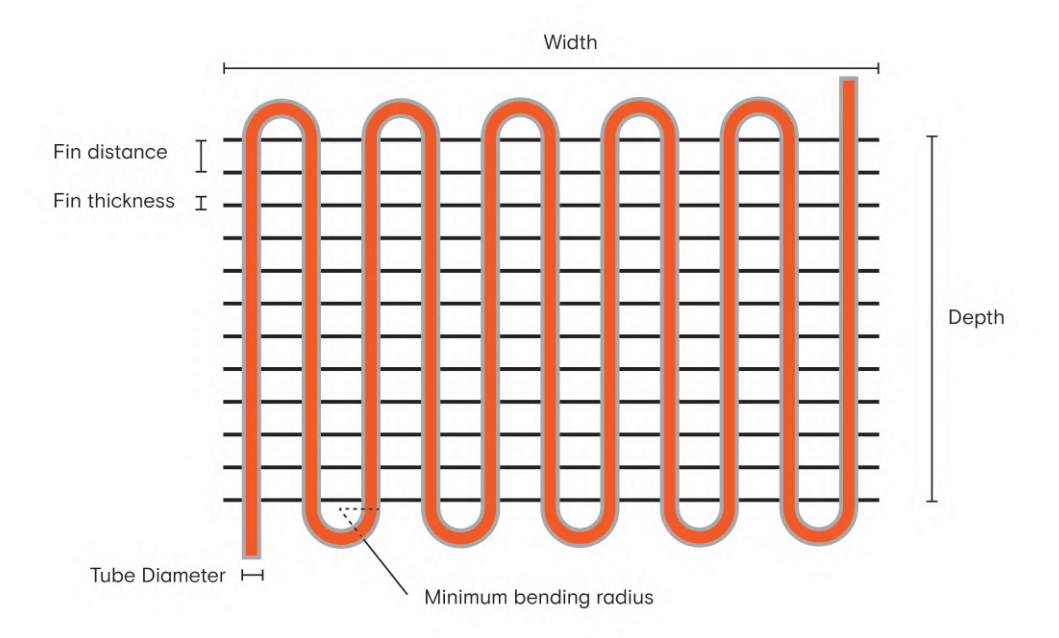


Figure 3.2: Schematic top-down depiction of the design concept showing the fins and tubes.

Modelling

This chapter details the modelling of the undefined variables from the previous chapter. The system will be modelled in three sections:

- The heat transfer to and from the tubes to the fins and PCM will be modelled using a 2D-finite difference system. This method will be outlined in section 4.1.
- The heat transfer from refrigerant to the system will be modelled using a condensation model for condensation inside horizontal tubes. This model is elaborated on in section 4.2.
- The heat transfer to the water from the PCM will be called the preheating side and will be calculated using known correlations in section 4.3.

4.1. Finite Difference Model

To adequately make design choices on the heat transfer on the PCM side, heat transfer models will be used to determine specific design parameters. The critical design parameters here are fin thickness and fin distance. The system will operate in two modes: the heating mode and the cooling mode. The model will need to accommodate both modes. To model this behaviour, a two-dimensional finite difference model is set up. The model only implements conductive heat transfer as the convective heat transfer is negligible in the solidification process. During the melting process, convective heat transfer plays a minor role, but this process is not the critical process as the buffer, in most cases, will receive excess heat compared to the amount of heat it delivers. A two-dimensional model will be used to make decisions on fin distance and fin thickness. While this approach potentially loses some information related to the third dimension around the tubes, it makes up for it in the model's simplicity and computation time.

Figure 4.1 shows a schematic depiction of the modelled area. The simulation contains three regions in two-dimensional space. The most significant part is comprised of the PCM and will be called the bulk. The second region is the conductive fin at the top of the model. The third region is the interface between the bulk and the fins. The tube wall will be modelled as a boundary condition which will be specified in section 4.1.2.

4.1.1. Bulk

The bulk simulations are made up of finite difference approximations for two-dimensional steady conduction. A mesh is generated to discretise space and time coordinates. Each node represents a control volume surrounding the node of size $\Delta x \cdot \Delta y \cdot 1$. Energy conservation is then applied to the volume element. As the system requires a transient solution, previous time steps are used to find values for the next time step. The explicit form is used. For the bulk Δx and Δy are the same. Therefore the simplified version below applies.

$$T_{m,n}^{i+1} = Fo(T_{m,n+1}^i + T_{m,n-1}^i + T_{m+1,n}^i + T_{m-1,n}^i) + (1 - 4Fo)T_{m,n}^i$$
(4.1)

26 4. Modelling

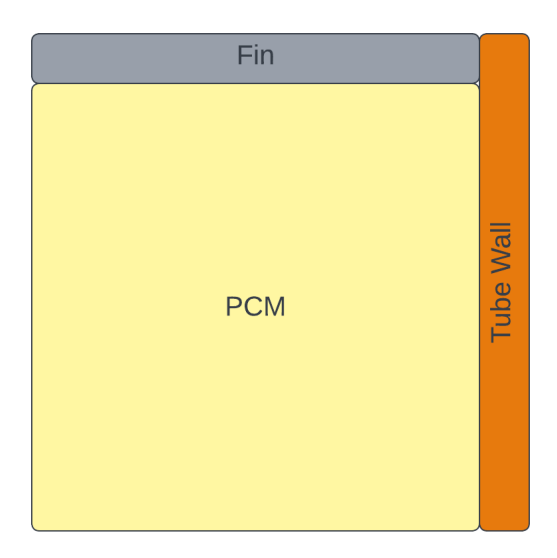


Figure 4.1: Schematic depiction of the modelled area

Here T gives the temperature at each location given by m and n and at each point in time given by i. Fo is the Fourier coefficient of the bulk material given by the following:

$$Fo = \frac{\alpha_{PCM}\Delta t}{\Delta x \Delta y} \tag{4.2}$$

where Δx and Δy are the horizontal and vertical between nodes respectively, Δt is the time-step for iteration and α_{PCM} is the thermal diffusivity of the PCM.

Equation 4.1 needs to be modified slightly for the heat transfer in the body of the fins.

$$T_{m,n}^{i+1} = \beta \Delta t \alpha_A \left(\frac{T_{m+1,n}^i - 2T_{m,n}^i + T_{m-1,n}^i}{\Delta x^2} + \frac{T_{m,n+1}^i - 2T_{m,n}^i + T_{m,n-1}^i}{\Delta y^2} \right) + T_{m,n}^i$$
 (4.3)

The fins have cells that are not square so the β function corrects for this. The alpha is also corrected to the values for aluminium. The aluminium has a constant α as it is not a function of temperature. The PCM, due to its phase change, does experience varying properties as a function of temperature. The chosen PCM is a blend of compounds to effectively achieve the required phase change temperature. This means the partial enthalpy distribution of the PCM is closer to a gaussian distribution than a single peak. Thus the partial enthalpy distribution was fitted to a gaussian distribution which includes temperature specific fourier coefficients. As the enthalpy is also dependent on whether the material is heating or cooling, two fits are made. They are both fitted to the following equation:

$$f(x_1, x_2, x_3, x_4, T) = x_1 + x_2 e^{-\frac{T - x_3^2}{x_4}}$$
(4.4)

The fit values for the melting fit are: 3.70, 114, 35.3, and 1.07. For the solidification fit they are 3.40, 99.6, 34.6, and 1.08. The model checks which state the system is in before choosing which fit to apply. These fits can be seen in figure 4.2.

The finite difference model has a stability condition for the time step that is based on the Fourier coefficient. In two dimensions, the Fourier coefficient must be less than 0.25 to ensure convergence when the mesh is square. The mesh in the fins is not square. As aluminium has a significantly higher heat conductivity rate, the required time step for stability is lower. To increase the simulation speed, this effect is counteracted. The node distance perpendicular to the fins is increased to increase the time step that converges. The node distance along the fin is still the same as in the PCM as the mesh is orthogonal. The converging time step is then calculated for both the bulk and the fins and the smaller time step is used.

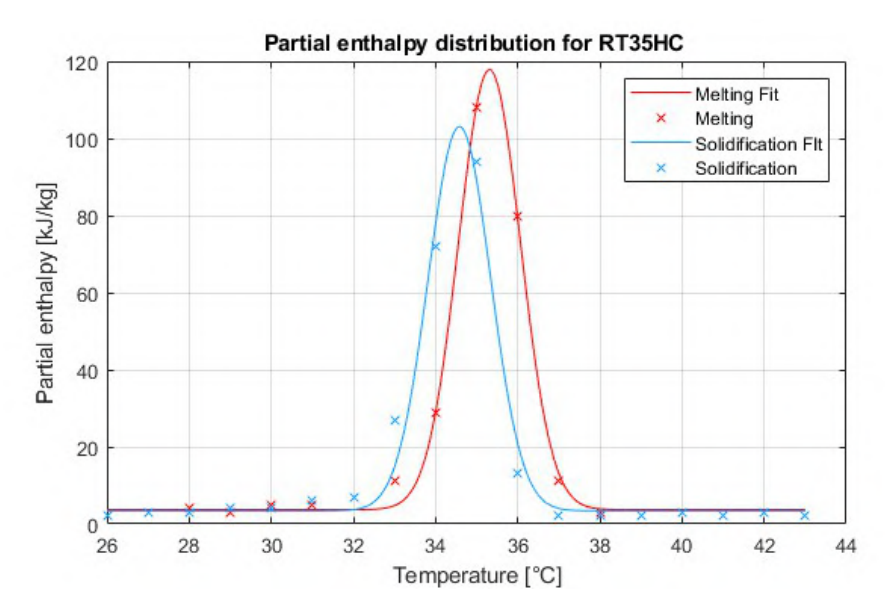


Figure 4.2: Partial enthalpy distribution of the PCM. Supplier data has been fitted with equation 4.4.

4.1.2. Boundary Conditions

The boundary conditions of the model are all unique. The model implements multiple axes of symmetry to simplify calculations. First of all, an axis of symmetry is placed through the centerline of the fins. This is based on the assumption that many fins will be placed after one another. The space behind the fin will be the same as in front. This boundary has no heat flux component in or out of the model. Secondly, another axis symmetry is placed at the plane equidistant to both fins. This is based on the same assumption in the other direction. The right side of the model correlates to a tube wall. The left side is another axis of symmetry.

To implement an axis of symmetry in the finite difference model, equations 4.1 and 4.3 can be used in their respective cases with slight modification. The non-existant terms are replaced by the term in the opposite direction due to the symmetry. For example in the case of the boundary condition on the left hand side $T_{m\,n-1}=T_{m,n+1}$.

4.1.3. Interface

The interface between PCM and fin needed to be correctly defined to calculate the heat transfer through the fins and then into the bulk. At the interface between the two materials, an interface node was defined where part of the control volume was aluminium and part was PCM. If a node on the top side of the model is taken as an example, the heat transfer in the positive y-direction is purely through aluminium. The heat transfer in the negative y-direction is purely through PCM, and the heat transfers in the x-direction are parallel heat transfers through PCM and Aluminium. The heat capacity of the node is directly proportional to the ratio between the volume of Aluminum and the volume of PCM. Figure 4.3 shows an example of an interface node at the top side of the model.

The tube side boundary is a Dirichlet boundary condition with the temperature set to either the condensation temperature of the condensing gas or the incoming water stream, depending on whether heating or cooling was being simulated. Figure 4.4 shows an example of a result from the model. This example depicts the output temperatures of the system after 10 seconds of cooling has been applied to the system. The depiction is not to scale as the top 3 nodes are spaced using the fin thickness. The top 3 nodes represent half the thickness of the fin. In this example, that is 0.15 mm. The lowest 20 nodes have a spacing related to the fin distance. In this case, the fin distance is 2 mm. The size of the interface node is dependent on both distances. This example shows a rapid heat transfer rate through the fin and a developing melting front away from the fin.

One of the valuable outputs of the model is the energy transfer into or out of the system per unit area and time. These values can be compared to determine the efficiency of the system. The system requires efficient heat transfer to and from the system without significantly compromising storage capacity. Another output of the system is the resulting temperature distribution after a certain period of

28 4. Modelling

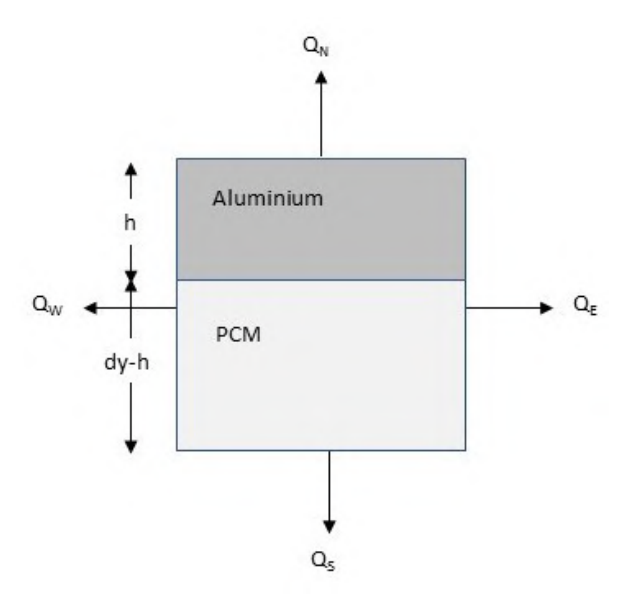


Figure 4.3: Diagram of Heat transfer through an interface node.

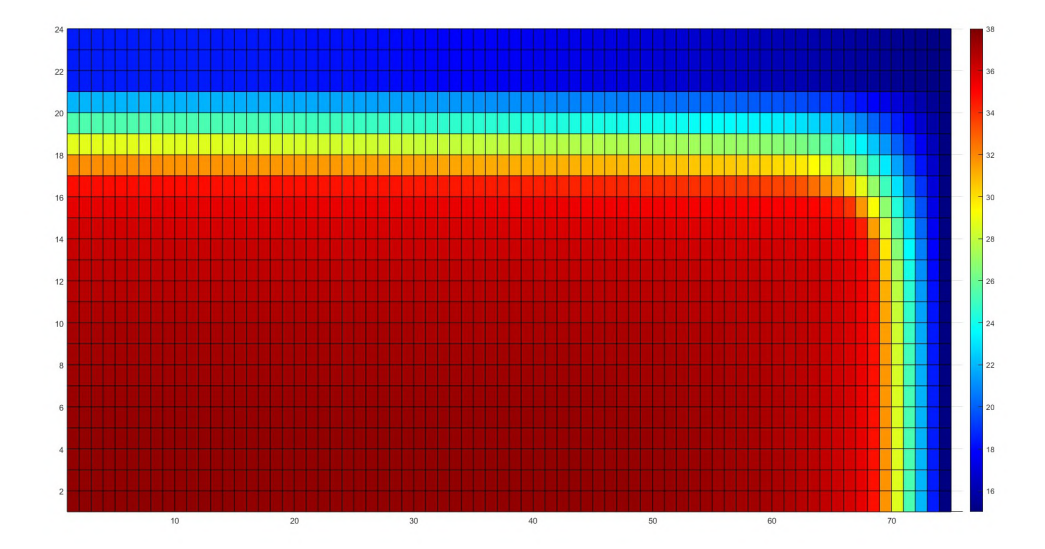


Figure 4.4: Finite difference model cooling from 38 °C. Fin separation is 2mm. The fin Thickness is 0.3 mm. The figure is not to scale as the fin node separation is significantly smaller than the PCM node separation. The top 3 nodes are fin nodes. The 4th is the interface node followed by PCM nodes. On the right-hand side, the furthest is the tube followed by an interface node.

heating or cooling. The model can then be used to change specific parameters and judge the effects on heat transfer to and from the system during heating and cooling. The parameters that will be varied here are fin distance and fin thickness.

4.1.4. Fin Thickness

In the mesh, the fin comprises three full nodes and part of the interface node. The thickness of the fin was thus adjusted by changing the distance between the nodes. As the fin thickness increases, the amount of heat transfer increases, but the total capacity of the system reduces as less space is available for PCM. It also decreases the area where the PCM is in direct contact with the tube.

The relation between the fin thickness and the amount of extracted energy is shown in figure 4.5. This simulation is run with a varying fin thickness from 0.2 mm to 0.7 mm. 0.2 mm is the minimum thickness that still maintains manufacturability. The PCM starts fully melted and the whole system

4.2. Condenser side 29

is at 38 °C. The tube side is set to 15 °C. As the figure shows, the energy released increases as the fin thickness reduces. This is due to the heat transfer being so much higher in the fins that a uniform temperature is achieved very quickly. The limiting factor in fin thickness design is thus the manufacturability.

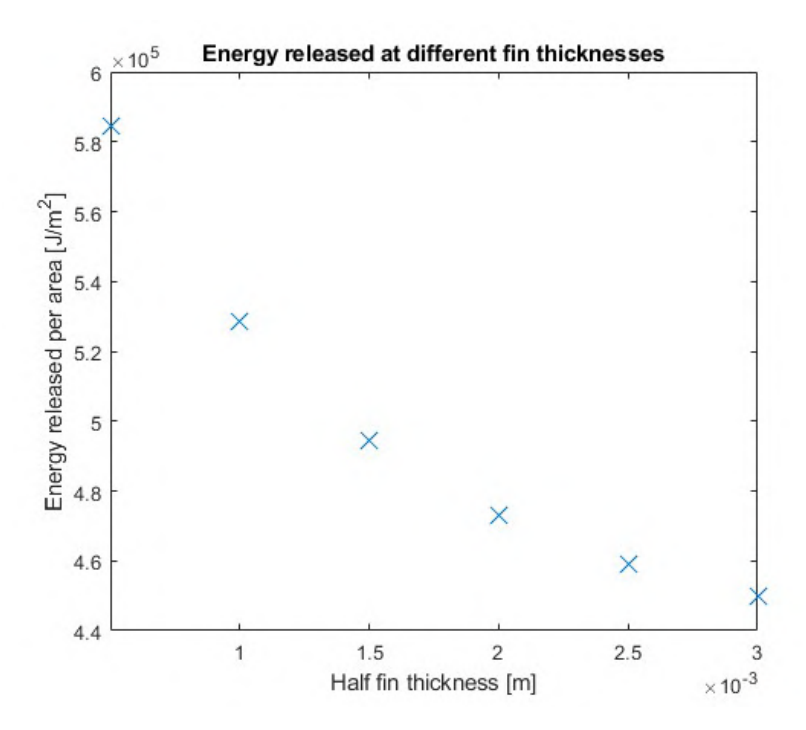


Figure 4.5: Energy extraction per unit area as a function of fin thickness.

4.1.5. Fin Distance

The distance between the fins is adjusted by changing the distance between nodes in the bulk mesh. The resolution of the model is not changed but the distance between the nodes was changed to then change the total distance between the fins. The recovered energy is calculated with the same method as with the varying fin-thickness. The correlation between fin distance and energy recovery is shown in figure 4.6. Here the optimum fin distance is shown to be at 2 mm.

4.2. Condenser side

The heat transfer on the condensing side is calculated using the method by Sinnott and Towler [38]. Condensation inside horizontal tubes depends heavily on the flow pattern present at that point. Two models can be used to estimate the mean condensation coefficient in these flow patterns. These are the models for annular flow and for stratified flow discussed in section 2.1.1. The stratified model is given below:

$$h_{c,s} = 0.76k_L \left[\frac{\rho_L(\rho_L - \rho_v)g}{\mu_L \Gamma_h} \right]^{1/3}$$
 (4.5)

The horizontal tube loading coefficient for the condensing stream is given by.

$$\Gamma_h = \frac{\dot{m}}{\pi d_i} \tag{4.6}$$

The coefficient for the annular flow can be estimated using the Boyjo-Kruzhilin equation:

$$h_t' = 0.021 \frac{k_L}{d_i} Re^{0.8} Pr^{0.43}$$
(4.7)

30 4. Modelling

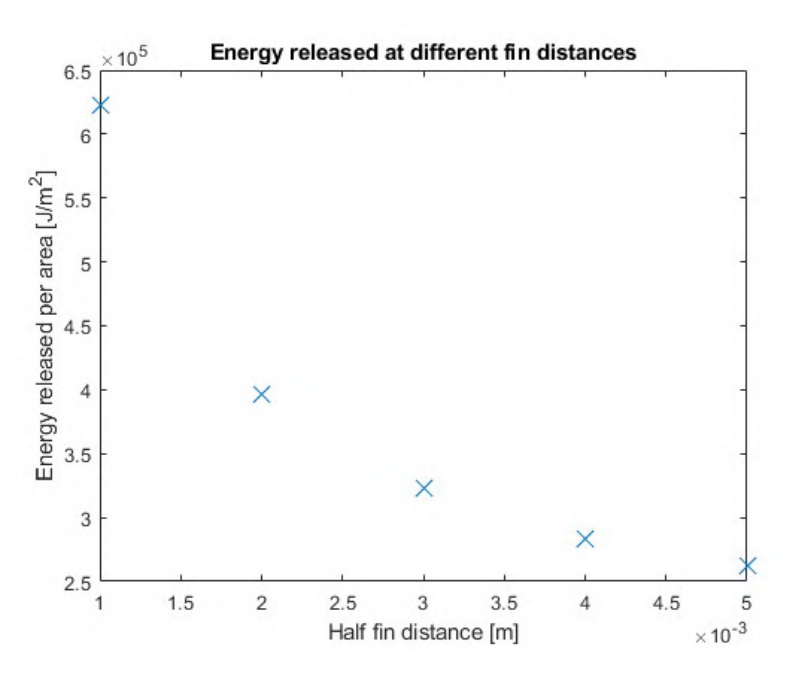


Figure 4.6: Energy extraction per unit area as a function of fin distance

Where Re is the film Reynolds number:

$$h_{c,a} = h_t' \frac{\sqrt{J_1} + \sqrt{J_2}}{2} \tag{4.8}$$

$$J = 1 + \frac{\rho_L - \rho_v}{\rho_v} x \tag{4.9}$$

All the symbols and further details on the equations can be found in section 2.1.1. The mean coefficients of both models were compared, and the higher coefficient was selected, namely the stratified flow model.

The conclusions lead to a required length for a specific ΔT to achieve full condensation. This allows the design requirements to be compared to performance requirements. Full condensation means all the available heat, namely 160W, will be applied to the system. By implementing the maximum length and maximum width of the system and minimum bending radii of different tube sizes, height becomes a free variable dependent on tube size. This can be graphed against the achievable ΔT . Increasing the tube diameter increases the surface area for condensation but reduces the number of tubes that fit the width of the system. Figure 4.7 shows this relation.

The graph shows clear jumps every time a new layer of tubes is required. The desired outcome is a low height and a low ΔT . The 10 mm tube was chosen with 5 passes per level and 4 levels. To ensure that pressure drop is not a problem this was calculated for each tube diameter using the equation [38] below.

$$\Delta P = 8j_f \left(\frac{L'}{d_i}\right) \frac{\rho u_t^2}{2} \tag{4.10}$$

Here ΔP is the pressure drop, j_f is the is the dimensionless friction factor, L is the pipe length, and u is the flow velocity. The resulting data is shown in figure 4.8.Its clear that for the smallest tubes the pressure drop is the highest. Even the highest value of 700 Pa is not very significant for the system. All tubes sizes are thus considered to have acceptable pressure drops.

4.3. Preheating side

The design of the preheating side of the prototype was done using the following formulas. The Reynolds number of the water stream was taken using its formula:

$$Re = \frac{\rho u D}{\mu} \tag{4.11}$$

4.3. Preheating side 31

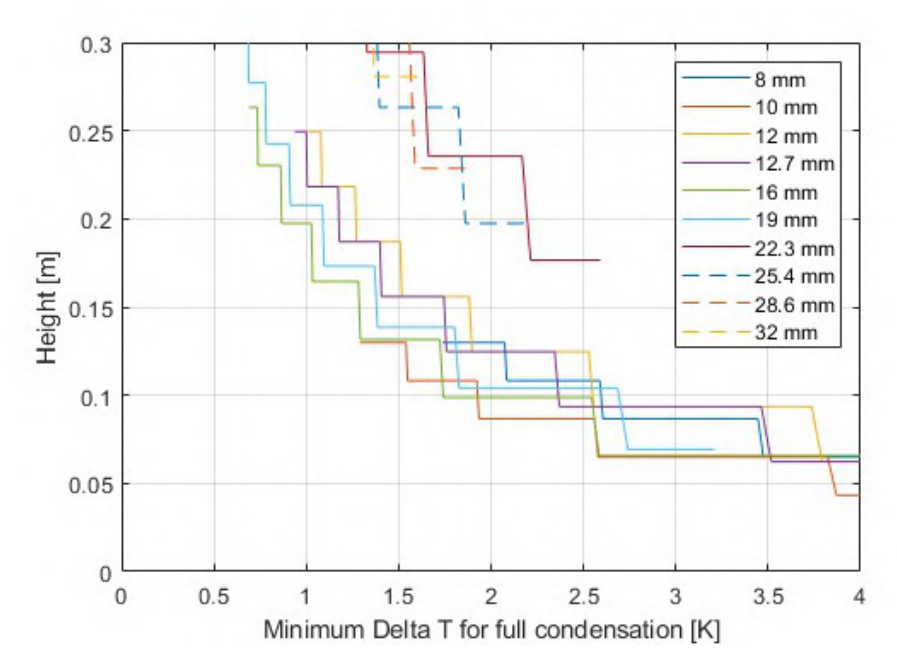


Figure 4.7: Height of the system given as a function of the achievable ΔT for different tube diameters.

For the stage of the calculation the flow will be assumed to be turbulent as this is the case for all but a few tube diameters. Once the diameter has been set, the Reynolds number can be checked to see if its turbulent. As the tube wall is smooth Petukhov's formula can be applied to calculate the friction factor:

$$f = (0.790ln(Re) - 1.64)^{-2} (4.12)$$

Where f is the friction factor and Re is the Reynolds number of the flow in the stream entering the system. Petukhov's formula has a lower bound to the applicable Reynolds number but when applying it to Gnielinski's formula the lower limit can be ignored according to Mills. Gnielinski's formula is as follows:

$$Nu_D = \frac{f}{8} \frac{(Re - 1000)Pr}{1 + 12.7(Pr^{2/3} - 1)(f/8)^{0.5}}$$
(4.13)

Where Nu_D is the Nusselt number, and Pr is the Prandtl number. The heat transfer coefficient h_c is described by a combination of Nusselt number Nu, thermal conductivity of water k and the tube diameter D shown in equation 4.14. This describes the rate of heat transfer between the tubes and the PCM.

$$h_c = \frac{Nu_D k}{D} \tag{4.14}$$

This gives an initial heat flow of 2150 W. To ease the manufacturing process, the diameter of the tubes will be the same as the condenser side. This will allow the holes in the conductive fins to be the same across the fin and the same tools to be used for further processing. Using the above formulas leads to a correlation between ΔT and the required tube distance. This leads to the system using five passes in a single level with a tube diameter of 10 mm to achieve a ΔT of 10 °C. This gives a Reynolds number of 7200 which is sufficient to satisfy turbulence. A more detailed description of the configuration will follow in the next chapter.

32 4. Modelling

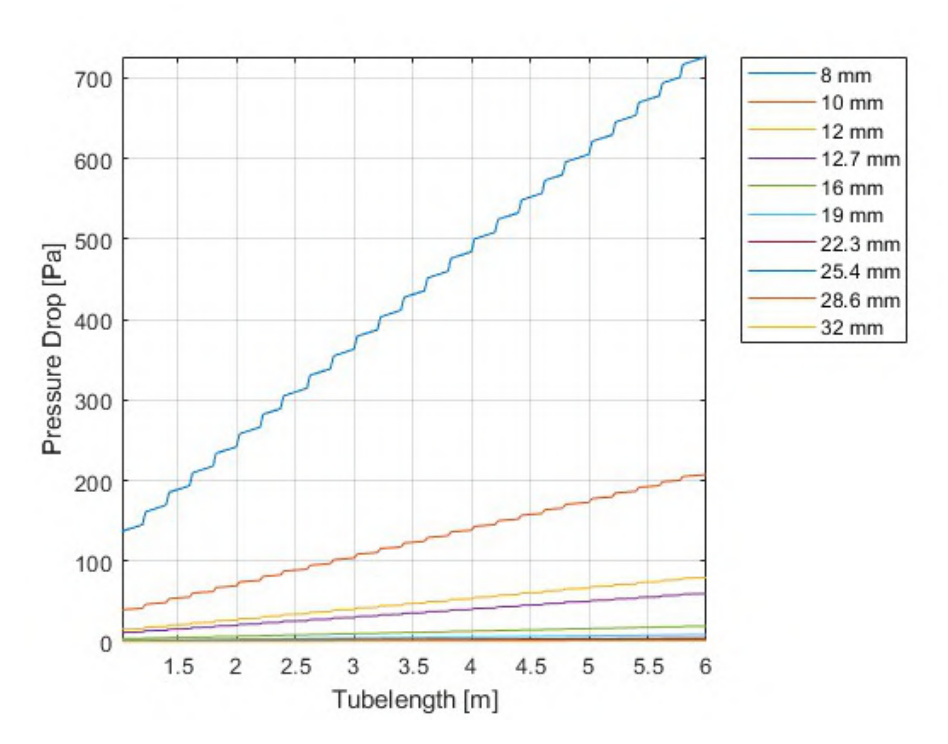


Figure 4.8: Pressure drop in the condenser for different tube lengths

Prototype design

This chapter builds on the design requirements and the modelling results to create a design of the prototype.

The modelling results showed that a minimal fin thickness was desirable. The model showed its best performance with a fin distance of 2 mm. It also delivered the requirements for the tube size and tube length as well as the number of passes for each stream. The waterside would be one layer of 5 passes with a pass length of 200 mm. The condenser side requires 18 passes with the same pass length.

5.1. Design Considerations

5.1.1. Heat Conduction from Tube to Fin

A key factor when implementing fins to increase the heat transfer rate is ensuring that the fins also transfer heat efficiently to the tubes. The solution used in this design is as follows. The fins were made up of laser-cut aluminium with holes cut at the specified locations. Collars were then pressed into the fins. These collars were dimensioned by lasercutting a hole smaller than the outside tube diameter. Multiple tests were run with different fin thicknesses to determine the optimal hole diameter for the collar. These were run by lasercutting a range of hole sizes into test strips of different thicknesses. Figure 5.1 shows a few of these strips.



Figure 5.1: Test strips used to dimension the collars. The thicker fins were capable of producing higher collars before tearing. The thicker fins are less flexible.

The tests showed that for the thinnest strips only small collars were possible before they would tear. Larger collars are desirable to ensure enough contact between the collars and the tubes. The thicker fins could create high collars but were a lot stiffer. With these strips it would be a lot more difficult to use the elasticity of the aluminium to ensure contact. The tubes are pressed through the fins causing the fins to deform to a position where they have full contact with the tubes. The best manufacturable

34 5. Prototype design

dimension of the hole diameter for the desired plate thickness of 2 mm was 6mm. This gave a collar height of around 2.05 mm. A single fin can be seen in figure 5.2.



Figure 5.2: Single cooling fin

5.1.2. Materials

To maximise the performance of the system, the materials of the parts need to be chosen specifically for the application. Using copper for the tubes maximises the heat transfer through the tubes into the PCM. Copper tubes are also readily available commercially and thus a beneficial choice. The fins will be made up of aluminium plates. The fins need good heat transfer properties but must also be malleable to create good contact surfaces with tubes. Aluminium still has a relatively high heat conductivity while being significantly cheaper than copper.

5.1.3. PCM Expansion

A vital design consideration is ensuring the PCM has enough space to undergo its phase change. Gravity will cause the PCM to reside at the bottom of the reservoir in a liquid state. Therefore, the system design has additional space above the PCM for it to expand into during melting. Secondly, the heating is applied at the top op of the PCM. This means the expansion will initiate at the top, where the extra room is present. The cooling will be applied at the bottom so that the contraction initiates there. This will ensure the PCM does not place excessive stresses on the heat exchanger and its casing.

5.1.4. Tube Arrangement

The arrangement of the tubes in the longitudinal direction determines how much heat the system can transfer, but other critical factors influence the decisions on the arrangement. The tube spacing is limited by the diameter of the tubes. Each different tube diameter has a minimum bending radius which will determine the minimum achievable distance between tubes. Table 5.1 shows the minimum centre distances for the U-bends at different tube diameters. A larger distance between tubes is undesirable as it decreases the rate of heat transfer. For this reason, the minimum distances will be used. The models showed that optimal spacing could be achieved with tubes with an outside diameter of 10mm. These have a bending radius of 12.5 mm. To maximise the heat transfer, the maximum amount of tubes are packed in the limited area. This is achieved using a triangular pitch with a centre distance of 25 mm. The other limiting factor affecting the tube arrangement is the distance between unconnected layers. These layers would not require the spacing necessary for the bending radius but would require spacing for manufacturing. The pressing of the collars requires space for two reasons. Firstly the collars pull surrounding materials towards them while being pressed. Sufficient material needs to be present, or the collars will tear. There also needs to be spacing for the tools to be applied to press the

Diameter [mm]	Center distance [mm]
8	25
10	25
12	36
12.7	36
16	38
19	40
22.3	68
25.4	76
28.6	88
32	108

Table 5.1: Diameters and centre distances of commercially available u-bends

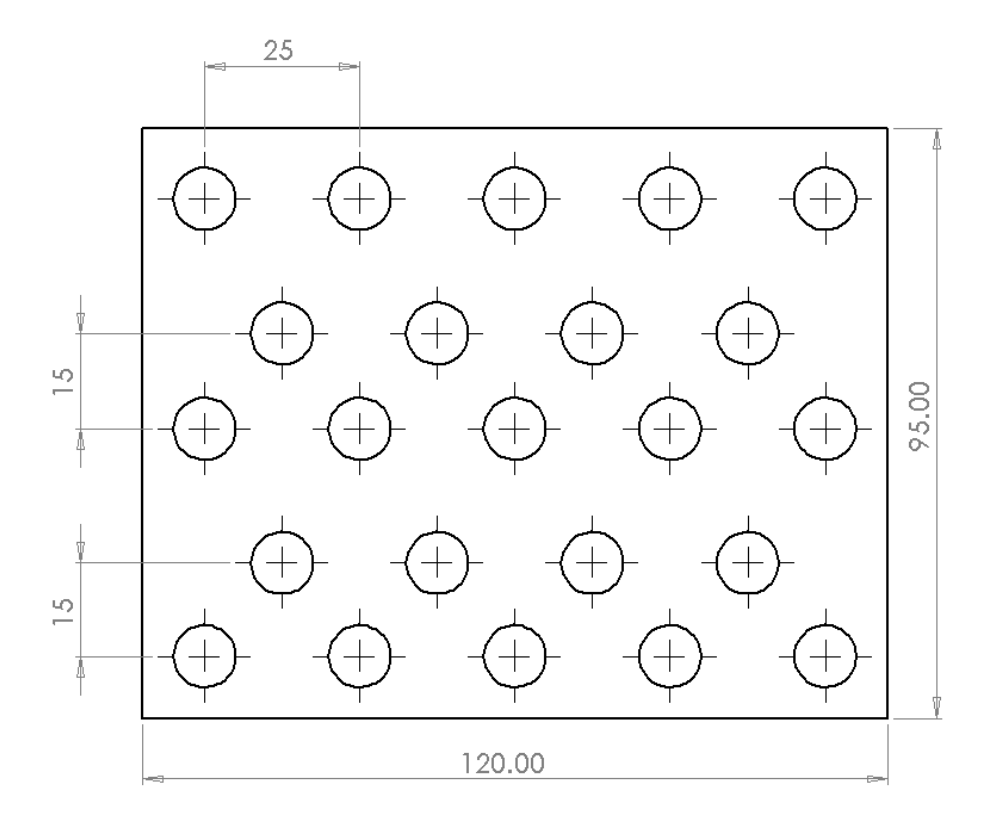


Figure 5.3: Tube arrangement on the heat transfer fin. Dimensions are in mm. The heat withdrawal stream is made up of the five tubes at the bottom, all separated by 25 mm. The 18 tubes at the top are for heat delivery. They are arranged in two sections with a triangular pitch with a 25 mm separation. The three layers are separated by 15 mm from each other.

collars. Experienced expert judgement determined the distance between the levels to be 15 mm. The modelling had determined the length of tube required and thus the number of tubes required.

5.2. Heat Storage Capacity

The modelling has determined the tube length to be 200mm. Implementing the criteria for the tube arrangement and PCM expansion led to the cross-sectional area of the PCM reservoir and hence the fin size, to be 120 mm by 90 mm. The dimensioning of the system leads to an available capacity of the system. The chosen PCM has a latent heat capacity of 210 kJ/kg. It has a liquid density of 770 kg/ m^3 [30]. The dimensions of the design are 200 mm in tube length, 95 mm in fin height and 120 mm in fin width. The area outside the fins will be ignored for the capacity as these areas will be significantly harder to heat and cool without the fins reaching these areas. These dimensions give a volume of 2.28 L. Using a fin spacing of 2 mm and a fin thickness of 0.3 mm, it can be seen that 15% of this volume

36 5. Prototype design

is made up of fins. The 23 tubes have an outside diameter of 10 mm, and a length of 200 mm. They remove a further 0.36 L from the available PCM volume. This leaves 1.58 L for the PCM. This equates to 1.21 kg of PCM and, thus a capacity of 255 kJ. This equates to slightly more than six litres of water that can be heated by 10 °C. This is significantly more than the average user demand of 2 L per day and more than the 3 L capacity of the boiling water reservoir.

5.3. Differences Between Prototype and End Product

Certain design choices were changed for the prototype that would be different in the final design. These changes were made for manufacturing reasons, testing reasons and functional reasons. First of all, the copper tube u-bends were replaced. Instead of using copper U-bends, PVC hose was used. This was done for manufacturability reasons. The copper u-bends would require welding, which was outside of the range of possibilities for this prototype. The heat transfer was designed for the surface area of the tubes without bends. The bends would add a slight positive effect to the measurements. This effect is not in the same order of magnitude as heat transfer across the tubes themselves. The hoses were attached using hose clamps. The second change made to the system was that the wall of the encasement was made from poly-carbonate rather than steel with insulating materials. This was done so that the melting and freezing fronts could be observed during testing. This leads to more heat loss through the walls. This effect is small compared to the heat being added and removed with the heating and cooling streams. The sizing of the encasement is also larger than necessary for manufacturing reasons. The hose and clamp system requires more accessibility than a welded system would need. The placement of thermocouples also requires additional room. As the lid of the encasement needed to stay removable, it was not sealed shut. for this reason, extra height was left so that expanding PCM would not leak out. This extra space causes the storage volume to be larger but without fins in these areas it will be very difficult to deliver and retrieve heat from these areas. In manufacturing the system, production variability led to the spacing between the fins being variant. The assumed fin distance is thus the total distance encompassed by the fins divided by the number of fins. The 77 fins take up 174 mm of space leading to an average fin spacing of 2.26 mm. Due to the fin thickness, the fin distance is 1.96 mm. In the bigger picture these differences will have slight effects on the measurements but the results should be sufficient for larger overarching conclusions regarding the concept.

5.4. Experimental Setup

Implementing all the design choices and considerations from the requirements and modelling led to the experimental setup that can be seen in figure 5.5 and 5.6. Figure 5.4 shows a schematic depiction of the experimental setup. The heat exchanger in the polycarbonate enclosure has two streams running through it. These are two input streams and two output streams. The cold water input was attached to the mains water line with a valve to control the flow rate and a T-junction piece where a thermocouple was inserted inline into the stream. The warm water was sourced from two 7L boiling water reservoirs connected to each other in series. The first reservoir would fill the second as the second is being depleted, and meanwhile, the first would fill with cold water and start heating. The output of the second boiling water reservoir was fed through a mixing valve, which could be manually set to the desired temperature. Both boiling water reservoirs contained a 2.2 kW heating element meaning that at low enough flow rates and low enough demand temperatures, infinite hot water could be produced even after the reservoirs' original water had been depleted. On colder days, when the incoming mains water line temperature was lower, the hot water supply was more limited. The incoming hot water stream also contained a thermocouple inline with the stream inserted through a T-junction. Both output streams emptied into the sink behind the setup. These streams also contained thermocouples inline. 12 other thermocouples were placed into the PCM at various locations through the top of the container. All thermocouple cables were fed into two dataloggers which were encased in foam to protect them from external thermal effects.

The four inline thermocouples were type K. The 12 thermocouples were type T. The thermocouples were calibrated before the measuring phase. All thermocouples were attached to each other and placed in the same container. This container was frequently stirred until it was thermally stable. The temperature was then recorded using all 16 thermocouples. The temperatures of each thermocouple were then compared to the mean temperature. This offset was very stable for each thermocouple. The process was repeated three times on different days, times and ambient temperatures, and the offset

still remained the same. The offsets per thermocouple are shown in table A.1 in the appendix.

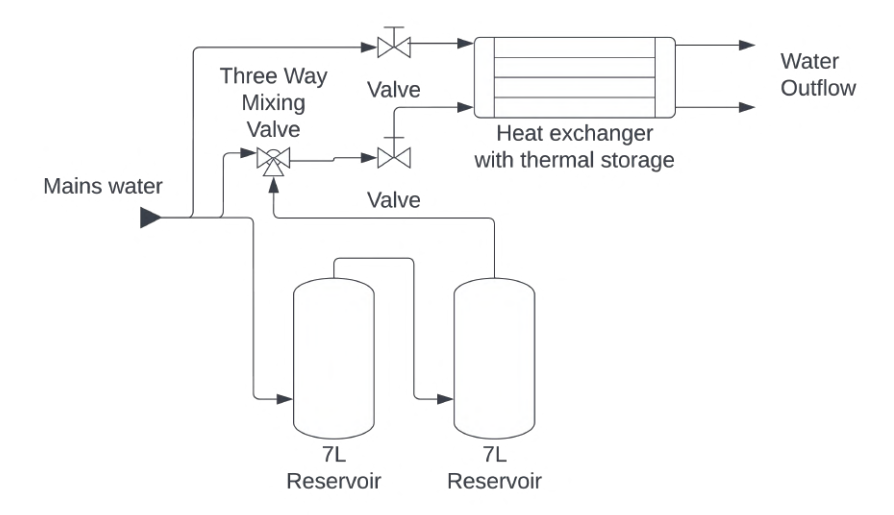
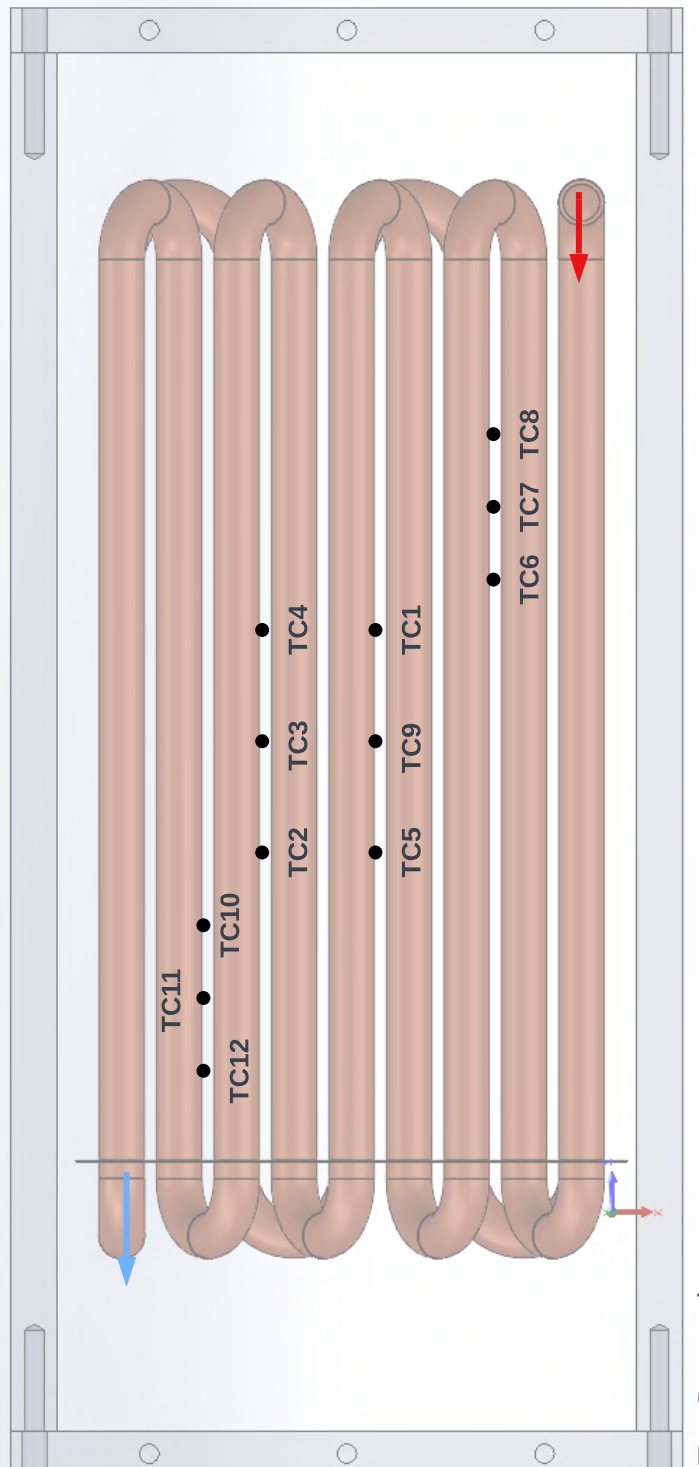


Figure 5.4: Schematic depiction of the experimental setup

5.4.1. Thermocouple Placement

The thermocouples in the PCM were placed in locations seen in the figure 5.7. 16 thermocouples were placed in the system. A thermocouple was placed in the flow of the entry and exit of both streams. A thermocouple was placed in the PCM near both streams' beginning, middle and end. The remaining thermocouples were spread around the system. Three different heights were used: next to the highest tube, between the two heating layers and next to the bottom tube.

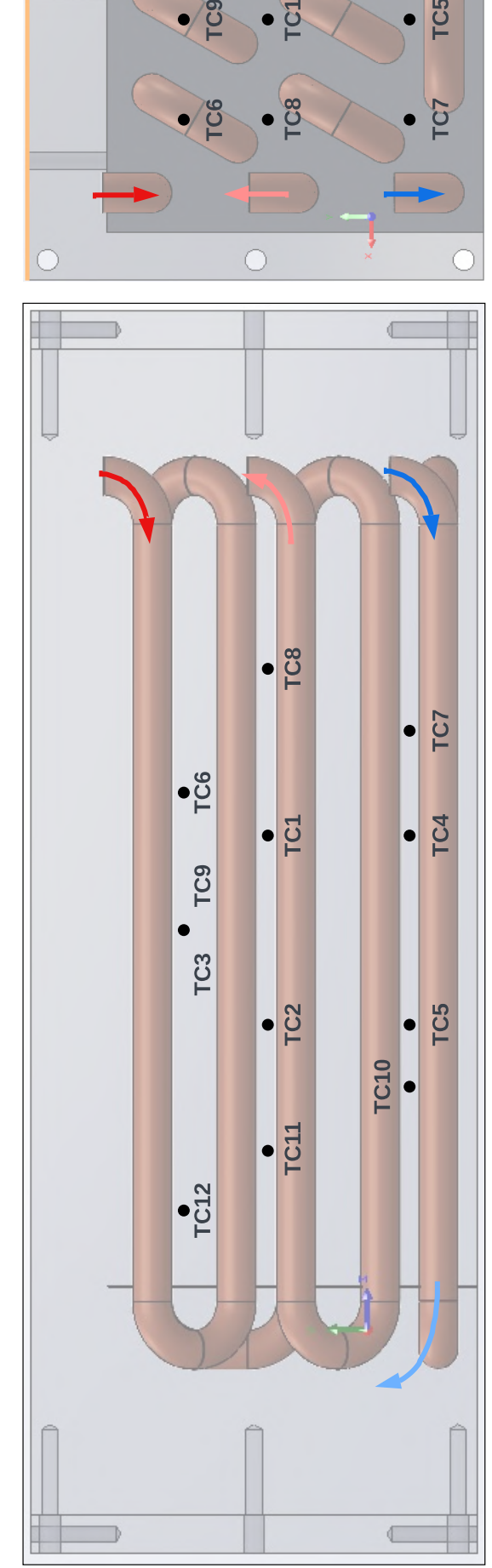


Warm InflowWarm Outflow

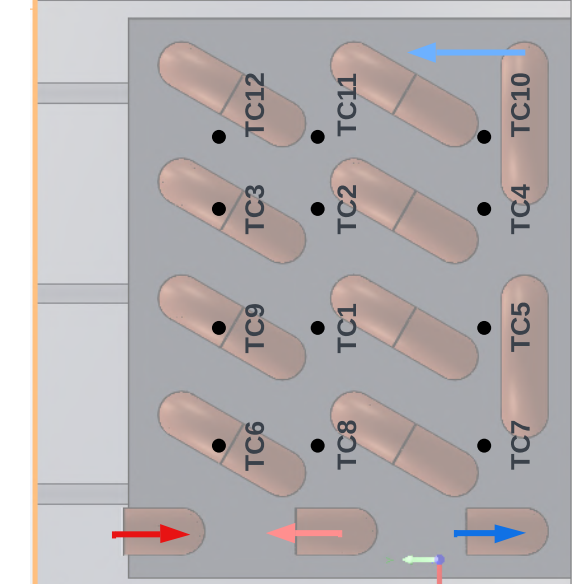
Cold Inflow Cold Outflow

Arrow Legend

Top Down view



Schematic depiction of the thermocouple locations and flow direction.



Right side view

Front view

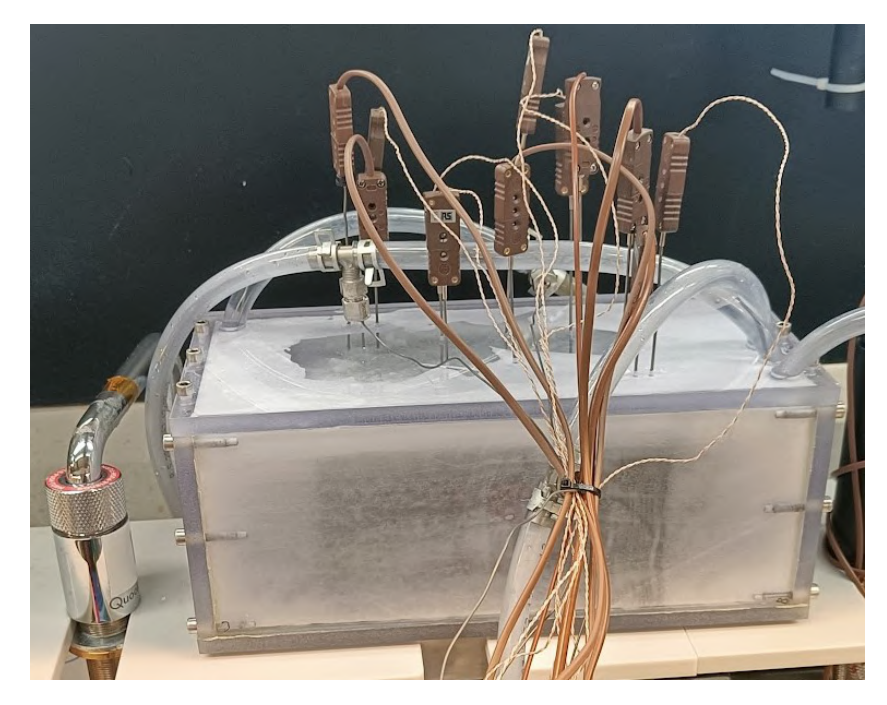


Figure 5.5: The experimental setup in its solid state. The thermocouples that are seen at the top all have the same length and are thus placed at varying heights within the system. The tap on the left is purely used as a safety release valve for the boiling water reservoirs.

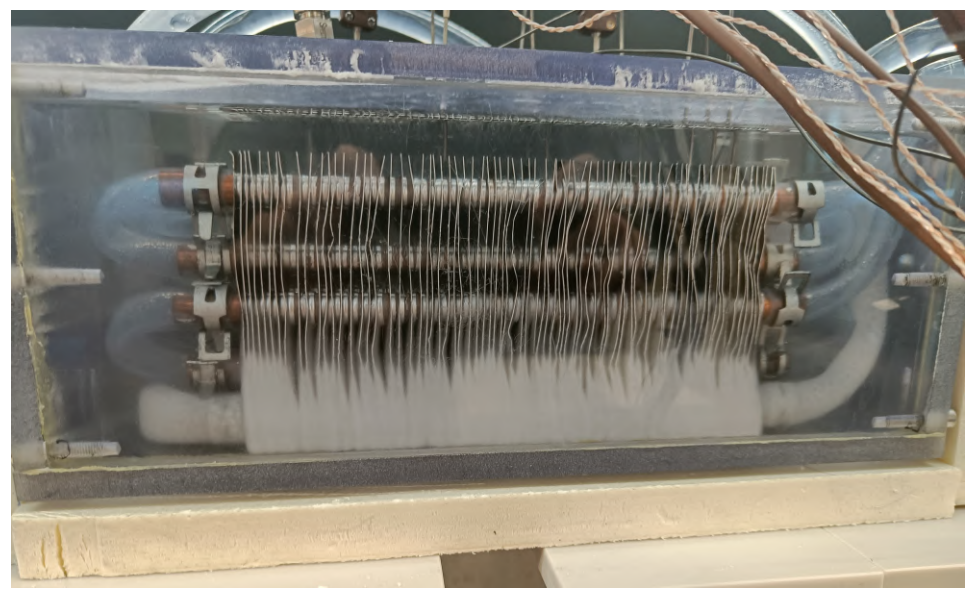


Figure 5.6: Image of the experimental setup where the heat exchanger is visible due to most of the PCM being molten.

40 5. Prototype design

5.5. Experimentation Method

Two different system situations were tested; therefore, two different measurement scenarios were used. The first involves applying heat to the system using warm water to simulate the condensation of R600a. The second scenario is the user demanding boiling water, simulated by running mains line tap water through the system. The thermal couple data was sampled once per second during measurements.

5.5.1. Heat Storage

For the heat storage tests, the system was first brought to a thermally stable state where all thermocouples gave a temperature near ambient temperature, and no significant variation in temperature was measured. In the meantime, both 7L tanks would have been filled and heated to ensure a large enough storage of hot water. The mixing valve was set to the desired temperature of 40 °C. The hot water tap was then opened. It was desirable to keep the flow rate constant throughout the measurement. For this reason, once the tap was opened, it was not adjusted until after the measurement was completed. This caused each measurement to have a different flow rate that needed to be accounted for. The temperature data would then be sampled once per second, and in the meantime, the flow would be measured using a stopwatch and a measuring cylinder. This process was repeated three times. The measurement was continued until either the hot water was finished or all thermocouples had reached a molten state.

5.5.2. Heat Withdrawal

The Heat withdrawal test was performed according to the following method. The system was brought to a fully molten state by continuously pumping warm water through the system. Once visual inspection revealed that the whole system was transparent, the system was deemed to be fully melted. This was quite a lengthy process as parts of the system, especially the parts further from the fins, were more challenging to reach. A higher temperature was applied to speed up this process. This meant that once the system was fully melted, the system was left to rest until the temperatures had restabilised, and the mean of the thermocouples had reached the desired starting point. From this point, the mains water tap was opened so that it would dispense water of around 2.5 L/min. The exact flow rate was then measured using a measuring cylinder and a stopwatch. The water was then sent through so that at least 7L of water had gone through the system. This method was then repeated several times.



Results

This section displays the results as collected and compares the results to the expectations from the modelling. The section is split into the heat delivery measuremntes and the heat extraction measurements. For both sets a single example test run is shown. The heat flow of all tests is graphed. The local heat transfer coefficients are also depicted for each thermocouple location.

6.1. Heat Delivery

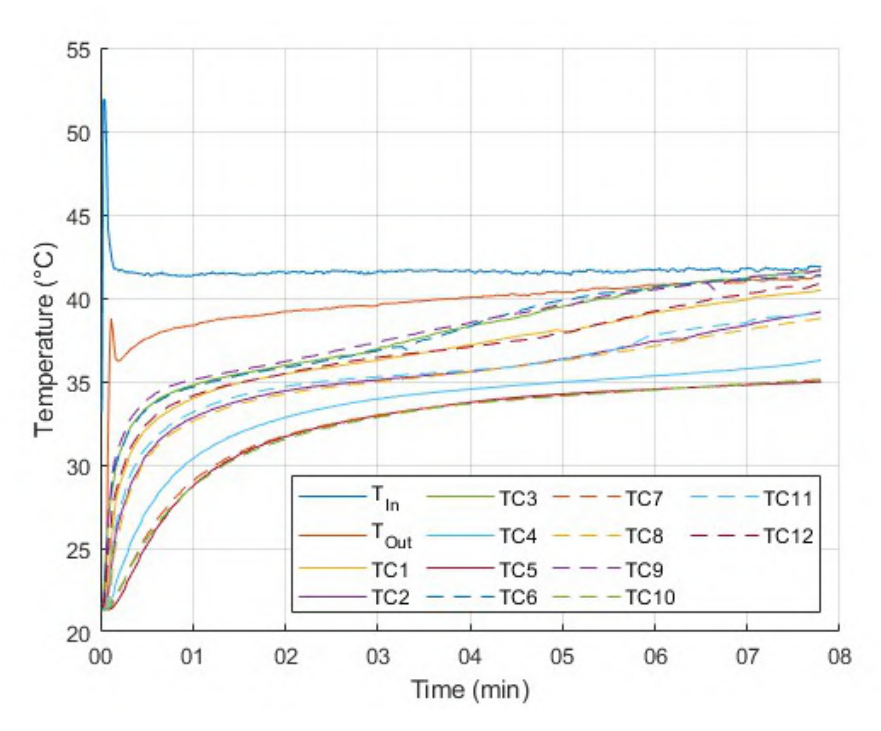


Figure 6.1: First test where hot water was sent through the storage system.

Figure 6.1 shows the first test where hot water was sent through the system to heat it. Three of these measurements were executed. The results of the other two are very similar and can be seen in Appendix C. The test starts in a steady state where the whole system is around ambient temperature. The warm water valve is then opened. This is immediately noticeable in the incoming temperature. The thermostatic valve quickly corrects the temperature to the desired set point. The valve has a quick yet noticeable reaction time causing the temperature to spike for a few seconds before balancing out. The test then runs until the reservoirs run out of boiling water, at which point the temperature will temporarily

42 6. Results

spike before dropping to the mains line temperature. The data used for calculation starts from the point where the incoming water temperature increases rapidly and ends at the point where this temperature increases once more due to the spike and thus impending drop to main lines temperature. The example in figure 6.1 also contains small sources of error in the measurement where the pressure dropped on the mains line momentarily due to external water use. The disturbances caused by these changes in temperature and pressure are negligible to the PCM temperatures.

First observations show that the temperatures in the PCM initially rapidly approach the temperature of the heat delivery. Once the thermocouple in the PCM reaches the melting zone, shown in table 3.2 in the design section, the temperature change seems to slow. This is in line with expectations as the energy being applied to the system is being used to convert the phase rather than increase the temperature. Another observation is the grouping of thermocouples. Thermocouples 9, 3 and 6 are the fastest to reach the phase transition. They are followed by thermocouples 12 and 1. Thermocouples 11, 2, and 8 also show similar reactions to the incoming heat. Thermocouples 10,7,5 are closely grouped at the bottom with thermocouple 4 slightly above them. This grouping can be seen across all the measurements.

From the temperature data the heat flow into the system was calculated for each test using the following equation:

$$\dot{Q} = mc_n dT \tag{6.1}$$

where \dot{Q} gives the heat transfer rate between the water and the system, m is the mass flow rate of the water. c_p is the specific heat capacity of water. dT is the temperature difference between the inflowing and outflowing streams with the time delay accounted for. The stream's flow rate and the tubing length were used to calculate the delay between the water flowing in and flowing out. The in-flowing temperature is compared to the out-flowing temperature after the delay. The \dot{Q} is then attributed to the moment of inflow into the system. The results of the heat flow can be seen in figure 6.2.

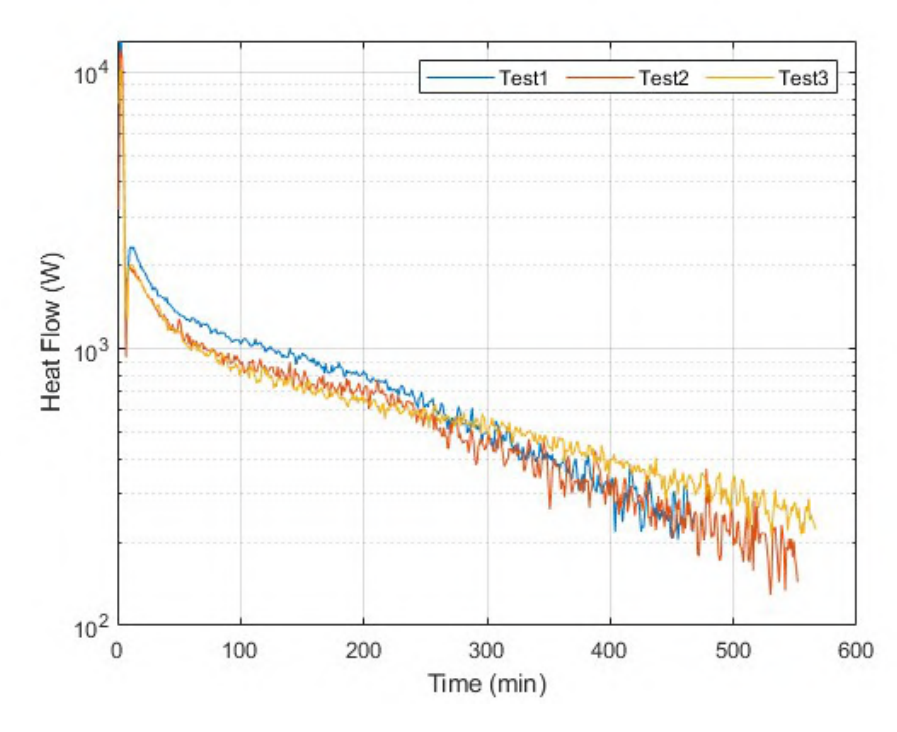


Figure 6.2: Energy flow into the system during the three heating tests.

The initial spike due to the reaction speed of the mixing valve is visible in the figure at the beginning. After the spike the initial heat flow is high as the temperature differences are still large. The heat flow decreases sharply at the start and then settles into a linear decrease. Note that the y-axis is logarithmic. This is inline with expectations as the first part represents the sensible heating after which most of the system reaches the phase change region.

6.1. Heat Delivery 43

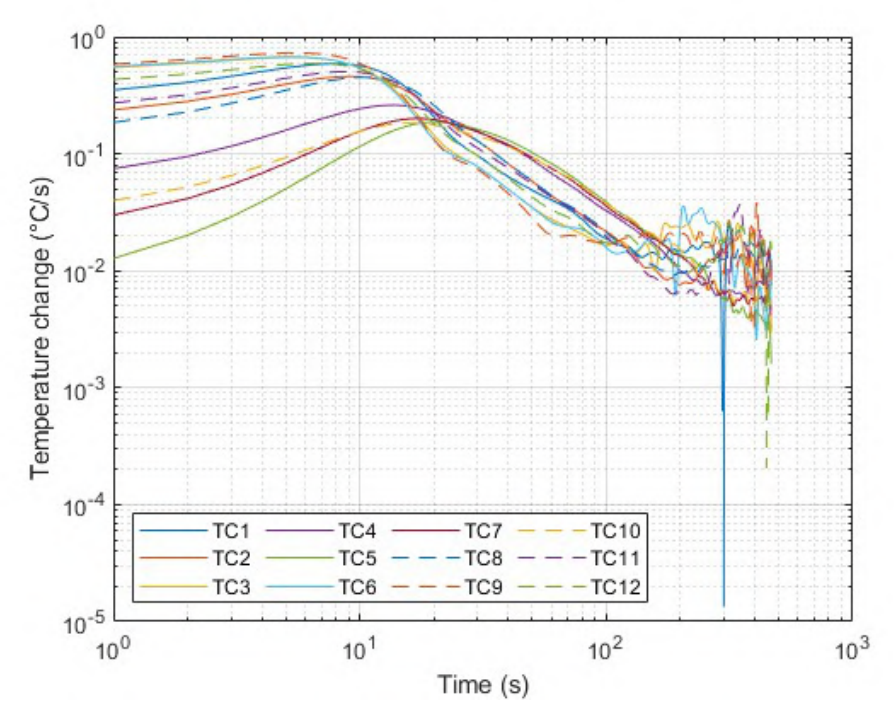


Figure 6.3: Logarithmic plot showing the forward difference of the temperature at each point in time for the first heating test. A low-pass filter has been applied to the temperature change data to remove random noise.

From the temperature the forward difference was calculated to determine the temperature change per second at every location. A low pass filter was then applied to the result to remove high frequency errors on the signal. The result for the first heating measurement is seen in figure 6.3. The other tests showed very similar results and can be seen in appendix C.

All measuring points show an initial increase in temperature until a maximum is reached after which they all decrease. This decrease can be attributed to the PCM surrounding the thermocouple reaching the phase change region. Towards the end of the measurement the temperature changes become very small causing the signalling become noisy regardless. One possible cause is that once the phase change region has been passed and the PCM is fully molten convection effects start to influence the measurement. It would be expected that once the phase transition had occurred the Temperature change would once again increase but as the temperature differences to the incoming heat are so small at that point, this effect is not visible in the data.

Just as in the raw temperature data, the same grouping can be seen in the temperature change calculation. The heat transfer rate is clearly different at different thermocouple locations transfer coefficient. This difference can almost solely be attributed to the location height. Thermocouples 3, 6, 9 and 12 are all located at the top level of the container. Thermocouples 1, 2, 8 and 11 are all located centrally in the container. Thermocouples 4, 5, 7, and 10 are all located near the bottom of the container. With the stream with the incoming heat located at the top of the container, the thermocouples near the top reside in an area that receives more heat compared to the lower thermocouples. This indicates that the fins are not transporting enough heat in the vertical direction.

44 6. Results

6.2. Heat Extraction

Figure 6.4 shows an example of a result from the cooling tests. The test starts in a state where the whole system is around 40 °C. The cold water valve is then opened. Like in the heat delivery measurements, this is immediately noticeable in the incoming temperature. Here there is no thermostatic valve, so there is no initial spike. The test then runs until at least 7L has passed through the system and enough time has passed for the flow rate measurements to take place at which point the tap is closed. This is also highly noticeable in the data as the temperature instantly starts rising rapidly. The data used for calculation starts from the point where the incoming water temperature starts decreasing and ends at the point where this temperature increases.

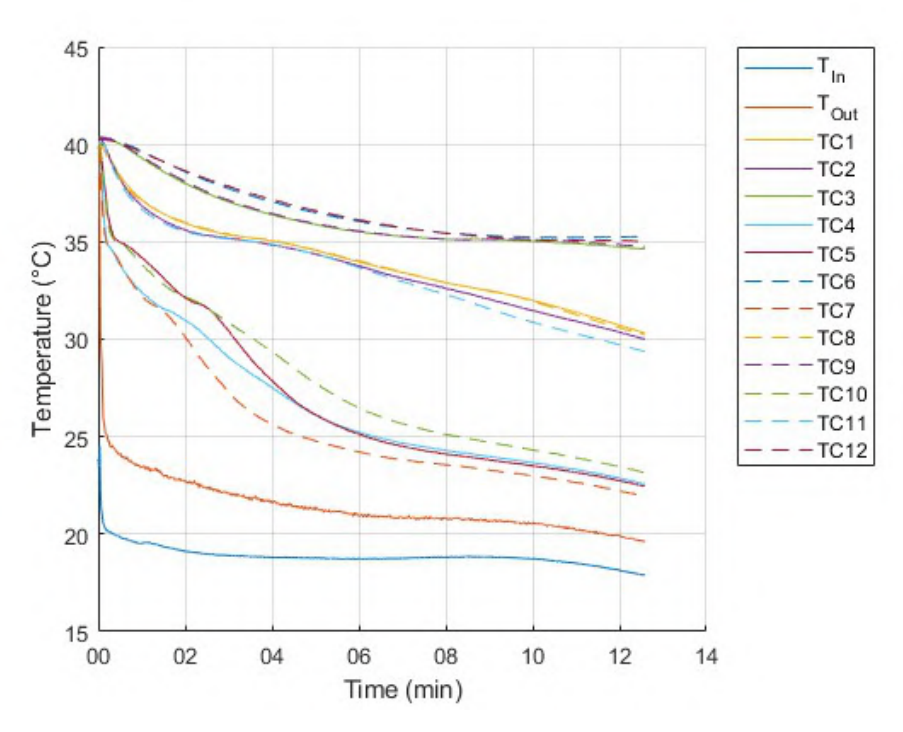


Figure 6.4: Example of a test where cold water was sent through the storage system.

The first observations show that the temperatures in the PCM initially drop rapidly to the phase change region. Once the region is reached, the temperature change seems to slow down. This is in line with expectations once again, as the energy being removed from the system is being drawn from the conversion of phase rather than the decrease in the temperature. Once again, the thermocouples are grouped quite closely. Thermocouples 4, 5 and 10 and 7 are the fastest to reach the phase transition. They are followed by thermocouples 1, 2, 8 and 11. Thermocouples 3, 9, 6 and 12 are the slowest to react.

Using the temperature data, the heat flow out of the system was calculated for each test in the same way as for the heat delivery tests except that here the positive heat flow is out of the system instead of into the system. The results of this calculation can be seen in figure 6.5. Here we can see that tests 1 and 3 follow a very similar path while test 2 follows a different path. Especially the increasing heat flow at the end of the measurement seems out of place. The cause of this irregularity can be clarified when the specific measurement is examined as the incoming temperature was varying rather significantly. The temperature profile of test 2 can be seen in appendix C. The heat flow profiles of test 1 and 3 are more realistic as they had a more stable incoming water temperature.

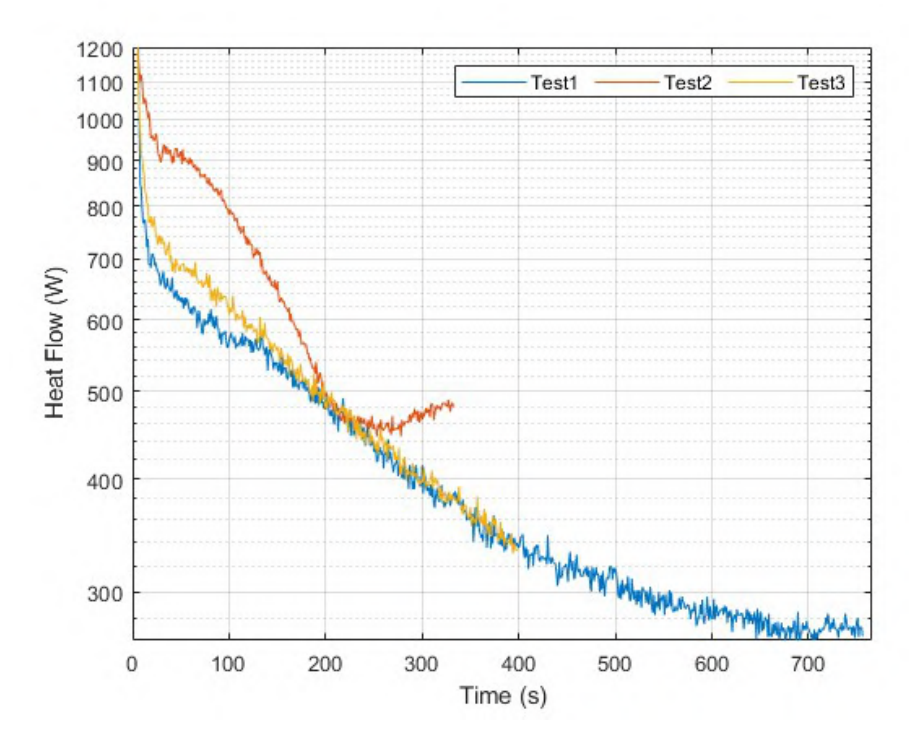


Figure 6.5: Energy flow out of the system during the three cooling tests.

Just like in the heat delivery section, the forward difference was calculated to determine the temperature change per second at every location but now for the measurements during the heat extraction process. As for the heat delivery, the low-pass filter was applied to remove the noise from the signal. The results for the first heat extraction test can be seen in figure 6.6. The other tests had comparable data. Their results are visible in appendix C.

In the temperature change figure of the heat extraction measurements all thermocouples start with a slight increase in heat transfer until their maximum is reached. The temperature change then drops. Unlike the heat delivery measurements where the full phase change was not visible, in these measurements a local minimum is visible. In some thermocouples it is more clear than others. Especially the thermocouples that reach the phase change first show a clear local minimum. This indicates that the rate of temperature change drops to accommodate the phase change and increases once the phase change has been completed.

The grouping is even more clear than in the in the raw temperature data. The heat transfer rate is clearly grouped into 3 levels. This difference is thus directly due to the location height. Thermocouples 3, 6, 9 and 12 are all located at the top level of the container. Thermocouples 1, 2, 8 and 11 are all located centrally in the container. Thermocouples 4, 5, 7, and 10 are all located near the bottom of the container. While the heat delivery stream reaches different heights within the system, the heat extraction stream soley runs along the bottom. This makes the effect of height significantly larger. This indicates once again that the fins are not transporting enough heat in the vertical direction.

6.3. Key Points of Interest

There are multiple key takeaways from the results. First of all, the initial heat transfer at the start of the measurements is significant. This implies that in the initial phase of the measurement when no phase change has occurred, the system can deploy or absorb significant amounts of heat. This also leads to the delivery and retention of more considerable temperature differences at the start of the measurements. Once the measurements continue and the phase boundary moves away from the tubes, the heat transfer coefficient drops significantly. This shows that the heat conduction methods from the tube to PCM were insufficient. Large parts of the capacity were being underutilised. This leads to the conclusion that the critical length of the system is not the distance from the fins. If this were the case, the heat transfer rates would be more similar to each other at the different thermocouple locations.

46 6. Results

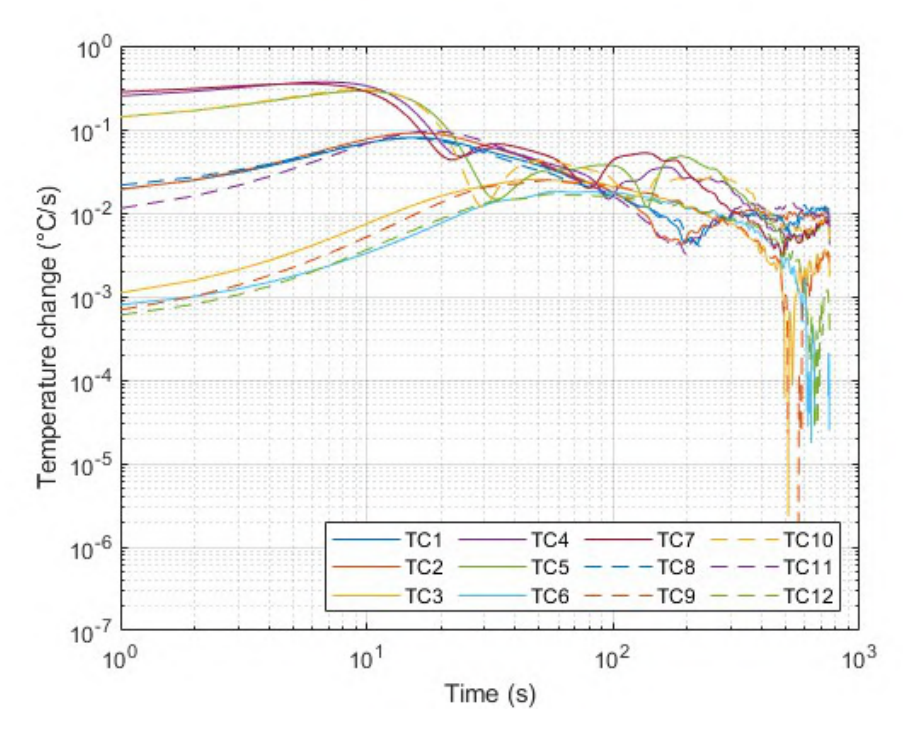


Figure 6.6: Logarithmic plot showing the forward difference of the temperature at each point in time for the first cooling test. A low-pass filter has been applied to the temperature change data to remove random noise.

Additionally, they would not be heavily grouped in categories depending on their height in the system. As the design goal is to uniformly heat or cool the whole system as rapidly as possible, the current design has room for improvement. The heat transfer near the tubes is still sufficient. The heat transfer in the vertical direction further away from the tubes is lower than required.

Economic case

The modelling and experimentation have shown the technical potential of the concept. This chapter discusses the economic potential of the system. The economic case for the system is built up in a few parts; the costs associated with manufacturing the system, the customer's monetary gains, and the added value from the improved product.

7.1. Costs

The costs of the system are built up from a few factors. These are the manufacturing of the condenser unit, the PCM material, the container, and the assembly and integration of the system into the current system. The condenser unit can be custom ordered as a unit and integrated into the current system during the cooling system manufacturing phase. The addition of this system to the current refrigeration system will be considered the condenser cost. The cost of the PCM ranges quite significantly depending on the quality and quantity ordered. For this cost estimate, the quantity used is 1 kg. The price is €7 per kg based on the product that was acquired for the experimentation. The container for the PCM does not have to be an expensive part. A plastic container with insulation is sufficient. Expert judgement estimates this to be around €1. The assembly costs will only be the added assembly costs due to the addition of this system. As the condenser and container will be implemented into the total cooling system externally, these costs are already factored in. The added assembly costs would be the steps required to integrate the system into the rest of the Quooker system. It is estimated that this would be four assembly actions associated with connecting the water streams on both ends. Each assembly action on the line should last around 15 seconds. Assuming an assembly cost of €60 per hour, €1 of assembly cost would be added per product. Additionally, retail prices are usually 2-3 times as high as the cost price, so to not skew the margins, this factor also needs to be applied. 2.5 will be used for these calculations. The costs are displayed in table 7.1.

Part	Part Cost (Euros)	
Condenser	10	
Container	1	
Assembly	1	
PCM	7	
Total	19	
Retail factor	2.5	
Total cost increase	47.50	

Table 7.1: System costs

7.2. Monetary Gains

The gains of the product can be categorised into two parts. These are monetary gains for the client and non-economic gains for Quooker. The client's savings potential heavily depends on a few highly volatile

48 7. Economic case

factors. Firstly the price of energy is currently in a very volatile state due to socio-political circumstances. For the rest of this calculation, the price ceiling for electricity, set by the Dutch government, will be used. This is set at €0.40 per kWh. The usage scenarios and environmental conditions are also of importance. In normal operating conditions, the Quooker system refrigeration cycle produces 160 Watts for 90 seconds every 20 minutes. This amounts to almost 0.3kWh per day. That amount of energy is purely to keep the cooled water reservoir at the required temperature. Any use of the cooled water increases the operating time of the compressor and, thus, the heat it produces. The energy the system can deliver depends on the system's design, the amount of heat demanded by the user and the temporal spacing between moments of demand.

While every user demand profile is different, this case will use the ultimate best-case scenario, the ultimate worst-case scenario and a typical user profile for the calculation. Judgments can be made with other profiles in mind compared to this profile.

7.2.1. Best-Case Scenario

In the most optimal energy-saving scenario, both boiling water and refrigerated water are heavily demanded. This will cause the compressor to deliver more heat than simply the standby heat with a maximum of 160W if it is in constant operation. By demanding large amounts of boiling water, the temperature differences will remain large in the system causing maximum heat to be transferred to the PCM and, subsequently, the water. This is limited by the rate at which the boiling water reservoir can heat its water. Once the 3L reservoir is empty, it takes around 20 minutes for the water to be at a temperature at which the user would want to dispense it. Thus with perfect optimal use, a theoretical gain of €1.53 per day. This scenario is clearly very unlikely, but it shows that the best use cases for this application are scenarios where both products are heavily used and intermittently spaced throughout the day.

7.2.2. Worst-Case Scenario

In the worst case, the user only demands cold water or does not use the system at all. In this scenario, the buffer will fill up with heat until it can not receive any more heat, and the excess heat will be rejected into the kitchen cabinet. This scenario has no economic gain. This scenario is highly unlikely, however, as it can be assumed that if a customer buys a product, they intend to use the product. While this scenario is quite farfetched, there are other scenarios that are more likely, which also have very poor economic performances. If all of the boiling water demanded is concentrated at one point in time, the performance is lower as the system does not have time to rebalance and reheat.

7.2.3. Average User Scenario

An average Quooker user uses 2L of boiling water every day. The quantities demanded will range from 100 ml for a small cup of tea, for example, to a litre or more to cook with. The smaller quantities will enjoy large heat transfer rates as less phase change has occurred, and the temperature differences between the fins and the water will be considerable. The larger demanded quantities will see less heat transfer towards the end. Using the current design and a demanded quantity of 200ml, the average temperature gain of the preheated water is up to 12 °C. If a litre is used as the quantity demanded, the average temperature gain drops to around 6 °C. This temperature output can be increased by improving the design but it will be used as an indication here. A hypothetical scenario for a user could involve five smaller uses of 200 ml throughout the day, followed by a larger use at dinner time for cooking. This leaves enough time for the PCM to regain all its temperature from the compressor in between uses. This scenario would see the user save 75 kJ or 0.02 kWh daily. This amounts to €3.05 per year. This can be used to equate the net present value. The average inflation rate over the last 20 years has been 2.5%. Using this as the discount rate gives a payback time of 20 years before the investment by the customer is recouped. This development of the payback period for the three cases is seen in figure 7.1. Both boundary cases are extreme scenarios, so almost all use cases will fall in between the two.

7.3. Economic Discussion

20 years is a timeline that is in line with expectations of how long the product should last, but this may not be a timeline in which consumers would be prepared to invest. Other factors that add value are thus important to consider. Saving energy and reusing energy are very important topics in today's society.

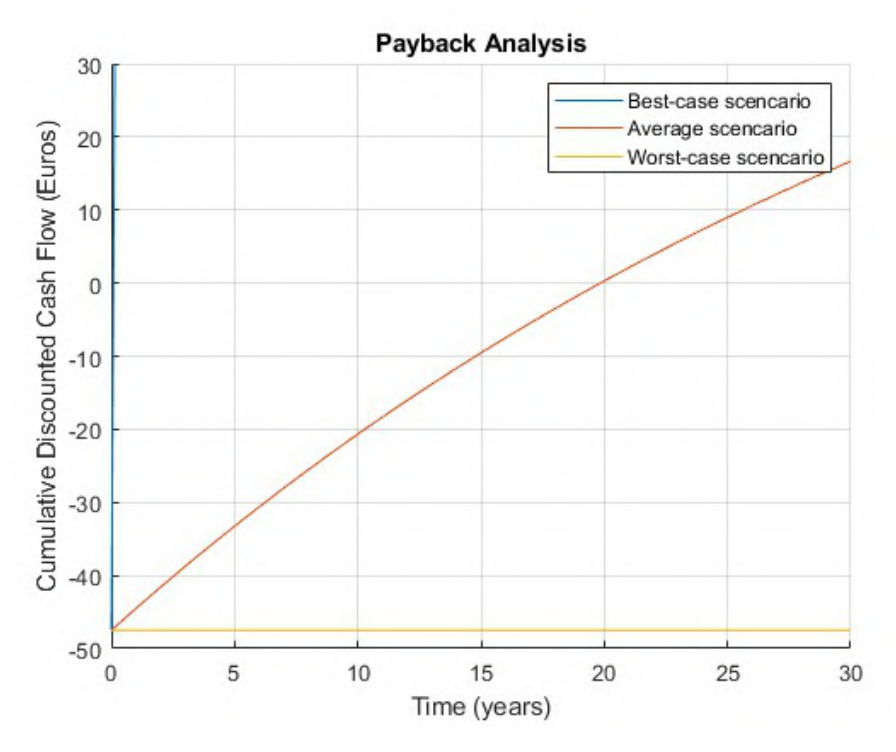
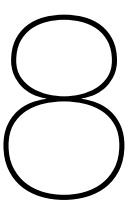


Figure 7.1: Graph showing the payback period of the system with an average user scenario.

There is additional value in products that save energy than purely monetary gain. By implementing more energy savings, the product can become more marketable. Another potential value is in compliance with potential future regulations or energy labels. As the globe tends to a more energy-efficient world, governments are also tightening environmental regulations and energy label requirements. A heat recovery system could be a potential future factor in passing these regulations or achieving these labels. This added value may even be more significant than the actual monetary gain. Future energy prices remain uncertain, leaving much speculation about how effective of an investment this system could be. While energy prices are currently very high, they may come down, pushing the payback period significantly, but increased design performance can potentially cancel this out.



Conclusions and Recommendations

8.1. Conclusions

The goal of this project has been to design a system with a lower energy demand than the current system while retaining all of the current system's capabilities. The conclusions from the literature showed that a system using a conventional refrigerant such as R600a would give the highest potential gains. The literature also showed that for an intermittent heating and cooling system, a latent thermal buffer can be effective if heat transfer additives are efficiently utilised. Based on these conclusions, the most effective and manufacturable system is a vapour compression system with a primary and secondary condenser where the primary condenser would act as a thermal energy store. This store could be deployed to preheat incoming water.

While most of the components of this system are readily available, this primary condenser with thermal storage would need to be designed from scratch. A finned heat exchanger encased in organic PCM was deemed to be the best design. Using the system requirements, design requirements and variables were set up that needed designing and modelling to solve to create the heat exchanger. The finite difference modelling and manufacturability requirements delivered theoretical optimal fin thickness and distance values. The fin thickness was set at 0.2 mm and the fin distance at 2 mm. The condensation models and other manufacturability requirements gave the tube diameter of 8 mm inside diameter. The tube arrangement followed from these same models coupled with the thermal expansion management ideas. The measurements showed that a phase change in PCM is an effective way to store energy. In the surroundings of the tubes, heat transfer was significant along the fins. The measurements also showed that height was critical in determining heat transfer and that more heat transfer through the fins was required. At further distances from the tubes, heat transfer was lacking. The expectation was that the distance from the fins would be the leading factor in determining efficiency. Distance from the tubes was more critical in the current configuration. The economic case for this system shows promise. In its current state with an average user, a payback period of 20 years can be expected. With design improvements, this can be brought down significantly. In addition, the added value of saving energy and being environmentally positive adds to the business case in a non-monetary manner.

8.2. Recommendations

This research has shown the conceptual feasibility of a PCM heat transfer and storage system that can be implemented into the Quooker system. Further research and testing are required to move it from this conceptual stage to a robust design and eventually implementation. Heat transfer rates can be significantly improved by implementing lessons learned from this research. The key problem is the vertical heat transfer between streams. A multitude of solutions exist to solve this problem

- By increasing the fin thickness, the vertical heat transfer can be increased. Thicker fins will lead
 to a higher vertical heat transfer and lower thermal capacity. Capacity was not an issue in this
 research.
- By decreasing the fin distance, the effective heat transfer goes up as there are more fins per volume of PCM, leading to more heat transfer.

• Thermal expansion of PCM was less of a problem than anticipated. A potential reason for this is the process being slower than expected. Research could be conducted into a design where the heating and cooling streams are interlaced. This decreases the distance between streams, drastically increasing heat transfer significantly. With this higher rate of heat transfer, the thermal expansion could pose problems again, though.

These solutions are all aimed at the increase in heat transfer rates. This project has not reached a phase where the design has been proven and can be directly implemented. Further development is required. The next phase of development should be focussed on dimensioning the system. The next phase should also involve using better materials that better represent the final design. The dynamic response of the system to different scenarios was ignored in this research as many factors were different compared to a potential final design. A next-stage prototype should thus use R600a instead of water, have fully welded joints instead of plastic tubing and a fully insulated exterior.

This project has also brought forth some recommendations to be used during experimentation in the further development phases. The experimental setup can be improved in a few ways. Firstly, a circular closed-off water system with a heating element would be beneficial. This would reduce the temperature variations due to external factors, and it would make the inflowing temperature actively controllable and more steady. The steady temperature would leave a clearer depiction of the change in flux due to internal factors rather than the change in inflowing temperature. The peaks caused by the slow reaction of the mixing valve would then also be removed, which would give more insight into the initial stages of the process. Secondly, the system should use a flow rate regulating valve so that the flow rate can be kept constant and controlled. This removes uncertainty from different flow rates in the system. Thirdly, large errors were caused by thermal effects near the thermocouple loggers influencing the cold junction temperature. Especially at these near-ambient temperatures, it is critical that the loggers are fully insulated and kept away from any potential heat source. By implementing these improvements into the next iteration of testing, a more decisive conclusion can be made about the success of the design concept presented in this paper.

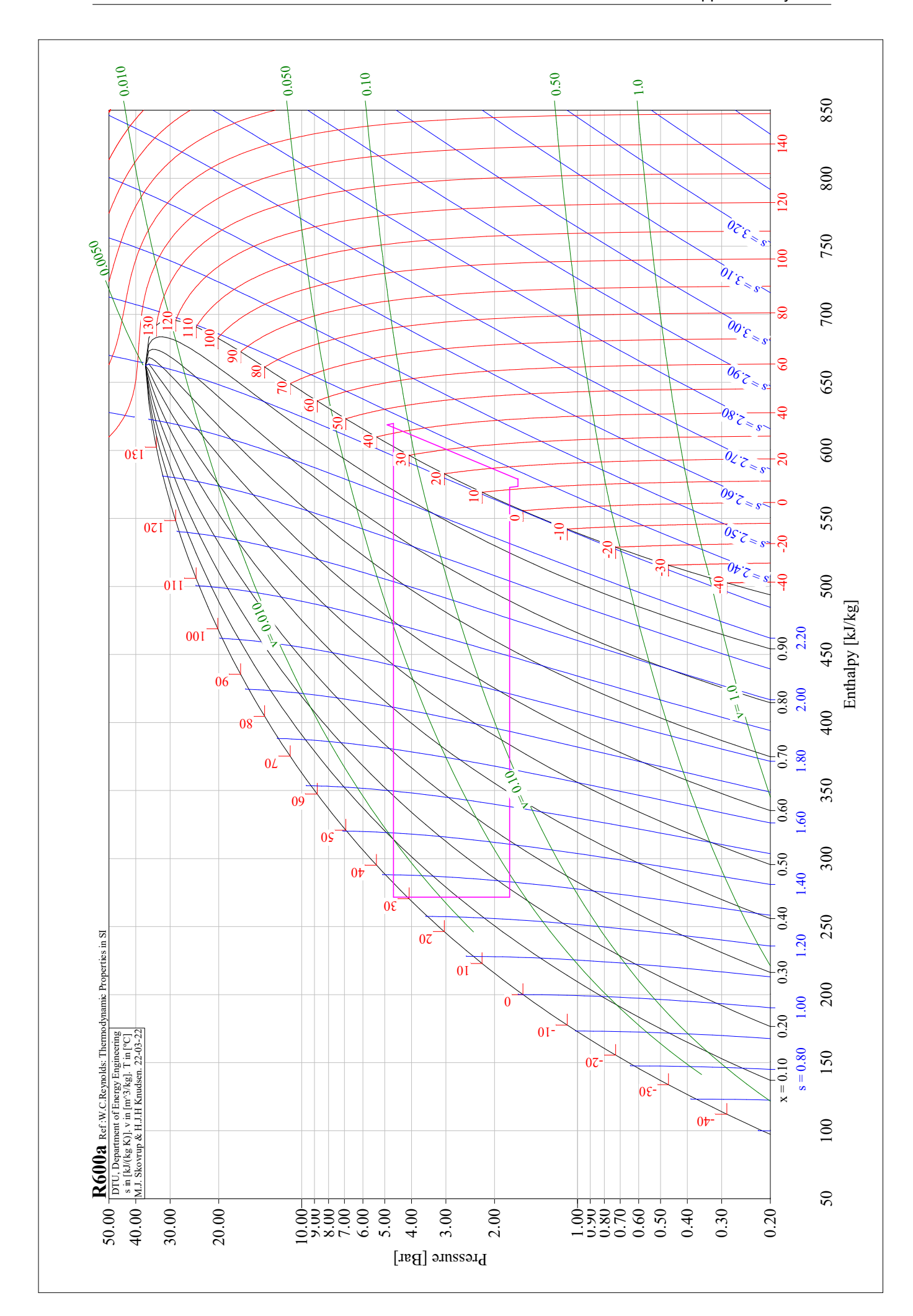


Supplementary Data

Thermocouple	Offset (K)		
Warm in	0.38		
Warm out	0.22		
Cold in	0.02		
Cold out	-0.35		
TC1	-0.38		
TC2	-0.03		
TC3	0.21		
TC4	0.36		
TC5	0.28		
TC6	0.15		
TC7	-0.03		
TC8	-0.39		
TC9	-0.53		
TC10	-0.18		
TC11	0.03		
TC12	0.22		

Table A.1: Thermocouple offsets

The refrigeration cycle of the current system is shown on the next page. The p-h diagram was generated using Coolpack [35].





Manufacturing process

The production of the prototype involved multiple different processes, some of which were performed in-house by myself or others at Quooker. Other processes were outsourced. Using the design requirements and the modelling results, designs were made for the different parts that need to be constructed. The different parts are the tubes, the tube corner pieces, the thermocouple t-junctions, and the container. Additionally, tools were manufactured for the tube bending and pressing of the fins.

B.1. Tubes

The tubes themselves were ordered to specification. The tube bends were then designed to fit over the tubes. To create the bends, a tube with an inside diameter of 10mm was acquired. It had an outside diameter of 13mm. This tube was then cut into pieces of around 100 mm. These pieces could be shortened later if necessary. It then needed to be bent into shape. Bending the tube in normal ambient conditions caused the tube to buckle, so a different solution was required. The first idea was to push the tube over a bent rod. A heat gun would then be applied to the tube, allowing the stresses in the tube to be relieved and the tube to bend without buckling. The rod was printed using a resin printer. Resin with a high temperature resistance was used. The first iteration of this idea had a problem associated with it that it was very challenging to push the plastic tube around the rod. For the second iteration, the tube diameter was reduced slightly, the vertical component was made longer to give a large portion where it could be held, and the chamfers on were made more significant and applied to both ends to make it easier to apply the tubes. Both iterations can be seen in figure B.2, and the technical drawing of the second iteration is shown in figure B.3. The second iteration still struggled with the same problems, and additionally, once the heat had been applied, it was very difficult to remove the rod.

To solve this problem, a new design was created. Instead of moulding the tube from the outside, it would be heated and subsequently placed in a mould, where it would be left to cool. To avoid the initial buckling of the tube, a silicon tube was acquired, which could be pulled through the tube using some wire. The drawing of the mould can be seen in figure B.4. This mould was also printed using the resin printer using the same temperature-resistant resin. The mould was printed twice so that both sides could be clamped around the tube once it had been heated. This process is shown in figure B.1.

B.2. Fins

The most critical parts of the prototype are the fins and tubes. The contact area needs to be maximised to ensure proper conduction between the fins and the tubes. To ensure maximum contact, collars were pressed into the fins. These collars were pressed from aluminium plates. A hole of a specific diameter would be laser-cut into the fin. The thickness was determined using the modelling. The height of the collars would be used to judge the spacing of the fins. Test strips were thus devised to evaluate which collar heights could be achieved at each fin thickness. By adjusting the diameter of the hole, the collars would be of different heights. As the plates got thinner, lower collar heights were achievable. This led to the final decision of 0.3 mm thickness and 1.5mm collar height. It was decided that the collars wouldn't have to be the critical factor in judging the spacing. The Friction between the fins and tubes would be



Figure B.1: Tube bending process where the tube has been heated with a heat gun and subsequently bent into shape and placed in the mould to cool. The silicon tube with attached wire can be seen still present within the tubing.



Figure B.2: Left: The first iteration bending tube with a shorter handle and larger tube diameter. Right: The second iteration bending tube with a larger handle, increased chamfer, and a smaller diameter.

B.3. Pressing 57



Figure B.3: Drawing of the first tube bending solution.

sufficient, so the fins would not necessarily need to be stacked. Figure B.5 shows a single fin with the collars pressed into it.

B.3. Pressing

Once the plates were cut and collared, they were ready to be pressed over the tubes. To properly press the fins, a tool was produced which could press the plates evenly over the tubes. This tool would need to apply pressure to the plates while letting the tubes through. The force of the press would also need to be distributed evenly.

The tool was designed considering structural integrity as well as material availability. 20 mm aluminium was structurally strong enough and available and was thus used. The tool consists of a bottom plate in which the tubes can stand, which is separate from the rest. The top plate can attach to the press and has 6 rods connecting to the bottom plate, which applies the pressure. Figure B.7 shows the design of the pressing plate, figure B.8 shows the design of the top plate, figure B.9 shows the design of the rods and figure B.10 shows the design of the rod holder. The three plates were milled into shape, and the holes were drilled.

The tool was then attached to the press, and the tubes were placed in the rack. The fins were then pressed over the tubes. This method of pressing led to a few problems. The stand in which the tubes were placed had too high of a gap tolerance causing the tubes to be loose and unaligned with each other while the first few fins were being pressed. As more and more plates were pressed onto the tubes, the tubes would be pushed back into alignment. In the next iteration, the tube tolerance should also be sharper. The current set of tubes contained a few tubes that were not as straight as the others, causing the alignment and stresses in the plates to vary as more plates were added to the system. Towards the end of the process, the alignment was off by such a large margin that significant pressing force was required to press the plates over the tubes. This increased pressure, along with the design of the press tool, caused the collar edges to be sucked into the press tool. Removing the plates after they had been pressed onto the ever-growing tube-and-plate-packet was increasingly difficult. As more plates were added, more force was required to remove the packet from the press. A removal tool

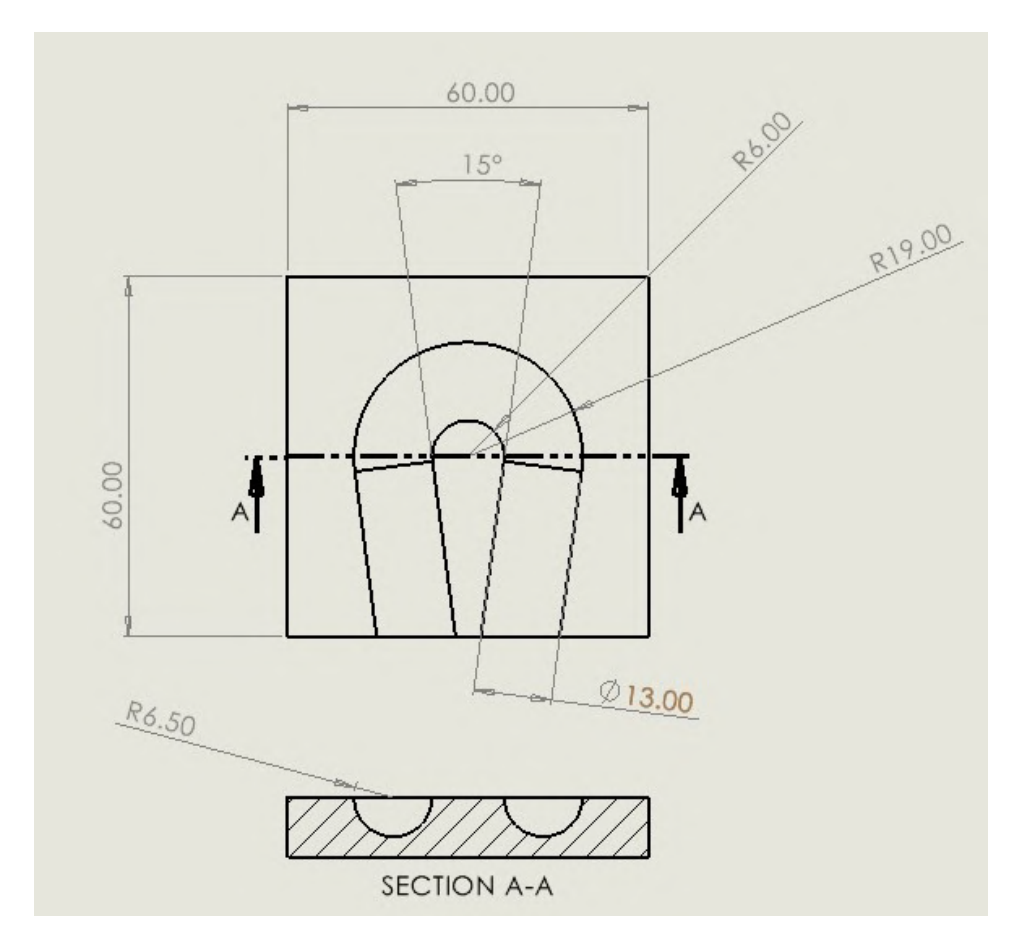


Figure B.4: Drawing of the mould for tube bending



Figure B.5: Image of fins with pressed collars form optimal thermal contact.

B.3. Pressing 59



Figure B.6: Image of the tool that was attached to the hydraulic press to press the fins over the tubes.

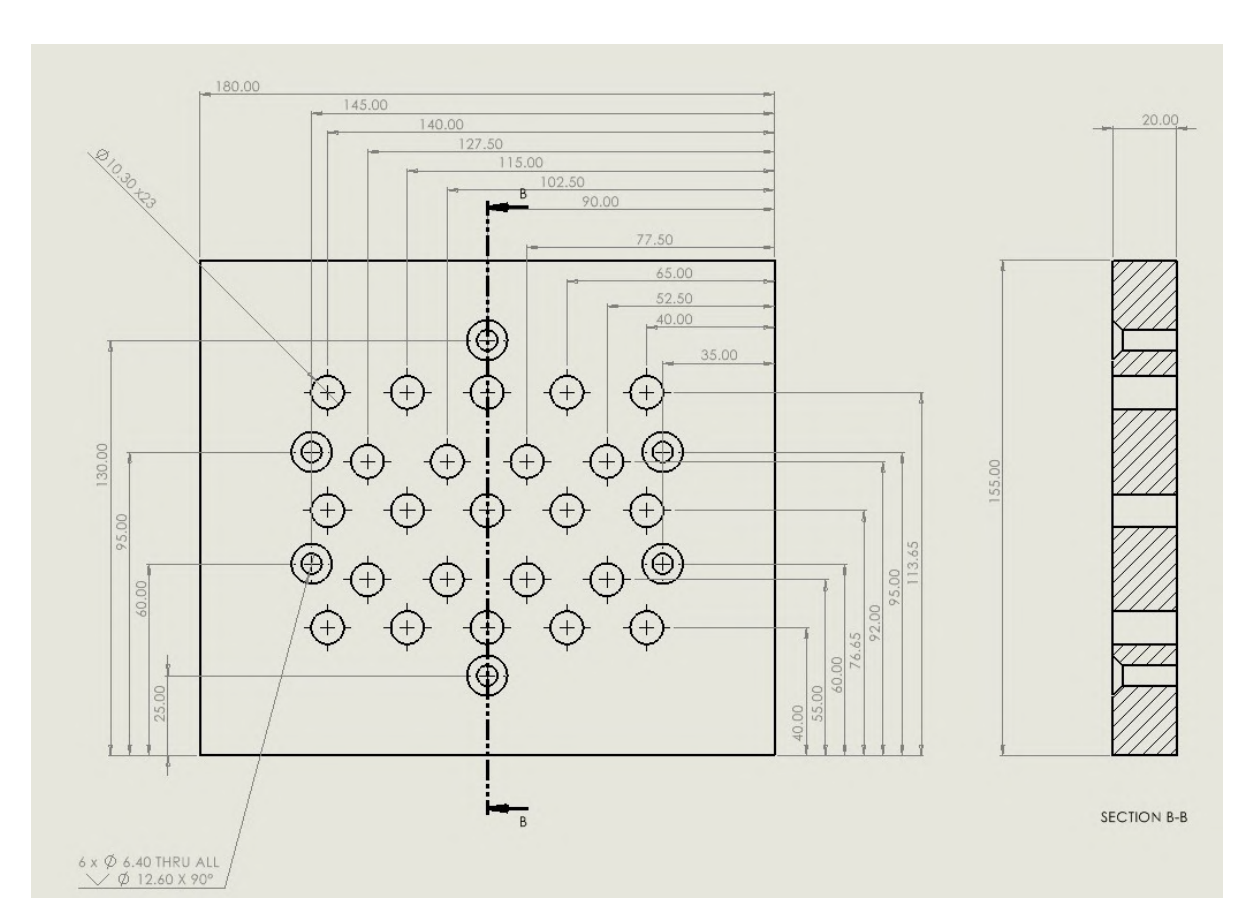


Figure B.7: Drawing of the press-plate of the pressing tool.

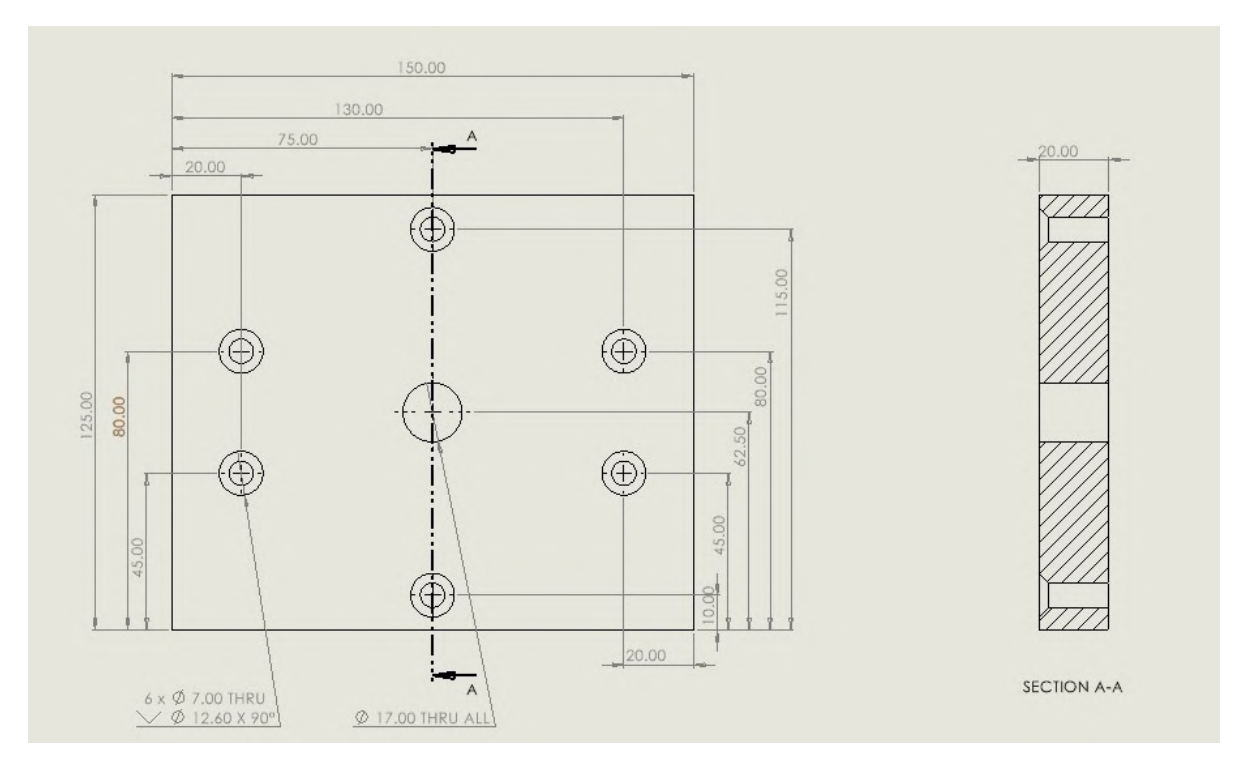


Figure B.8: Drawing of the top plate of the pressing tool

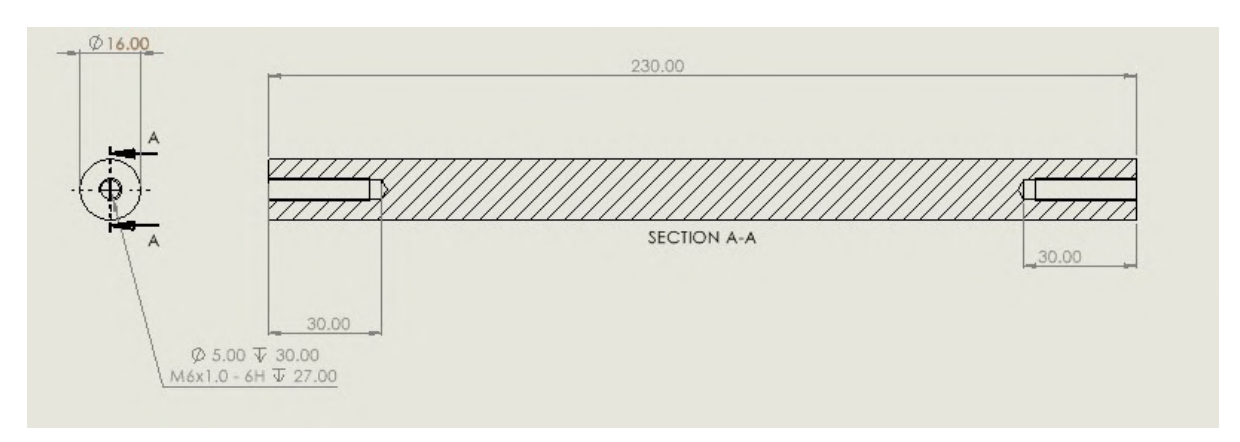


Figure B.9: Drawing of the rods used in the pressing tool.

B.4. Container 61

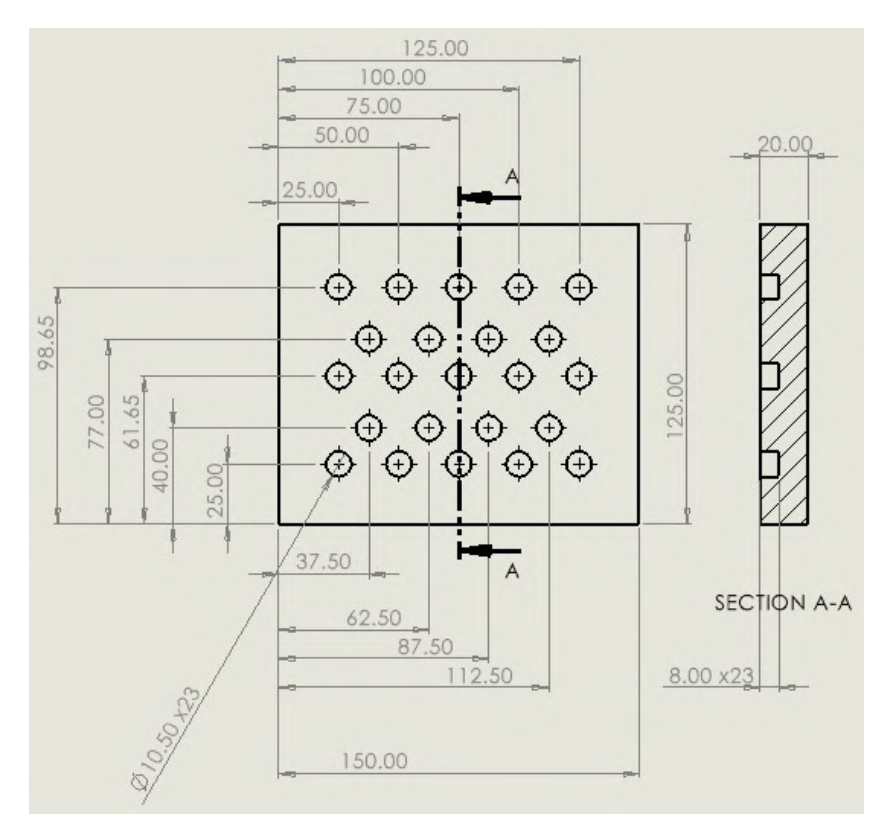


Figure B.10: Drawing of the rack in which the tubes stand while pressing.

had not been designed, meaning rudimentary methods such as prying with a screwdriver were used to separate the packet from the tool. Unfortunately, this also led to plate deformation, causing the plate distance to become very non-uniform.

B.4. Container

The container was made up of six plates of polycarbonate, which had been ordered to fit from a water-cutting firm. Holes were then drilled into the sides of the plates with thread so the plates could be attached. Holes were also drilled in the top where the tubes could pass through as well as smaller holes for the thermocouples. Figure B.11,B.12, and B.13 show the designs of the top, short side and long side, respectively. The bottom is the same as the top, without holes for tubes and thermocouples.

Once the holes had been drilled, the container could be bolted together and glued. A two-component adhesive was used to ensure a proper seal between the edges of the container. Figure B.14 shows the glueing process. The table clamps were used to position the separate pieces of the container from which the pieces could be removed and replaced one by one to apply the adhesive. The seals were then tested by filling the container with water and letting it set for an hour. After this period of time, no water was found under the container, so it was deemed leak tight. Figure B.15 shows the setup for the leak test.

B.5. Thermocouple T-junctions

The thermocouples needed to be inserted in the flow to measure the temperature there accurately. Long flexible thermocouples were thus purchased along with thermocouple seals. These seals were welded onto steel tubes which had had a hole drilled into the side of them. These tubes could then be clamped to the rest of the system in line with the flow. The thermocouple could be inserted through the seal into the stream.

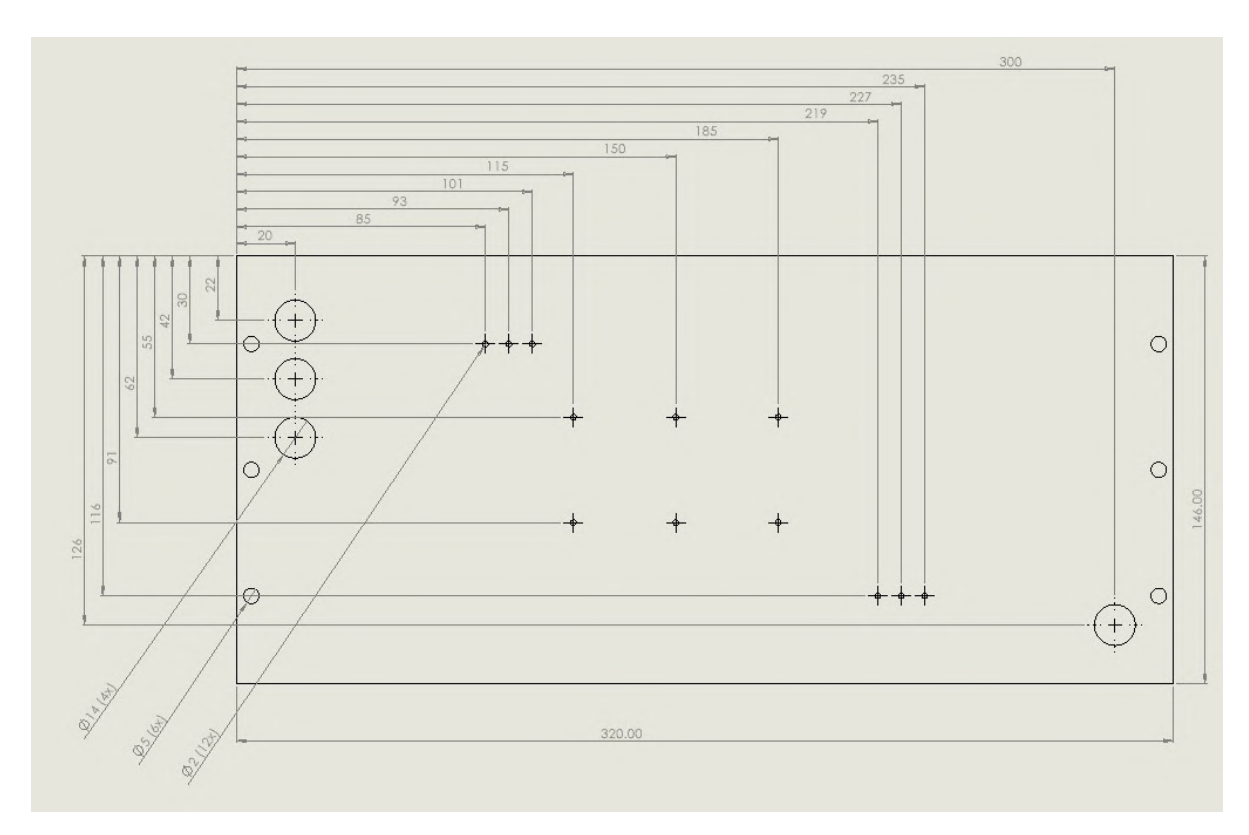


Figure B.11: Drawing of the PCM container lid.



Figure B.16: Image of a welded thermocouple t-junction

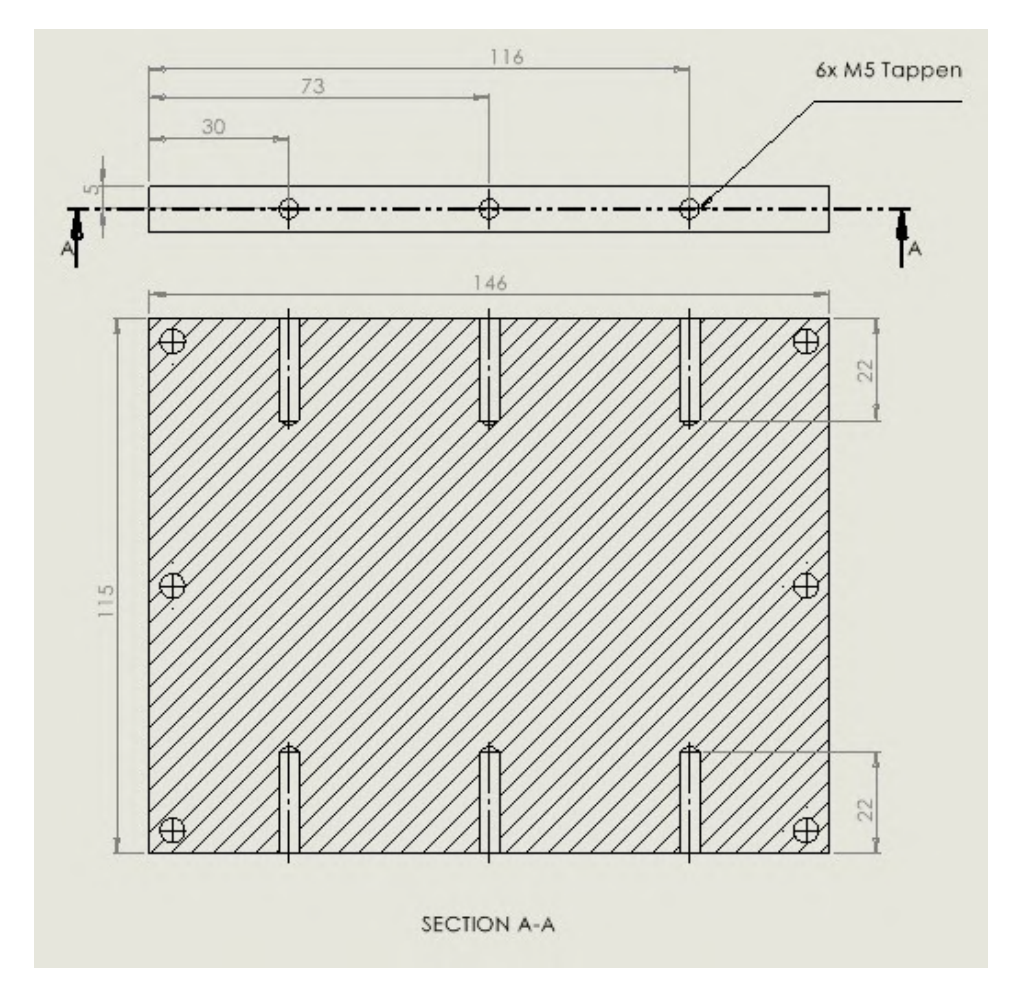


Figure B.12: Drawing of the short sides of the PCM container.

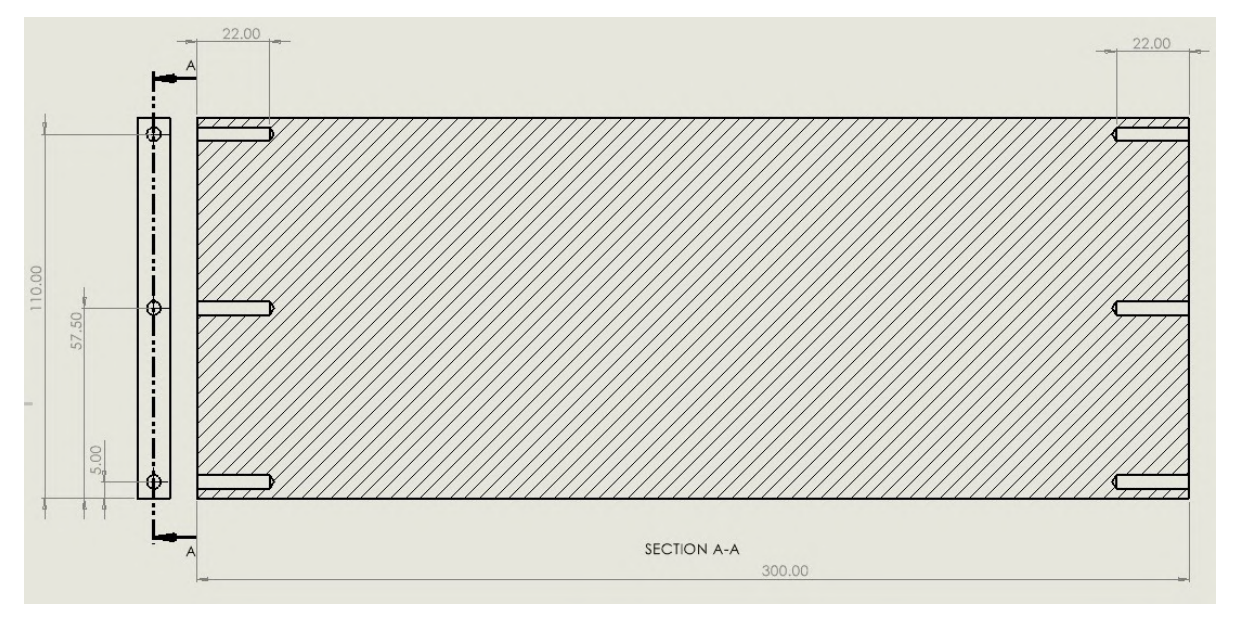


Figure B.13: Drawing of the long sides of the PCM container.



Figure B.14: Image of the glueing process of the PCM container.

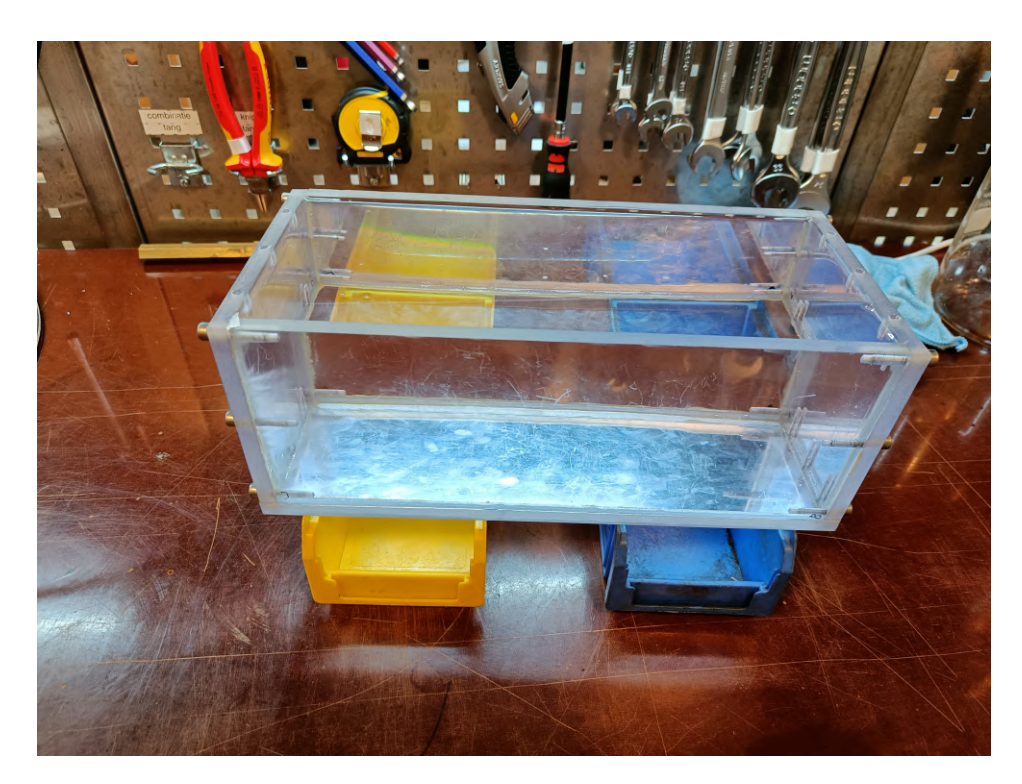
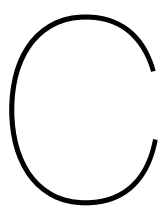


Figure B.15: Image of the PCM container leak test.



Measurements

These are the six measurements that were run along with the heat transfer coefficients for each thermocouple during each measurement.

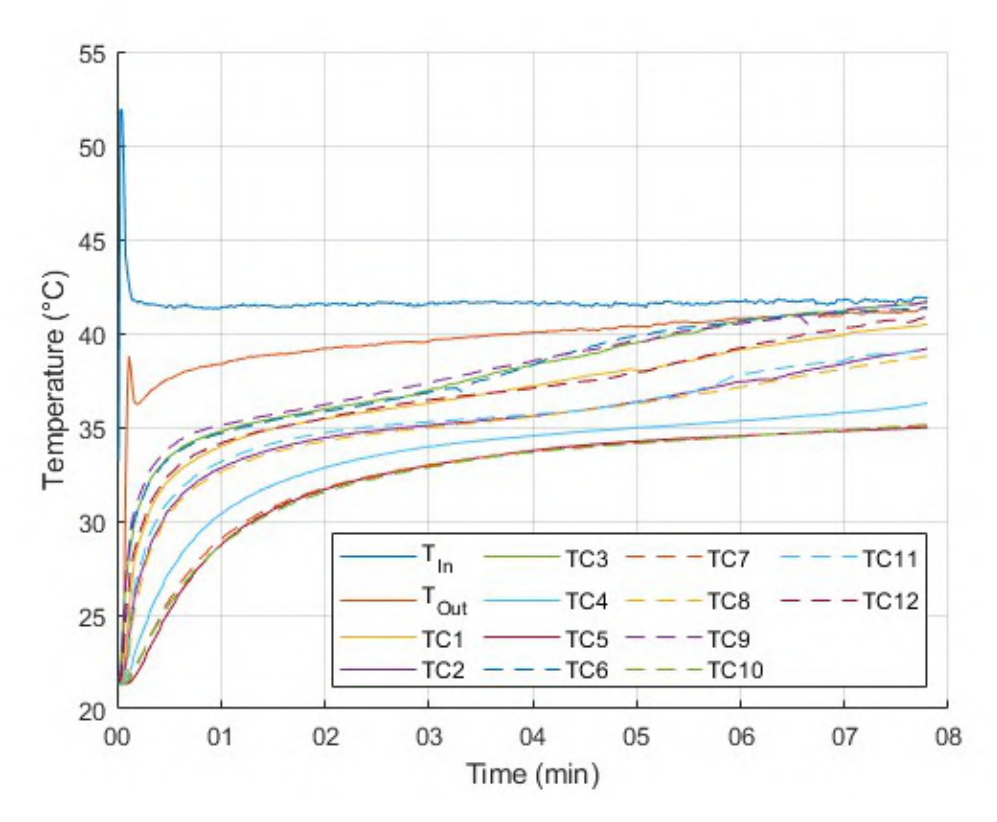


Figure C.1: First heating measurement.

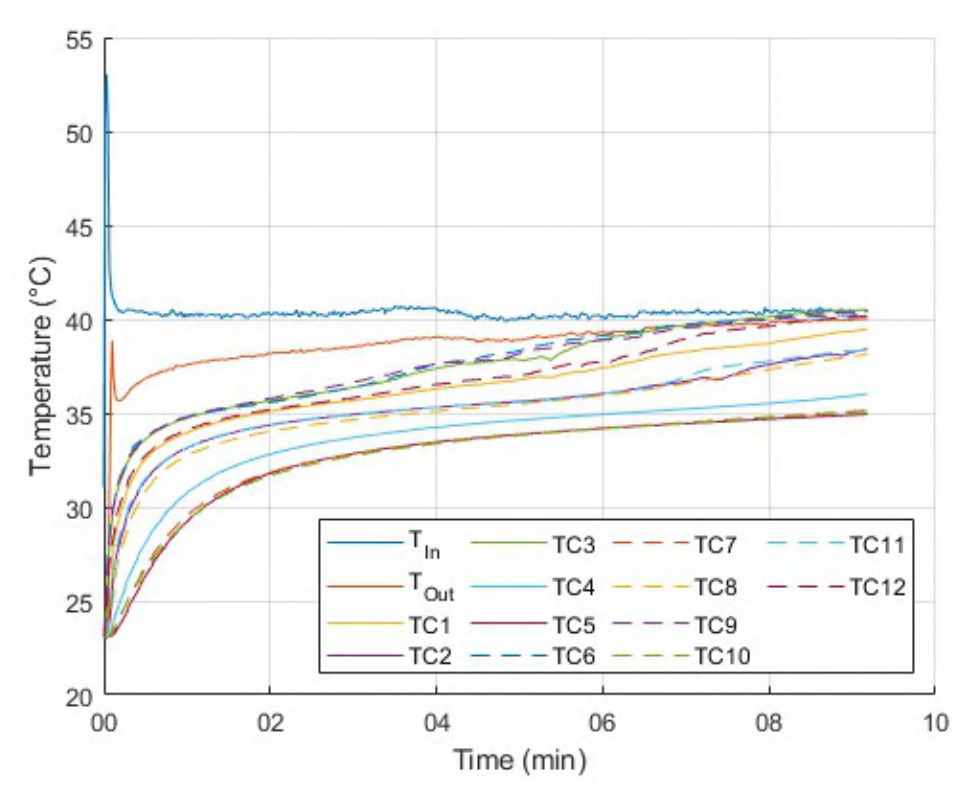


Figure C.2: Second Heating measurement.

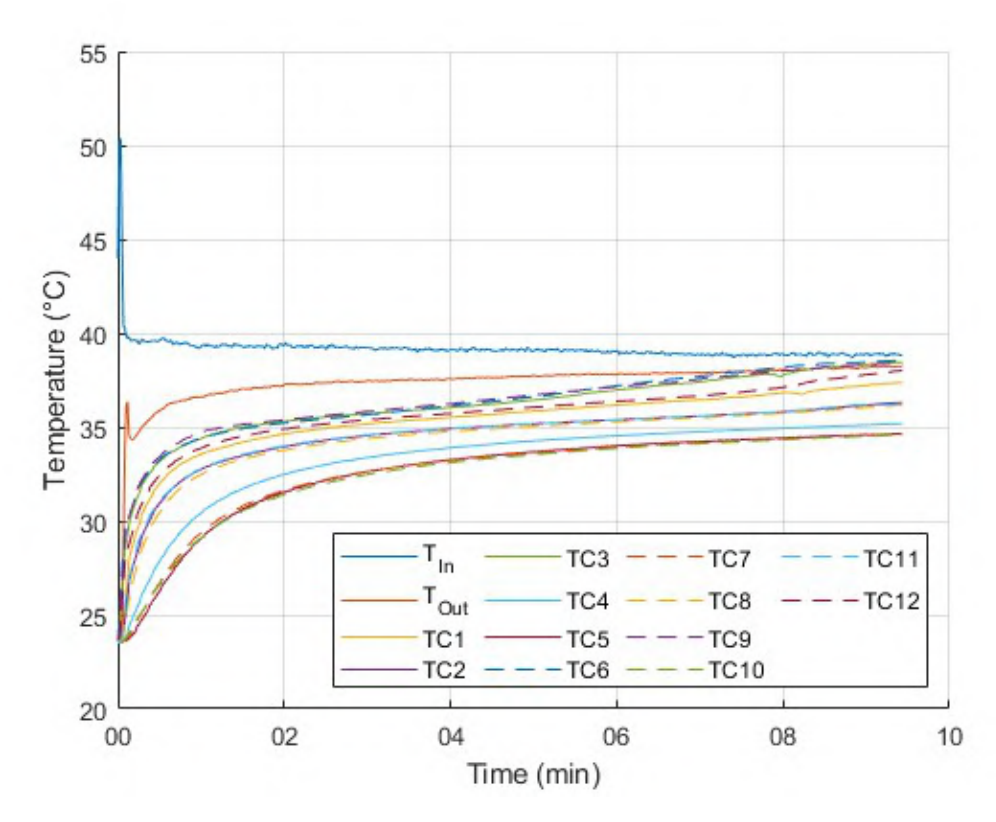


Figure C.3: Third heating measurement.

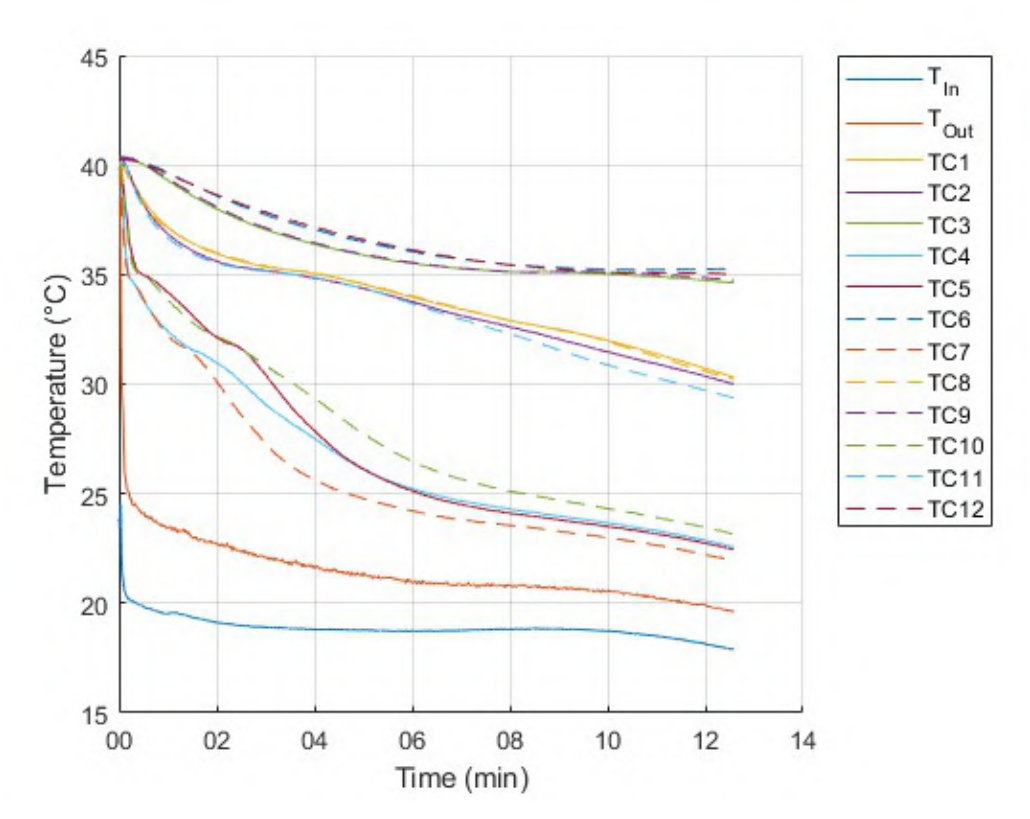


Figure C.4: First cooling measurement.

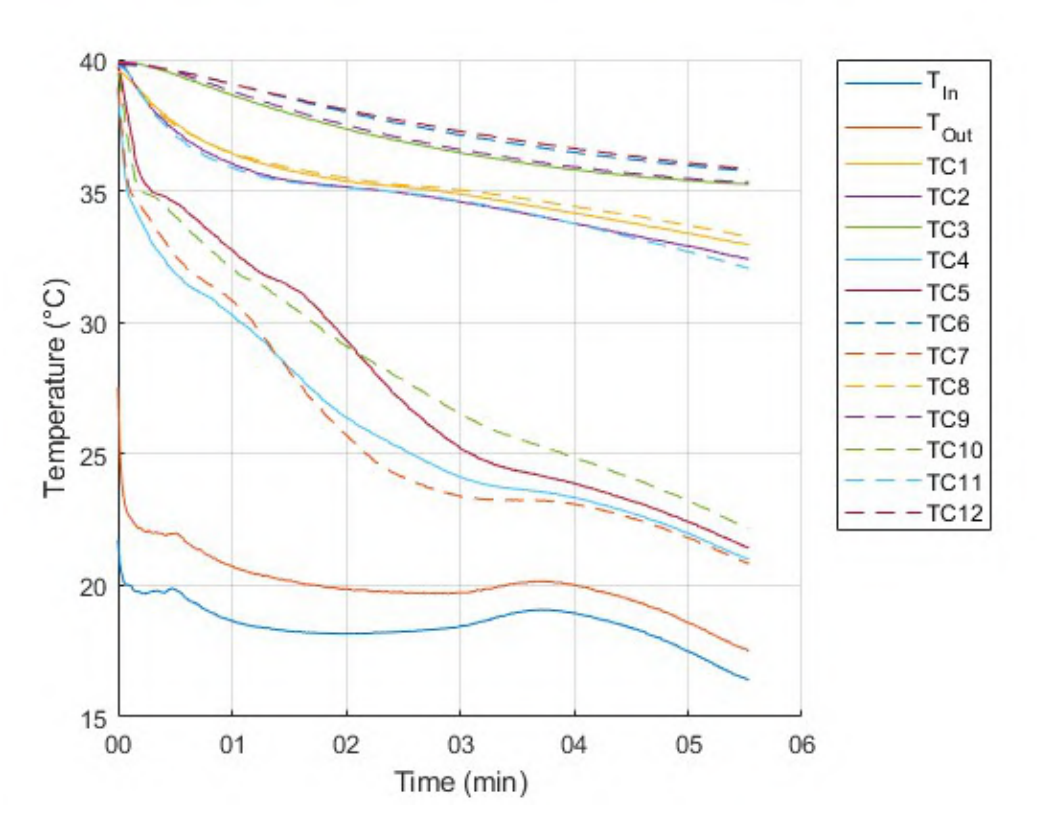


Figure C.5: Second cooling measurement.

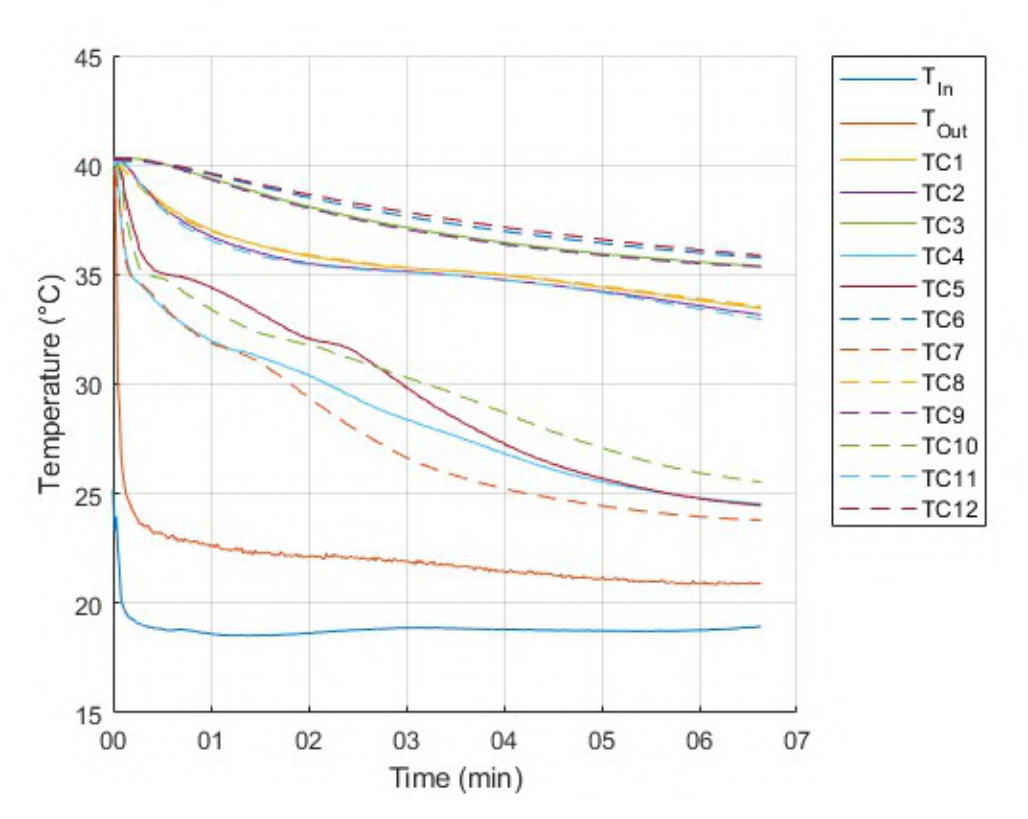


Figure C.6: Third cooling measurement

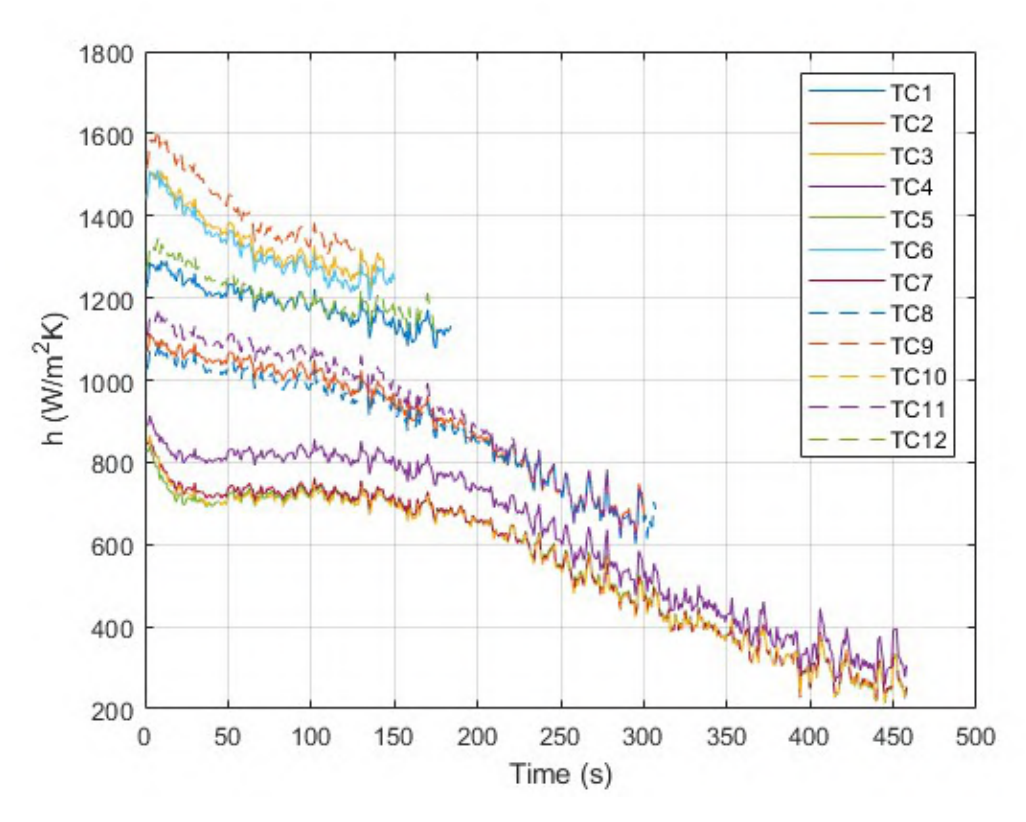


Figure C.7: Heat transfer coefficients of the first heating measurement.

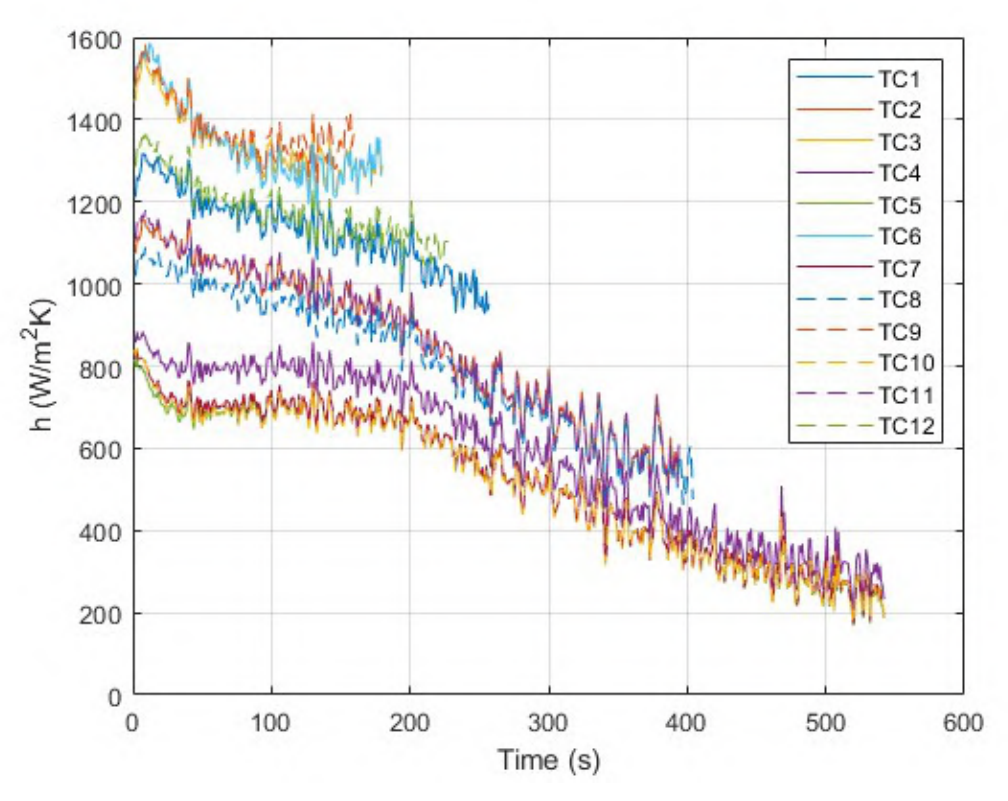


Figure C.8: Heat transfer coefficients of the second heating measurement.

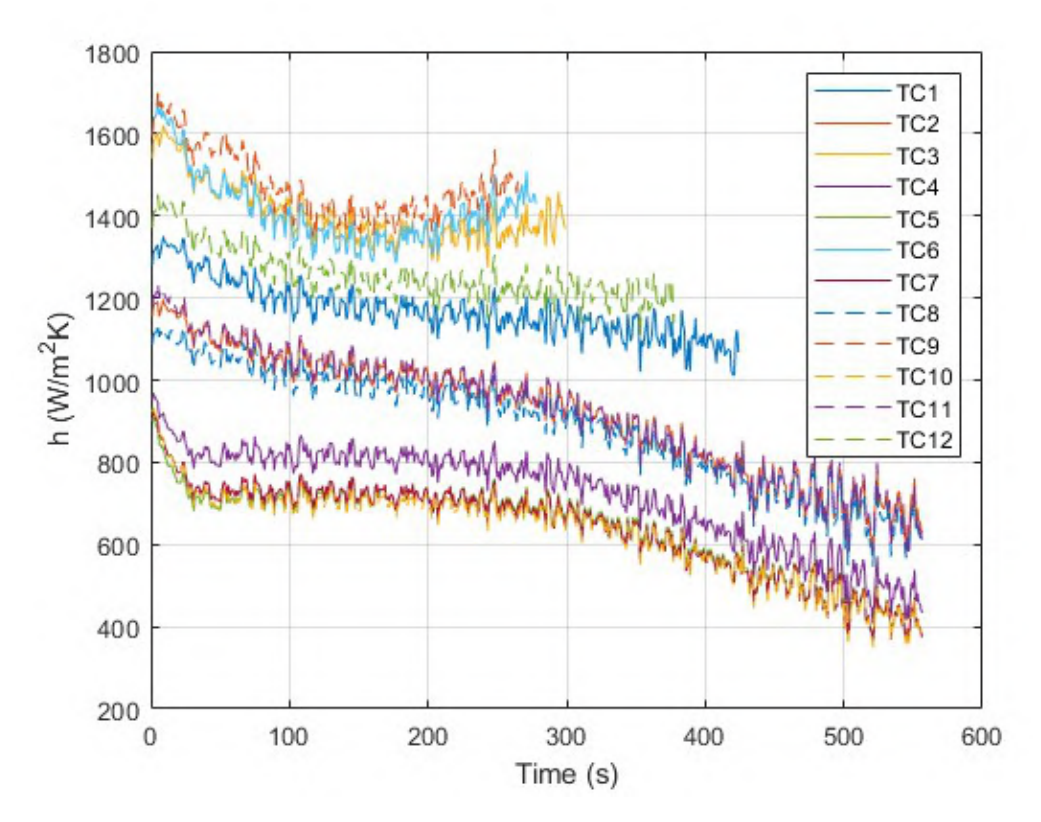


Figure C.9: Heat transfer coefficients of the third heating measurement.

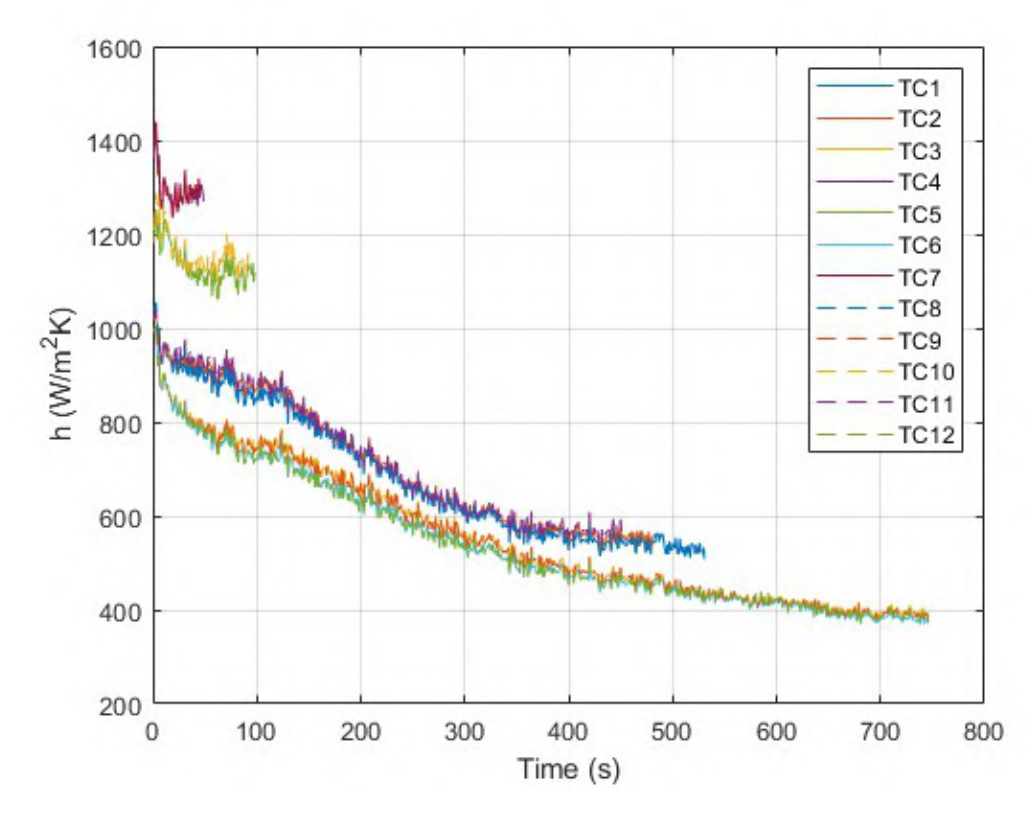


Figure C.10: Heat transfer coefficients of the first cooling measurement.

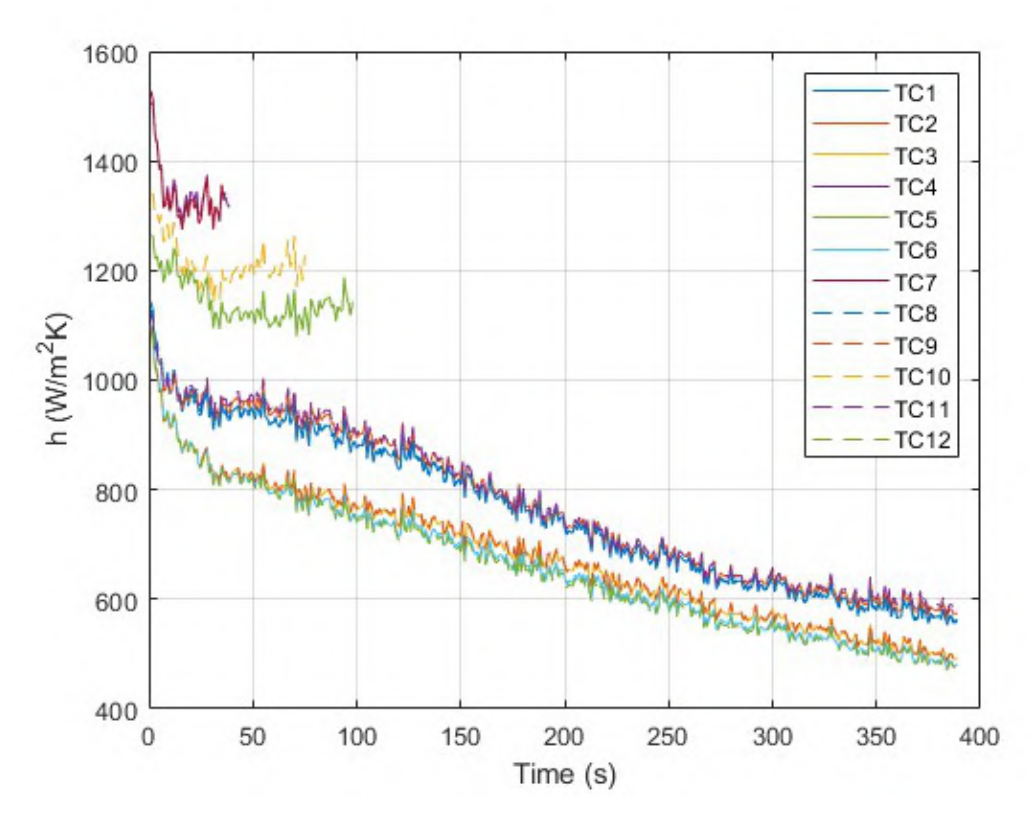


Figure C.11: Heat transfer coefficients of the second cooling measurement.

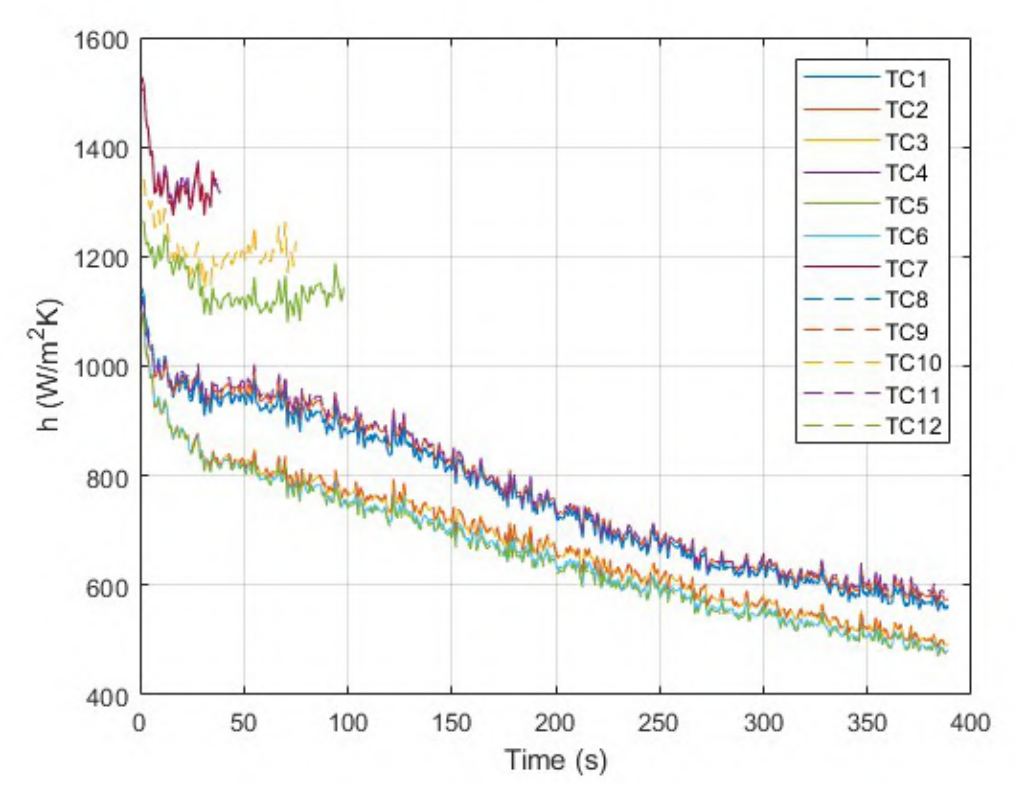


Figure C.12: Heat transfer coefficients of the third cooling measurement.

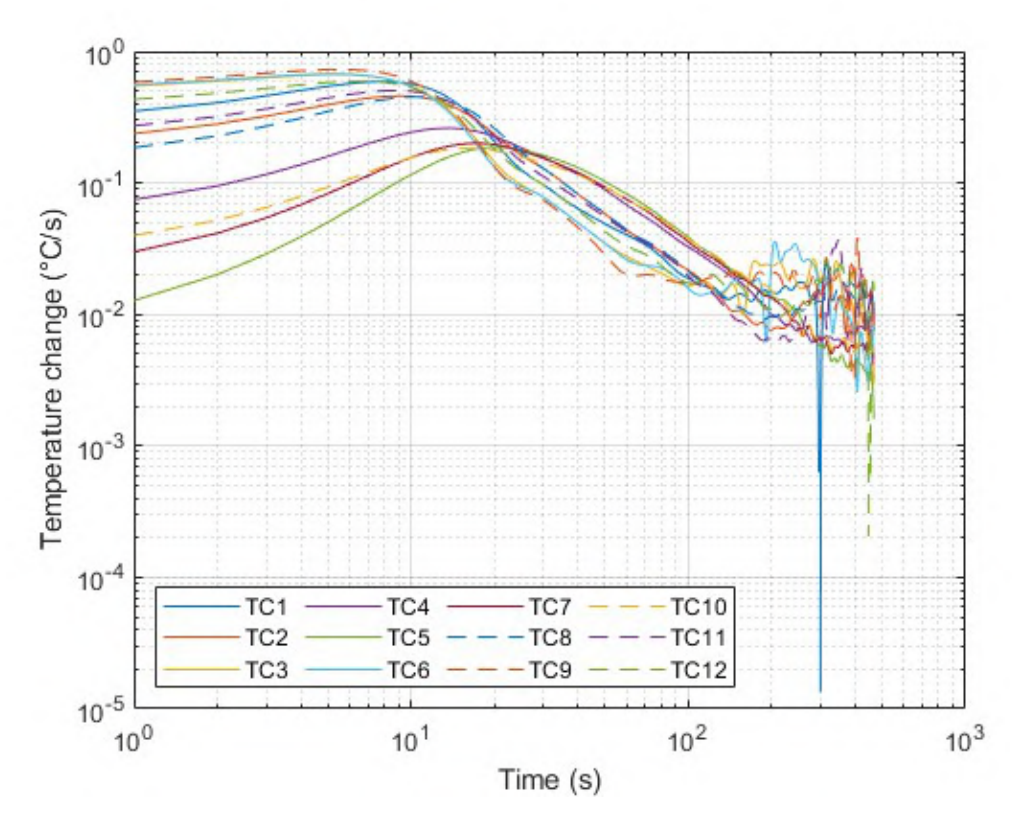


Figure C.13: Change in temperature per second at each thermocouple during the first heating measurement.

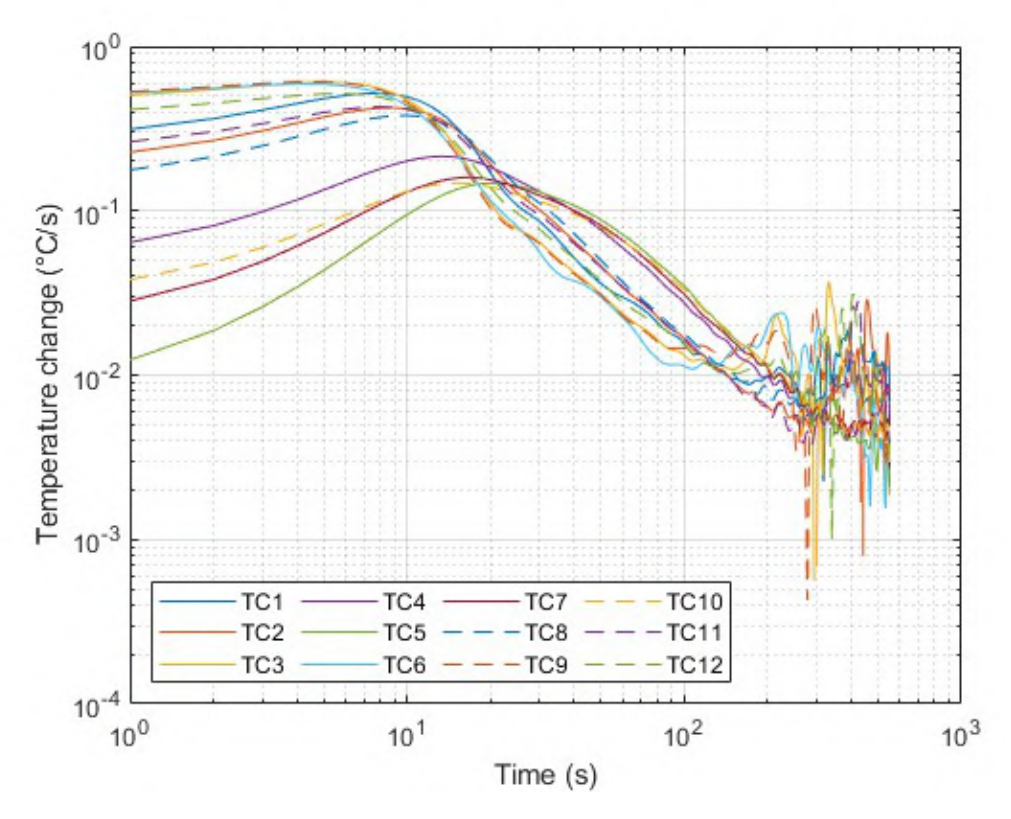


Figure C.14: Change in temperature per second at each thermocouple during the second heating measurement.

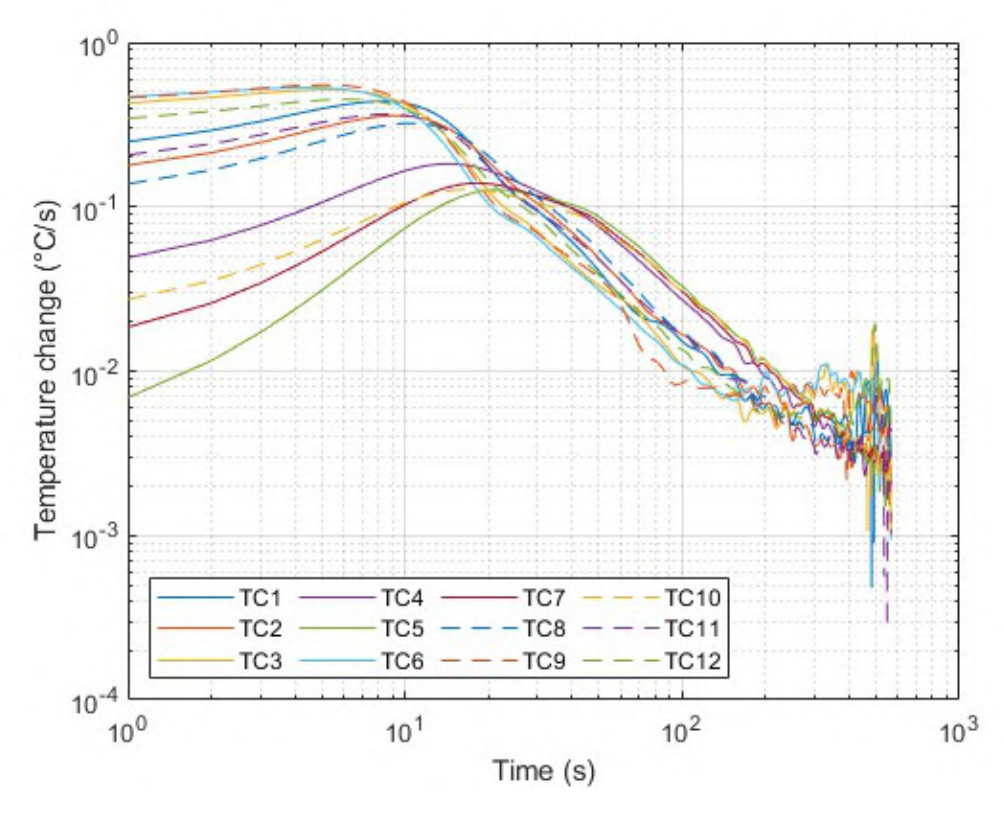


Figure C.15: Change in temperature per second at each thermocouple during the third heating measurement.

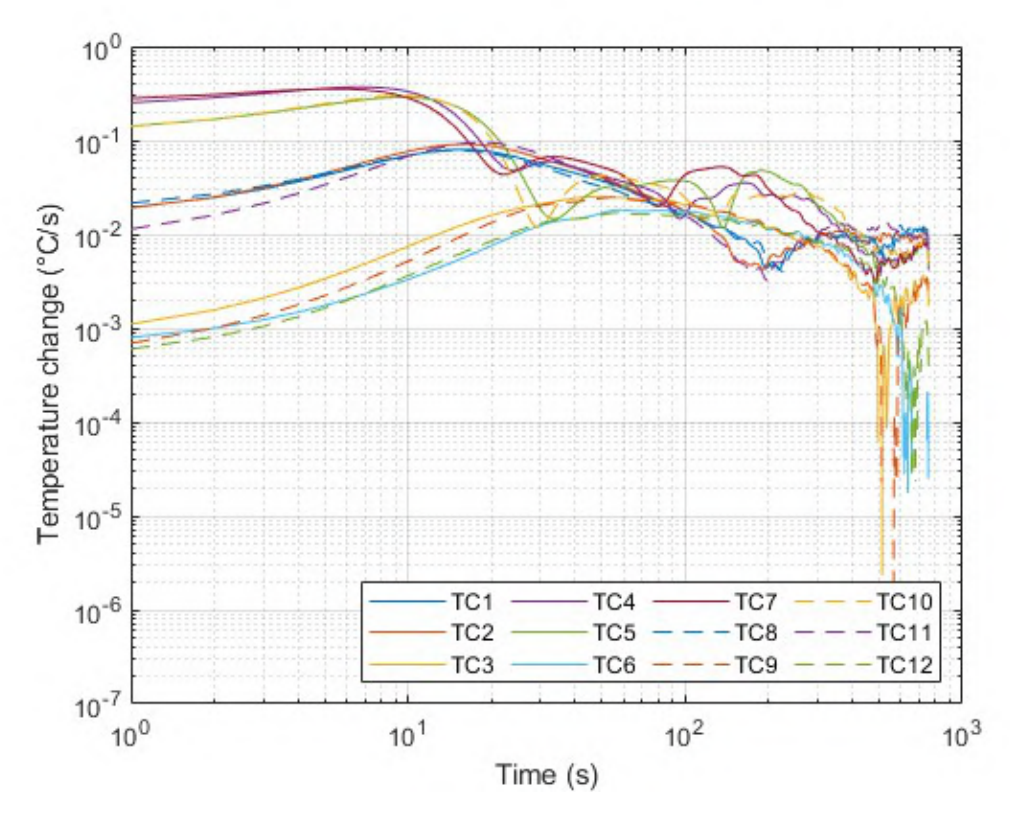


Figure C.16: Change in temperature per second at each thermocouple during the first cooling measurement.

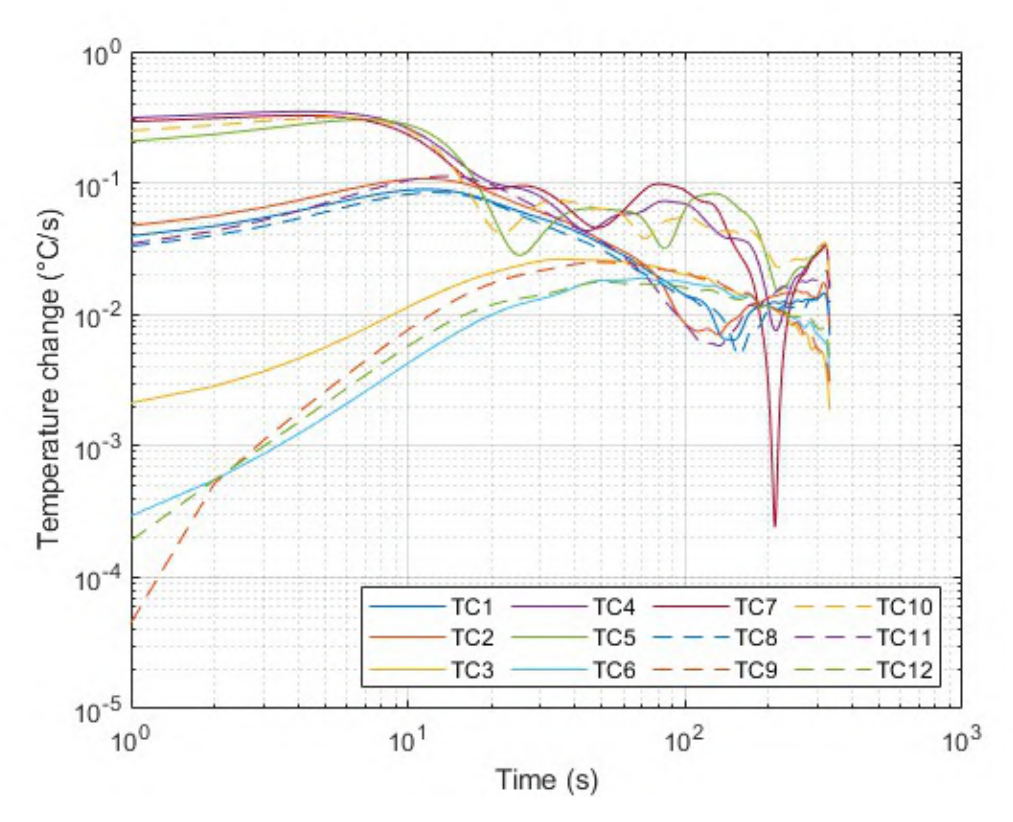


Figure C.17: Change in temperature per second at each thermocouple during the second cooling measurement.

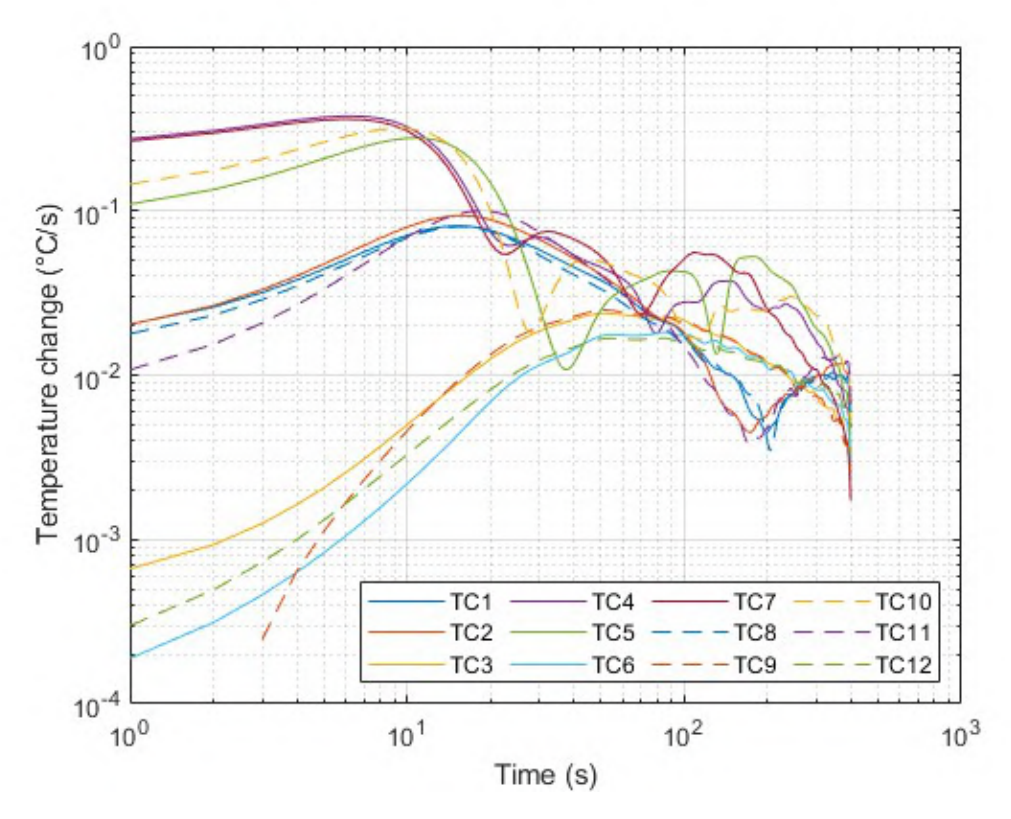


Figure C.18: Change in temperature per second at each thermocouple during the third cooling measurement.

Bibliography

- [1] Hussein Akeiber et al. "A review on phase change material (PCM) for sustainable passive cooling in building envelopes". In: *Renewable and Sustainable Energy Reviews* 60 (July 2016), pp. 1470–1497. ISSN: 1364-0321. DOI: 10.1016/J.RSER.2016.03.036.
- [2] Guruprasad Alva, Yaxue Lin, and Guiyin Fang. "An overview of thermal energy storage systems". In: *Energy* 144 (Feb. 2018), pp. 341–378. ISSN: 03605442. DOI: 10.1016/j.energy.2017. 12.037. URL: https://linkinghub.elsevier.com/retrieve/pii/S036054421732056X.
- [3] Brian T. Austin and K. Sumathy. "Transcritical carbon dioxide heat pump systems: A review". In: Renewable and Sustainable Energy Reviews 15.8 (Oct. 2011), pp. 4013–4029. ISSN: 1364-0321. DOI: 10.1016/J.RSER.2011.07.021.
- [4] Pradeep Bansal, Edward Vineyard, and Omar Abdelaziz. "Advances in household appliances-A review". In: *Applied Thermal Engineering* 31.17-18 (Dec. 2011), pp. 3748–3760. ISSN: 1359-4311. DOI: 10.1016/J.APPLTHERMALENG.2011.07.023.
- [5] F. Bruno et al. "Using solid-liquid phase change materials (PCMs) in thermal energy storage systems". In: *Advances in Thermal Energy Storage Systems*. Elsevier, Jan. 2015, pp. 201–246. DOI: 10.1533/9781782420965.2.201. URL: https://linkinghub.elsevier.com/retrieve/pii/B9781782420880500092.
- [6] CBS. Huishoudens nu. 2021. URL: https://www.cbs.nl/nl-nl/visualisaties/dashboard-bevolking/woonsituatie/huishoudens-nu#:~:text=Begin%202021%20waren%20er%208,gemiddelde%20huishoudensgrootte%20nog%203%2C54..
- [7] Vijayaraghavan S. Chakravarthy, Ramesh K. Shah, and G. Venkatarathnam. "A Review of Refrigeration Methods in the Temperature Range 4–300 K". In: Journal of Thermal Science and Engineering Applications 3.2 (June 2011). ISSN: 1948-5085. DOI: 10.1115/1.4003701. URL: https://asmedigitalcollection.asme.org/thermalscienceapplication/article/doi/10.1115/1.4003701/469408/A-Review-of-Refrigeration-Methods-in-the.
- [8] Seyoung Choi et al. "Review: Recent advances in household refrigerator cycle technologies". In: Applied Thermal Engineering 132 (Mar. 2018), pp. 560–574. ISSN: 13594311. DOI: 10.1016/j.applthermaleng.2017.12.133. URL: https://linkinghub.elsevier.com/retrieve/pii/S1359431117354674.
- [9] Roy J. Dossat. Principles of Refrigeration. 1996. ISBN: 0132333716.
- [10] Environmental Protection Agency. ENVIRONMENTAL PROTECTION AGENCY 40 CFR Part 82 Protection of Stratospheric Ozone: Listing of Substitutes for Ozone-Depleting Substances-Hydrocarbon Refrigerants. Dec. 2011. URL: www.epa.gov/ozone/snap/regs..
- [11] Annette Evans, Vladimir Strezov, and Tim J. Evans. "Assessment of utility energy storage options for increased renewable energy penetration". In: *Renewable and Sustainable Energy Reviews* 16.6 (Aug. 2012), pp. 4141–4147. ISSN: 1364-0321. DOI: 10.1016/J.RSER.2012.03.048.
- [12] Gas Servei. CFC REFRIGERANTS. 2022. URL: https://gas-servei.com/en/products/refrigerants/cfc-refrigerants/#:~:text=Prior%20to%20this%2C%20in%20the,due%20to%20methy1%20chloride%20leaks..
- [13] Yu G Gurevich and G N Logvinov. "Physics of thermoelectric cooling". In: Semiconductor Science and Technology 20.12 (Dec. 2005), R57–R64. ISSN: 0268-1242. DOI: 10.1088/0268-1242/20/12/R01. URL: https://iopscience.iop.org/article/10.1088/0268-1242/20/12/R01.

76 Bibliography

[14] Selvaraj Jegadheeswaran, Athimoolam Sundaramahalingam, and Sanjay D Pohekar. "Alternative Heat Transfer Enhancement Techniques for Latent Heat Thermal Energy Storage System: A Review". In: *International Journal of Thermophysics* 42.12 (Dec. 2021), p. 171. ISSN: 0195-928X. DOI: 10.1007/s10765-021-02921-x. URL: https://link.springer.com/10.1007/s10765-021-02921-x.

- [15] Jisoo Jeon et al. "Thermal performance enhancement of a phase change material with expanded graphite via ultrasonication". In: *Journal of Industrial and Engineering Chemistry* 79 (Nov. 2019), pp. 437–442. ISSN: 1226-086X. DOI: 10.1016/J.JIEC.2019.07.019.
- [16] Burcu Koçak, Ana Ines Fernandez, and Halime Paksoy. "Review on sensible thermal energy storage for industrial solar applications and sustainability aspects". In: *Solar Energy* 209 (Oct. 2020), pp. 135–169. ISSN: 0038-092X. DOI: 10.1016/J.SOLENER.2020.08.081.
- [17] Gang Li. "Sensible heat thermal storage energy and exergy performance evaluations". In: Renewable and Sustainable Energy Reviews 53 (Jan. 2016), pp. 897–923. ISSN: 13640321. DOI: 10.1016/j.rser.2015.09.006. URL: https://linkinghub.elsevier.com/retrieve/pii/S1364032115009764.
- [18] Abdur Rehman Mazhar, Ashish Shukla, and Shuli Liu. "Numerical analysis of rectangular fins in a PCM for low-grade heat harnessing". In: *International Journal of Thermal Sciences* 152 (June 2020), p. 106306. ISSN: 12900729. DOI: 10.1016/j.ijthermalsci.2020.106306. URL: https://linkinghub.elsevier.com/retrieve/pii/S1290072919317065.
- [19] Mark O. McLinden, Christopher J. Seeton, and Andy Pearson. "New refrigerants and system configurations for vapor-compression refrigeration". In: *Science* 370.6518 (Nov. 2020), pp. 791–796. ISSN: 0036-8075. DOI: 10.1126/science.abe3692. URL: https://www.science.org/doi/10.1126/science.abe3692.
- [20] MLDS. Zo drink je met gemak voldoende water per dag. 2022. URL: https://www.mlds.nl/hoe-gezond-is-jouw-buik/artikelen/zo-drink-je-voldoende-water/#: ~:text=Het%20wordt%20ons%20aanbevolen%20zo,in%20de%20Schijf%20van%20Vijf..
- [21] Michael J Moran et al. *FUNDAMENTALS OF ENGINEERING THERMODYNAMICS Eighth Edition*. 8th. Wiley, 2014. ISBN: 978-1-118-41293-0. URL: www.wiley.com/college/moran..
- [22] Kashif Nawaz et al. "R290 (propane) and R600a (isobutane) as natural refrigerants for residential heat pump water heaters". In: *Applied Thermal Engineering* 127 (Dec. 2017), pp. 870–883. ISSN: 13594311. DOI: 10.1016/j.applthermaleng.2017.08.080. URL: https://linkinghub.elsevier.com/retrieve/pii/S1359431117335494.
- [23] NIST. NIST Chemistry WebBook. URL: https://webbook.nist.gov/.
- [24] Ohio Heating. Why Use Ammonia in Commercial Refrigeration Equipment? July 2015.
- [25] Quooker B.V. Onze collectie reservoirs. 2022. URL: https://www.quooker.nl/reservoirs.
- [26] Hazel Reardon. *Thermoelectric materials*. Apr. 2021. URL: https://chem.au.dk/forskning/forskningscentre/center-for-materials-crystallography/research/energy-materials/thermoelectrics.
- [27] Refrigeration and Air-condition Genuine Information and Service. Subcooling and Superheat.

 URL: https://refandaircongenuineservice.wordpress.com/2017/09/13/subcooling-and-superheat/.
- [28] S. B. Riffat and Xiaoli Ma. "Thermoelectrics: a review of present and potential applications". In: *Applied Thermal Engineering* 23.8 (June 2003), pp. 913–935. ISSN: 1359-4311. DOI: 10.1016/S1359-4311 (03) 00012-7.
- [29] Rajib Rony et al. "Recent Advances in Transcritical CO2 (R744) Heat Pump System: A Review". In: *Energies* 12.3 (Jan. 2019), p. 457. ISSN: 1996-1073. DOI: 10.3390/en12030457. URL: https://www.mdpi.com/1996-1073/12/3/457.
- [30] Rubitherm Technolgies GmbH. RT35HC. Berlin, Oct. 2020.

Bibliography 77

[31] Ioan Sarbu and Alexandru Dorca. "Review on heat transfer analysis in thermal energy storage using latent heat storage systems and phase change materials". In: *International Journal of Energy Research* 43.1 (Jan. 2019), pp. 29–64. ISSN: 0363-907X. DOI: 10.1002/er.4196. URL: https://onlinelibrary.wiley.com/doi/10.1002/er.4196.

- [32] Ioan Sarbu and Calin Sebarchievici. "A Comprehensive Review of Thermal Energy Storage". In: Sustainability 10.1 (Jan. 2018), p. 191. ISSN: 2071-1050. DOI: 10.3390/su10010191.
- [33] Atul Sharma et al. "Review on thermal energy storage with phase change materials and applications". In: Renewable and Sustainable Energy Reviews 13.2 (Feb. 2009), pp. 318–345. ISSN: 13640321. DOI: 10.1016/j.rser.2007.10.005. URL: https://linkinghub.elsevier.com/retrieve/pii/S1364032107001402.
- [34] R.E. Simons and R.C. Chu. "Application of thermoelectric cooling to electronic equipment: a review and analysis". In: Sixteenth Annual IEEE Semiconductor Thermal Measurement and Management Symposium (Cat. No.00CH37068). IEEE, 2000, pp. 1–9. ISBN: 0-7803-5916-X. DOI: 10.1109/STHERM.2000.837055. URL: http://ieeexplore.ieee.org/document/837055/.
- [35] Morten Juel Skovrup et al. Coolpack. 2012.
- [36] S.A. Tassou et al. "A review of emerging technologies for food refrigeration applications". In: Applied Thermal Engineering 30.4 (Mar. 2010), pp. 263–276. ISSN: 13594311. DOI: 10.1016/j.applthermaleng.2009.09.001. URL: https://linkinghub.elsevier.com/retrieve/pii/S1359431109002737.
- [37] N. H.S. Tay, F. Bruno, and M. Belusko. "Experimental validation of a CFD and an ε-NTU model for a large tube-in-tank PCM system". In: *International Journal of Heat and Mass Transfer* 55.21-22 (Oct. 2012), pp. 5931–5940. ISSN: 0017-9310. DOI: 10.1016/J.IJHEATMASSTRANSFER. 2012.06.004.
- [38] Gavin Towler and Ray Sinnott. "Heat-Transfer Equipment". In: Chemical Engineering Design. Elsevier, 2013, pp. 1047–1205. DOI: 10.1016/B978-0-08-096659-5.00019-5. URL: https://linkinghub.elsevier.com/retrieve/pii/B9780080966595000195.
- [39] U.S. Bureau of Labor and Statistics. *American Time Use Survey*. 2019. URL: https://www.bls.gov/tus/.
- [40] Binbin Yu et al. "An updated review of recent advances on modified technologies in transcritical CO2 refrigeration cycle". In: *Energy* 189 (Dec. 2019), p. 116147. ISSN: 0360-5442. DOI: 10. 1016/J.ENERGY.2019.116147.
- [41] Belén Zalba et al. "Review on thermal energy storage with phase change: materials, heat transfer analysis and applications". In: *Applied Thermal Engineering* 23.3 (Feb. 2003), pp. 251–283. ISSN: 13594311. DOI: 10.1016/S1359-4311(02)00192-8. URL: https://linkinghub.elsevier.com/retrieve/pii/S1359431102001928.
- [42] Dongliang Zhao and Gang Tan. "A review of thermoelectric cooling: Materials, modeling and applications". In: *Applied Thermal Engineering* 66.1-2 (May 2014), pp. 15–24. ISSN: 13594311. DOI: 10.1016/j.applthermaleng.2014.01.074. URL: https://linkinghub.elsevier.com/retrieve/pii/S1359431114000854.
- [43] X. Zheng and T. S. Ge. "Other types of solar-powered cooling systems". In: *Advances in Solar Heating and Cooling* (June 2016), pp. 382–396. DOI: 10.1016/B978-0-08-100301-5.00014-X. URL: http://dx.doi.org/10.1016/B978-0-08-100301-5.00014-X.